The evolution of the Brosterlea Volcanic Complex, Eastern Cape, South Africa

by

GRANT BRADLEY SURTEES
B.Sc. (Hons)

A thesis submitted in fulfillment of the requirements for the degree of

MASTER OF SCIENCE

RHODES UNIVERSITY

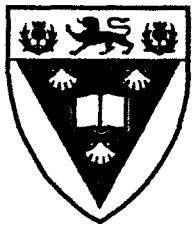

August 1999

ABSTRACT

Detailed field mapping (Map, Appendix B) has been conducted in and around the boundaries of a 14x18km, volcanic complex 35km northeast of Molteno in the Eastern Cape Province, South Africa. The structure is interpreted as a subsidence structure, and is filled with two volcaniclastic breccias, numerous lava flows, a number of sedimentary facies, and lies on a base of Clarens Formation overlying Elliot Formation rocks. This is an important study because widespread, voluminous fields of basaltic breccias are very rare (see Hanson and Elliot, 1996) and this is the first time that this type of volcanic complex and its deposits have been described.

Detailed analyses of the two volcaniclastic breccias revealed changes in colour, clast types, clast sizes, and degree of alteration over relatively short distances both vertically and laterally within a single breccia unit. The variation in clast sizes implies a lack of sorting of the breccias.

The lower of the two volcaniclastic breccias fills the subsidence structure, and outcrops between the Stormberg sedimentary sequence and the overlying Drakensberg basalts and was produced from phreatomagmatic eruptions signalling the start of the break-up of Gondwanaland in the mid-Jurassic. The upper volcaniclastic breccia is interbedded with the flood basalts and is separated from the lower breccia by up to 100m of lava flows in places, it is finer-grained than the lower volcaniclastic breccia, and it extends over 10km south, and over 100km north from the volcanic complex. The upper breccia is inferred to have been transported from outside the study area, from a source presumably similar to the subsidence structure in the volcanic complex. The pyroclastic material forming the upper breccia was transported to the subsidence structure as a laharic debris flow, based on its poorly sorted, unwelded and matrix-supported appearance However, both breccias are unlikely to have been derived from epiclastic reworking of lava flows as they contain glass shards

which are atypical of those derived from the autoclastic component of lava flows. The breccias are therefore not "secondary" lahars. There is also no evidence of any palaeotopographic highs from which the breccias could have been derived as gravity-driven flows.

Based on the occurrence of three, 1m thick lacustrine deposits, localised peperite, fluvial reworking of sandstone and breccia in an outcrop to the south of the subsidence structure, and channel-lags encountered only in the upper units of the Clarens Formation and only within the subsidence structure, the palaeoenvironment inferred for the subsidence structure is one of wet sediment, possibly a shallow lake, in a topographic depression fed by small streams. Magmatic intrusions below the subsidence structure heated the water-laden, partly consolidated Clarens Formation sandstones, causing the circulation of pore fluid which resulted in the precipitation of minerals forming pisoliths in the sandstones. Intruding magma mixed, nonexplosively, with the wet, unconsolidated sediments near the base of the Clarens Formation (at approximately 100m below the surface), forming fluidal peperite by a process of sediment fluidisation where magma replaces wet sediment and cools slowly enough to prevent the magma fracturing brittly. Formation of fluidal peperite may have been a precursor to the development of FCIs (Fuel Coolant Interactions) (Busby-Spera and White, 1987). The breccias may represent the products of FCIs and may be the erupted equivalents of the peperites, suggesting a possible genetic link between the two. The peperites may have given way to FCI eruptions due to a number of factors including the drying out of the sediments and/or an increase in the volume of intruded magma below the subsidence structure which may have resulted in a more explosive interaction between sediment and magma.

Phreatic activity fragmented and erupted the Clarens Formation sandstone, and stream flows reworked the angular sandstone fragments, pisoliths and sand grains into channelised deposits. With an increase in magmatic activity below the subsidence structure, phreatic activity became

phreatomagmatic. The wet, partly consolidated Clarens Formation, and underlying, fully consolidated Elliot Formation sediments were erupted and fragmented. Clasts and individual grains of these sediments were redeposited with juvenile and non-juvenile basaltic material probably by a combination of backfall, where clasts erupted into the air fell directly back into the structure, and backflow where material was erupted out of the structure, but immediately flowed back in as lahars. This material formed the lower volcaniclastic breccia.

A fault plane is identified along the southwestern margin of the subsidence structure, and is believed to continue up the western margin to the northwestern corner. A large dolerite body has intruded along the inferred fault plane on the western margin of the structure, and may be related to the formation of the lower volcaniclastic breccia, either directly through fluidisation of wet sediment during its intrusion, or as a dyke extending upwards from a network of sill-like intrusions below the subsidence structure.

Geochemical analysis of the Drakensberg basalt lava flows by Mitchell (1980) and Masokwane (1997) revealed four distinct basalt types; the Moshesh's Ford, the Tafelkop, the Roodehoek, and the Vaalkop basalts. Basalt clasts sampled from the lower volcaniclastic breccia were shown to belong to the Moshesh's Ford basalt type which does not outcrop *in situ* within the subsidence structure. This implies that the Moshesh's Ford basalts were emplaced prior to the formation of the lower volcaniclastic breccia, and may have acted as a "cap-rock" over the system, allowing pressure from the vaporised fluids, heated by intruding basalt, to build up. The Moshesh's Ford basalt type was erupted prior to the resultant phreatomagmatic events forming the lower volcaniclastic breccia.

ACKNOWLEDGEMENTS

I would like to express my thanks to my supervisors, Dr. Ian Skilling, Prof. Julian Marsh, and Dr. Octavian Catuneanu for their constant support and guidance throughout this study; both in the department and the field. I wish to thank Harilaos Tsikos for his helpful suggestions, and the rest of the students and staff of the Geology Department for their friendliness, encouragement and support during my career at Rhodes University.

I am grateful to the Foundation for Research Development for their financial assistance of this study.

Lastly I wish to thank my parents, friends and family for their encouragement, help and understanding in the last couple of years. I love you all, and appreciate all you have done for me.

CONTENTS

1.0 INTRODUCTION

The study area is a volcanic complex located approximately 35km north-east of Molteno, Eastern Cape, South Africa. The study concerns the phreatomagmatism which occurred between the deposition of the Stormberg Group and the emplacement of the Drakensberg Group flood basalts. The flood basalts are part of the Karoo Igneous Province (KIP).

Continental flood basalts (CFBs) represent one of the largest known volcanic episodes on earth (Mahoney and Coffin, 1997). One of the largest flood basalt provinces in the world is the Karoo Igneous Province (Marsh *et al.*, 1997; Bristow and Saggerson, 1983; Eales *et al.*, 1984).

In South Africa during the Ordovician the establishment of a deepening, latitudinal trough south of 21°S preceded the Karoo volcanism. The trough is located on an eroded basement of Pan-African medium-grade metamorphic rocks and intrusive granites (Eales *et al.*, 1984). Sediments which collectively constitute the Cape Supergroup accumulated in the trough. These sediments originated from the north and north-west. A hiatus separates these sediments from the overlying Karoo Supergroup (Figure 1), of which the uppermost formations, the Elliot and Clarens, had a wider distribution than the Molteno Formation. The Molteno Formation is restricted to the trough or Karoo basin, overstepping the basin to the north (Eales *et al.*, 1984). The supply of sediment to the southern part of the Karoo basin switched from the north for the Cape Supergroup to the south for the Karoo Supergroup.

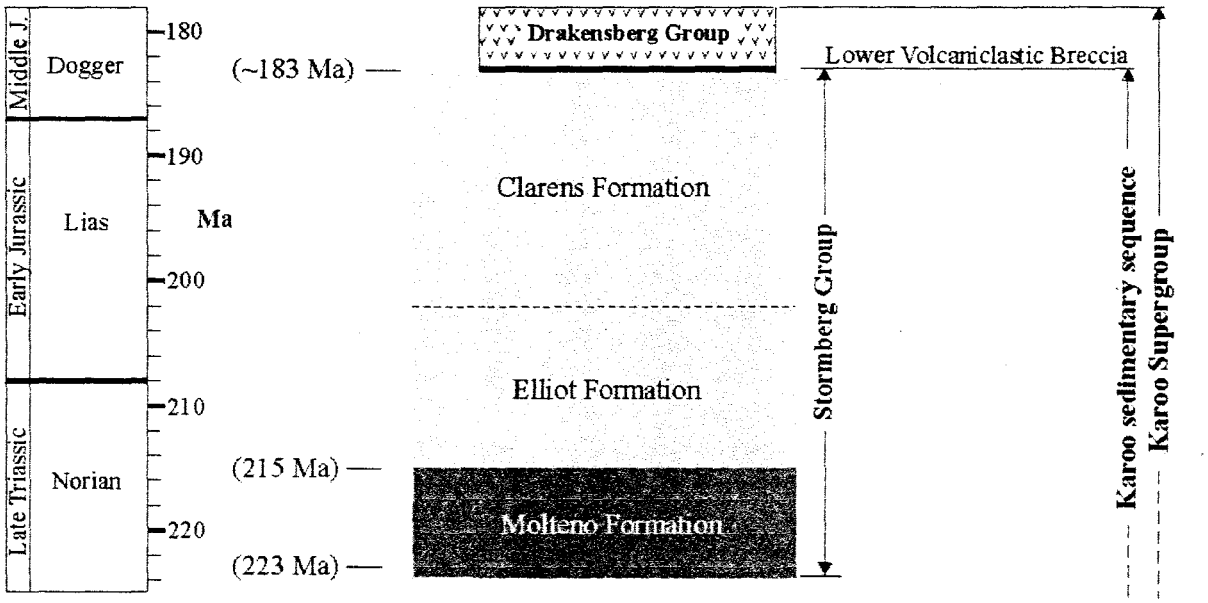

Figure 1: Stratigraphic column of the upper part of the Karoo Supergroup. The Elliot and Clarens formations of the Stormberg Group outcrop in the study area, along with the Drakensberg Group.

During the deposition of the final "Stormberg" sediments, the intruding magma associated with the emplacement of the Karoo flood basalts caused many phreatic (often forming sand-filled "diatreme" necks like Witkop to the north-east of the study area, and another Witkop between Dordrecht and Rossouw) and phreatomagmatic eruptions upon contact with the wet sediments near the surface. The eruptions occurred where the intruding magma came into contact with wet, unconsolidated sediment, and this level is estimated to have been near the base of the Clarens Formation (~ 60m below the palaeosurface) because the sedimentary clasts observed in the volcaniclastic breccias are predominantly Clarens Formation sandstone, rather than Elliot Formation sandstone and shale. Explosive vents formed, producing a large volume of volcaniclastic breccia which are preserved in two main areas: the Lesotho border - Barkly East area, and the Molteno - Jamestown area (Figure 3).

Following the initial phreatic and phreatomagmatic events, flood basalts were emplaced and occur as erosional remnants throughout southern Africa. The area covered by the volcanic remnants amounts to approximately 140,000km^2 (Bristow and Saggerson, 1983; Eales *et al.*, 1984; Marsh *et al.*, 1997), with outcrops occurring within an area extending from Zambia, Zimbabwe, Botswana, and southern Namibia, southwards through Lesotho, into the Eastern Cape Province (Figure 2). Marsh and Eales (1984) estimate the initial volume of the igneous rocks to be in excess of 1.5 x 10^6 km^3. These flood basalts represent the tholeiitic magmatism related to the early stages in the break-up of Gondwana and form what is referred to as the Karoo Igneous Province (KIP). The largest African remnant of the continental flood basalts extends from the Eastern Cape Province, through Lesotho, and into Natal (Figure 3).

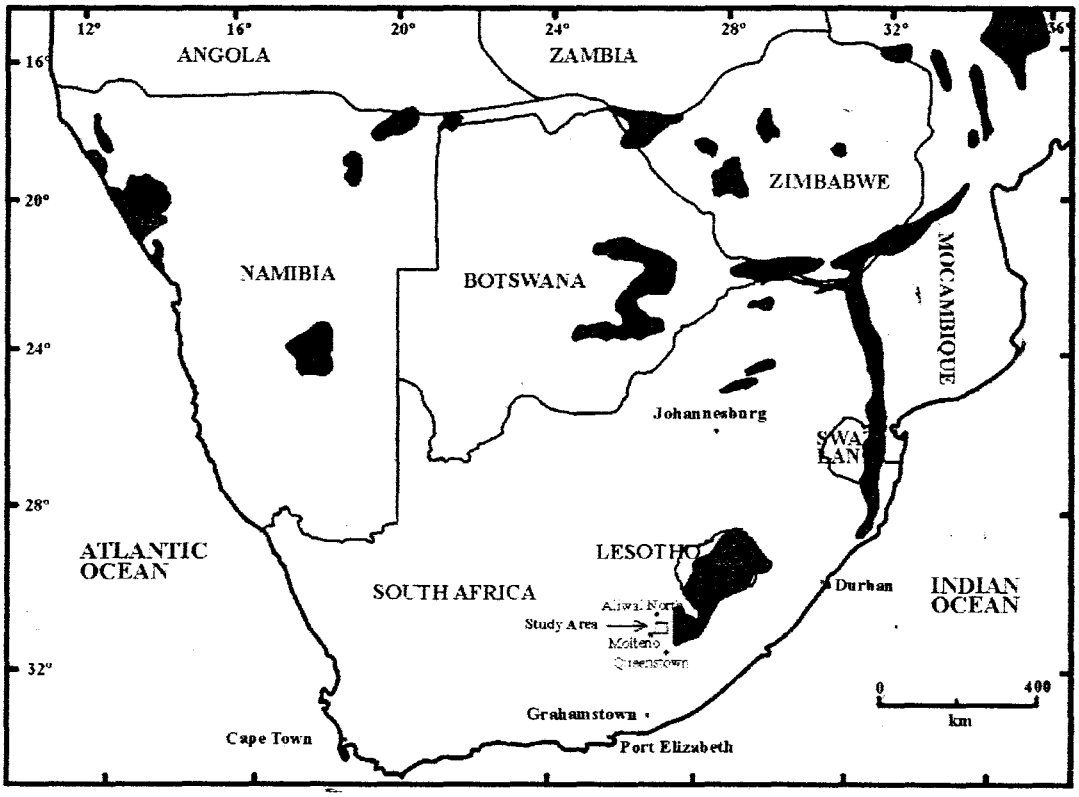

Figure 2: Generalised map showing the distribution of flood basalts and acid lavas in southern Africa and the location of the study area. After Bristow and Saggerson (1983), and Smith *et al.* (1993).

Similar volcanic rocks which occur in Antarctica and Australia as the Ferrar-Dufek Province correlate in age and composition with the Karoo rocks, and together with the Karoo volcanic rocks covered large areas of the Gondwanaland supercontinent (Duncan *et al.*, 1997). The volume of the combined Karoo-Ferrar-Dufek province is approximately 2.5 x 10^6 km^3, which makes it one of the largest continental flood basalt events (Duncan *et al.*, 1997).

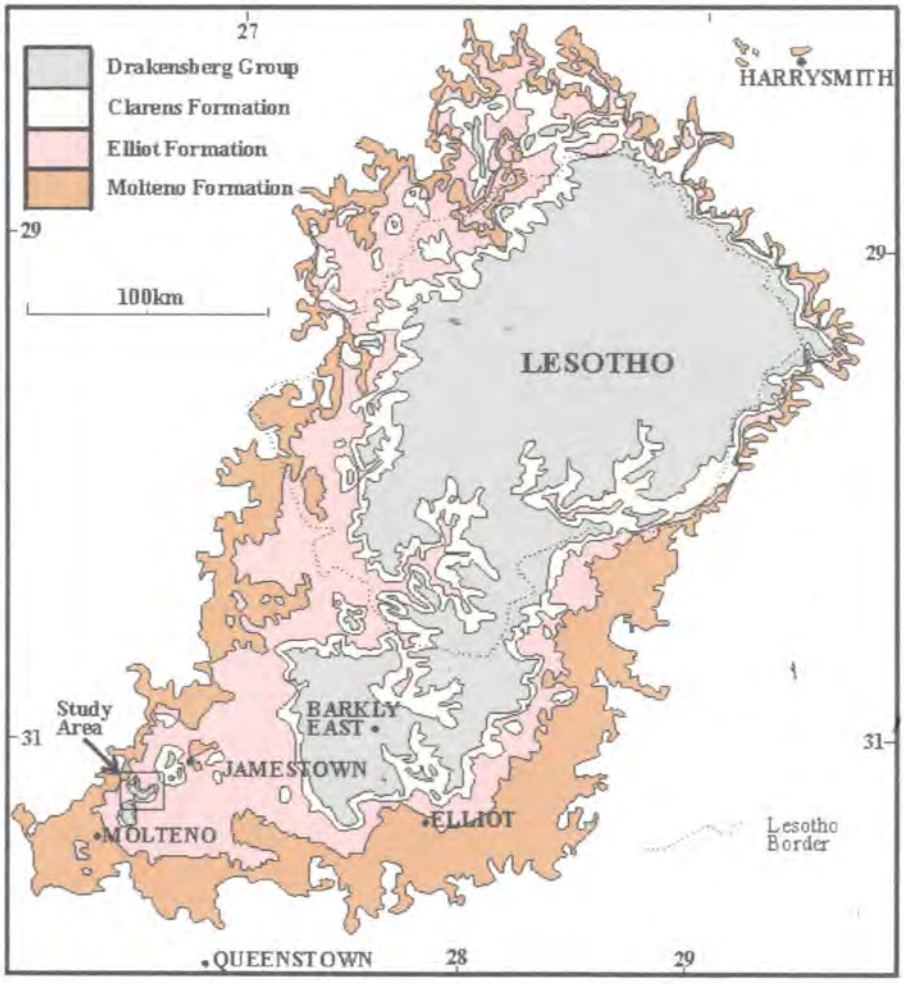

Figure 3: Location of study area, and distribution of the Drakensberg Group and the Molteno, Elliot and Clarens formations of the Stormberg Group in the main Karoo Basin. After Dingle *et al.* (1983).

Duncan *et al.* (1997), conducted ^{40}Ar - ^{39}Ar incremental heating experiments on feldspars and whole rock throughout the KIP, and concluded that the basal flows of the volcanic section in the Lesotho region were emplaced during the mid-Jurassic between 179 and 184 Ma. The majority of the flood basalt emplacement occurred at 183 ± 1Ma (Duncan *et al.*, 1997). The underlying volcaniclastic breccias that form the basis of this study are undated, but are probably of a similar age.

Hanson and Elliot (1996) have studied laharic breccia deposits from the Ferrar-Dufek province in Antarctica, which they describe as consisting of "accidental lithic fragments and sand grains from underlying strata, juvenile, vitric basaltic pyroclasts and minor amounts of dense basaltic lithic debris". These deposits are very similar in appearance, composition, age and structure to the breccia deposits encountered in the Karoo. The phreatomagmatic activity in Antarctica is inferred to have occurred in a groundwater-rich topographic basin linked to an evolving rift zone (Hanson and Elliot, 1996), and a similar environment is inferred for the phreatomagmatic activity occurring at the same time in southern Africa. These deposits are discussed in detail later in the text.

This research project is focussed on a roughly circular volcanic complex, approximately 270km^2 in area, which outcrops approximately 35km ENE of Molteno near Queenstown (Figures 3, and 4, and Map, Appendix B; Cross-sections in Appendix C and Figure 5). This complex was generated immediately prior to the onset of flood basalt volcanism. The structure is filled with volcaniclastic breccia that is associated with dolerite intrusions and erosional remnants of early flood basalts. The basalt flows occur in the area around the volcaniclastic breccias and partly cover them. The volcanic complex outcrops on the farms Noordhoek, Roodekloof, Strypoort,

Swartfontein, Streepfontein, Sterkfontein, Randfontein, Rooipoort, Roodehoek, and Brosterlea (Map, Appendix B) and is hereafter referred to as the Brosterlea Volcanic Complex.

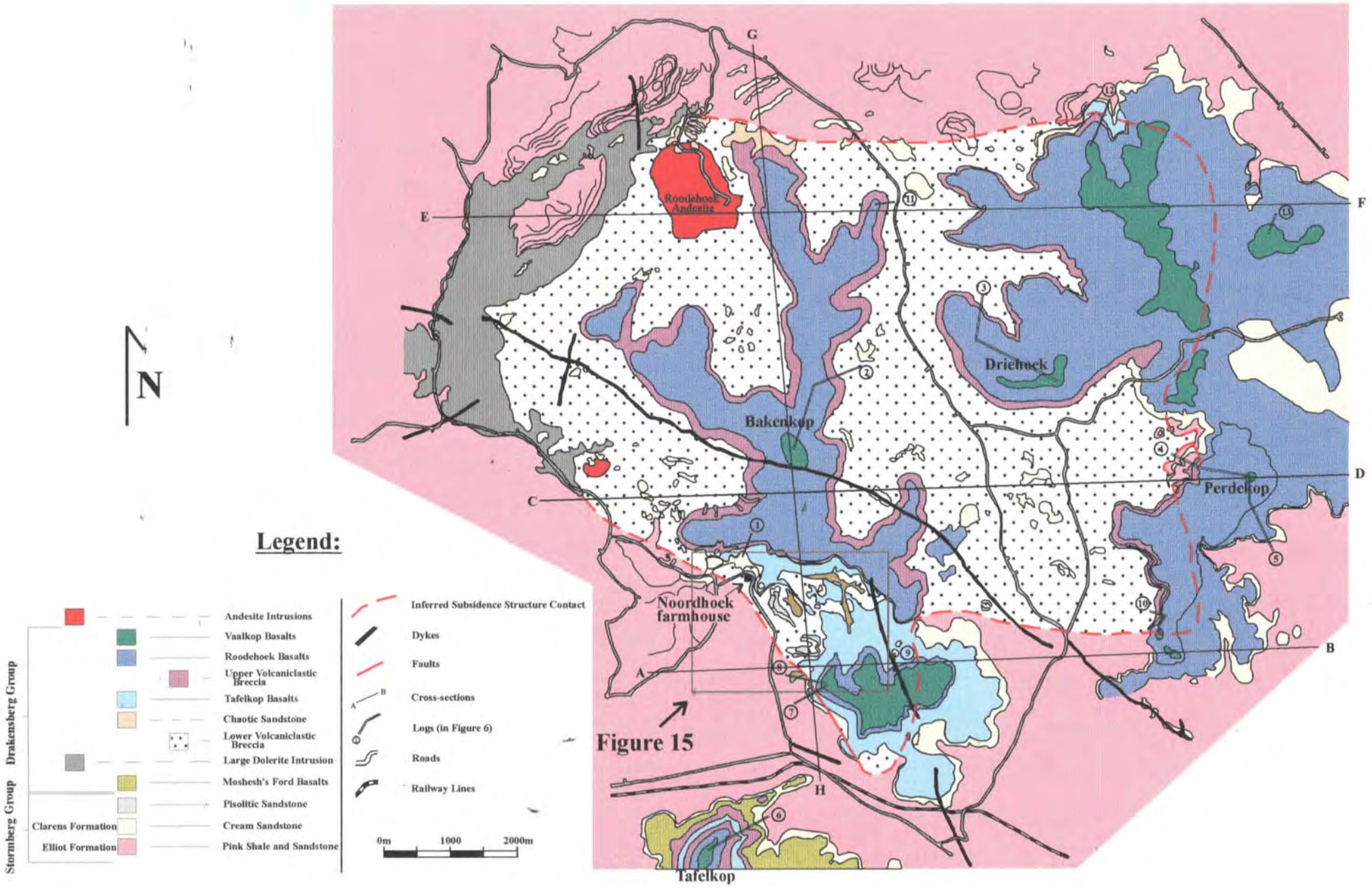

Figure 4: Geological map of study area with boundary of volcanic complex outlined in red. Positions of cross-sections, stratigraphic logs, and important sites, as well as names of main hill tops are included. Note that location of Figure 15 is also illustrated. This geological map is a smaller version of the Map (Appendix B).

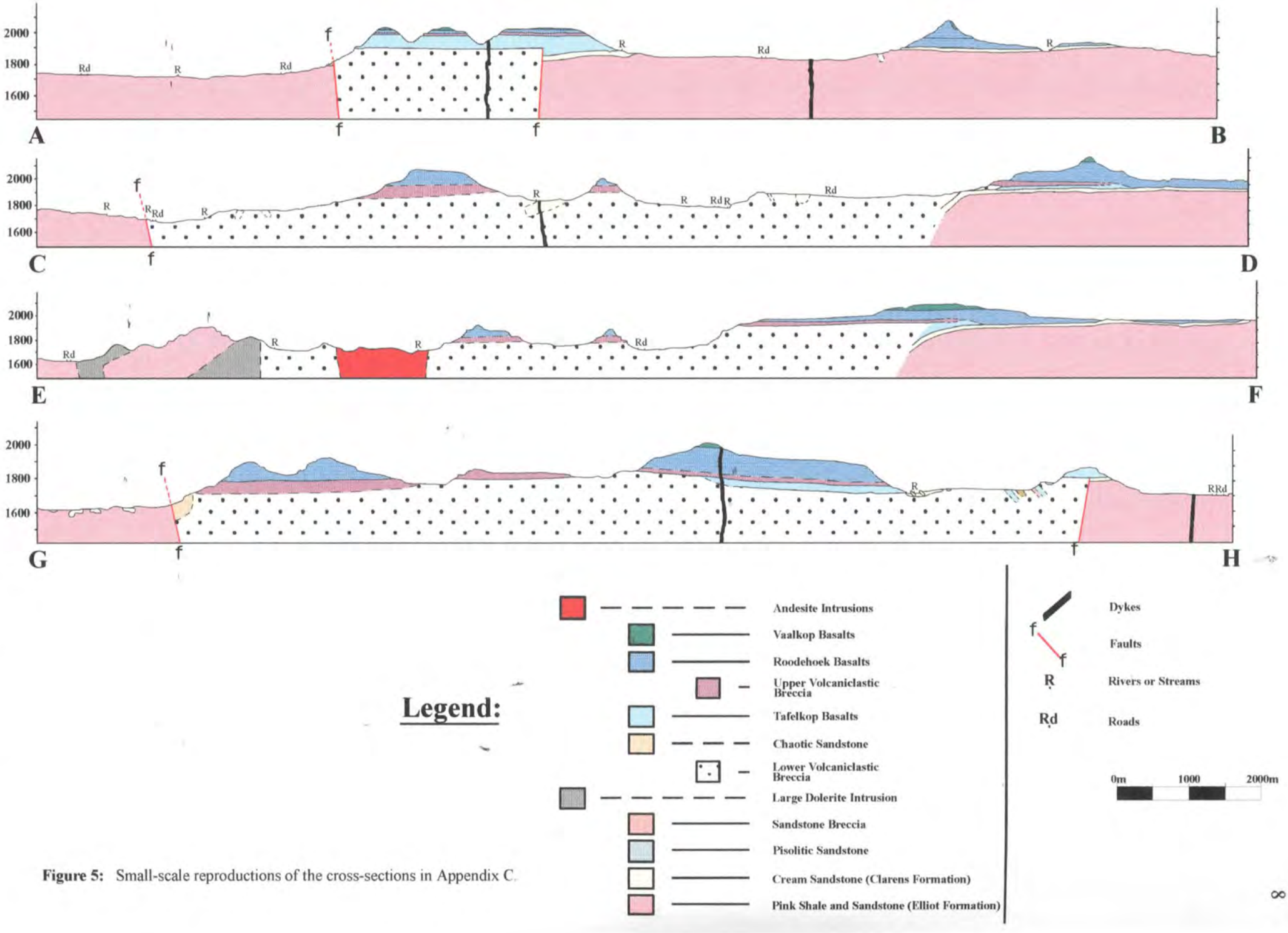

Figure 5: Small-scale reproductions of the cross-sections in Appendix C.

2.0 AIMS

The aim of this project is to provide detailed information on the origin of a large volcanic complex in the Eastern Cape province, and to describe the lithologies associated with it, particularly the volcaniclastic breccia filling the structure, and to discuss the palaeoenvironment. Eruption and emplacement mechanisms are also discussed.

This study involved detailed geological mapping of the complex and surrounding areas. Field studies were complemented by petrographical, geochemical, and statistical analyses. All data were integrated into a model for the origin of the complex. An important aspect of this study is that it has implications for the emplacement of volcaniclastic breccias erupted as precursors to flood basalts in the Ferrar Province, and possibly in other flood basalt provinces.

3.0 PREVIOUS WORK

Much work has been done on the Elliot and Clarens Formations, and the Karoo volcanics further north in the Barkly East area, Lesotho, and Natal, and comprehensive descriptions are available in many papers (eg. Rogers and du Toit, 1909; Du Toit, 1954; Mountain, 1960; Botha, 1968; Lock *et al.*, 1974; Visser *et al.*, 1980; Eriksson, 1981, 1984, 1985, 1986; Dingle *et al.*, 1983; Visser, 1984; Turner, 1986; Smith *et al.*, 1993; Eriksson *et al.*, 1994; Duncan *et al.*, 1997). Du Toit (1904, 1954) describes the breccias as agglomerates and pyroclastic rocks in the Belmore, Kelvin Grove, Broadford, and Glen Fillan central vent-type structures in the Barkly East district. Gevers (1927) described similar deposits from his work in the Dordrecht area, and at Tulloch in the Elliot district. Gevers (1927) and Mitchell (1980) describe volcaniclastic breccia material at Modderfontein and Zwartfontein in the Molteno-Jamestown district.

One large outcrop in the Molteno-Jamestown district has been associated with a collapsed caldera by Gevers (1927) and Mitchell (1980), who referred to it as the Brosterlea Caldera. This is the site of the present study area (Figures 3 and 4, and Map, Appendix B). A classic caldera contains ring faults, and forms through the collapse of the roof of the chamber (Walker, 1984). Field evidence in the study area suggests that the volcanic complex does not represent a classic caldera, but may represent a normal-faulted, partial downsagged "trapdoor" caldera. Few papers (eg. Gevers, 1928) include descriptions of the Brosterlea Volcanic Complex and the lithologies adjacent to it (eg. Rogers and du Toit, 1909). A textbook by du Toit (1954) also described the lithologies nearer the Brosterlea Volcanic Complex. Information from a number of unpublished Rhodes University Honours and Masters projects (eg. Rumble, 1979; Mitchell, 1980;

Masokwane, 1997; Makadzange, 1998) involving work conducted on areas within the present study area, as well as areas adjacent to the present study area (eg. Robey, 1973), has been incorporated into the present research. These Rhodes University authors have mapped different areas within the present study area, and Gevers (1928) has published a generalised map that includes the present study area. Papers on diatremes and maar craters (eg. Lorenz, 1973, 1986; White, 1990) provide detailed information on similar structures and deposits to those encountered in the Brosterlea Volcanic Complex.

4.0 METHODS

Field work comprised standard geological mapping using aerial photographs with tracing paper overlays, and topographic and geological maps. Contacts observed in the field were marked on the overlay, and a map at an appropriate scale was constructed from the overlays (Map, Appendix B). Lithology and various field descriptions were recorded, and structural readings of bedding and contact planes were taken at some outcrops, particularly large sandstone blocks within the lower-most volcaniclastic breccia in the Brosterlea Volcanic Complex. The blocks lie at non-horizontal attitudes. Analyses of clast type in the volcaniclastic breccias were conducted in an attempt to be able to correlate or separate the different outcrops of volcaniclastic breccia into separate flows. The understanding of the relationship of the different volcaniclastic breccias was aided by modal analyses of the breccias (Figures 58 - 61), cross-sections (Appendix C) and stratigraphic logs (eg. Figures 7and 8) through the area.

Stratigraphic Logs: The stratigraphic logs (Figures 6, 7 and 8) were measured to facilitate correlations of facies over the study area. Detail of units and internal structure in vertical sections was recorded using an altimeter for greater accuracy. These data cannot be represented adequately on a geological map. The units in the logs do not always correlate laterally, due to thinning, thickening and pinching out of basalt units through the study area. An exception is the basalt capping on top of the sequences which can be correlated laterally throughout the volcanic complex. The scaling of the logs is in metres and represents altitude above sea level.

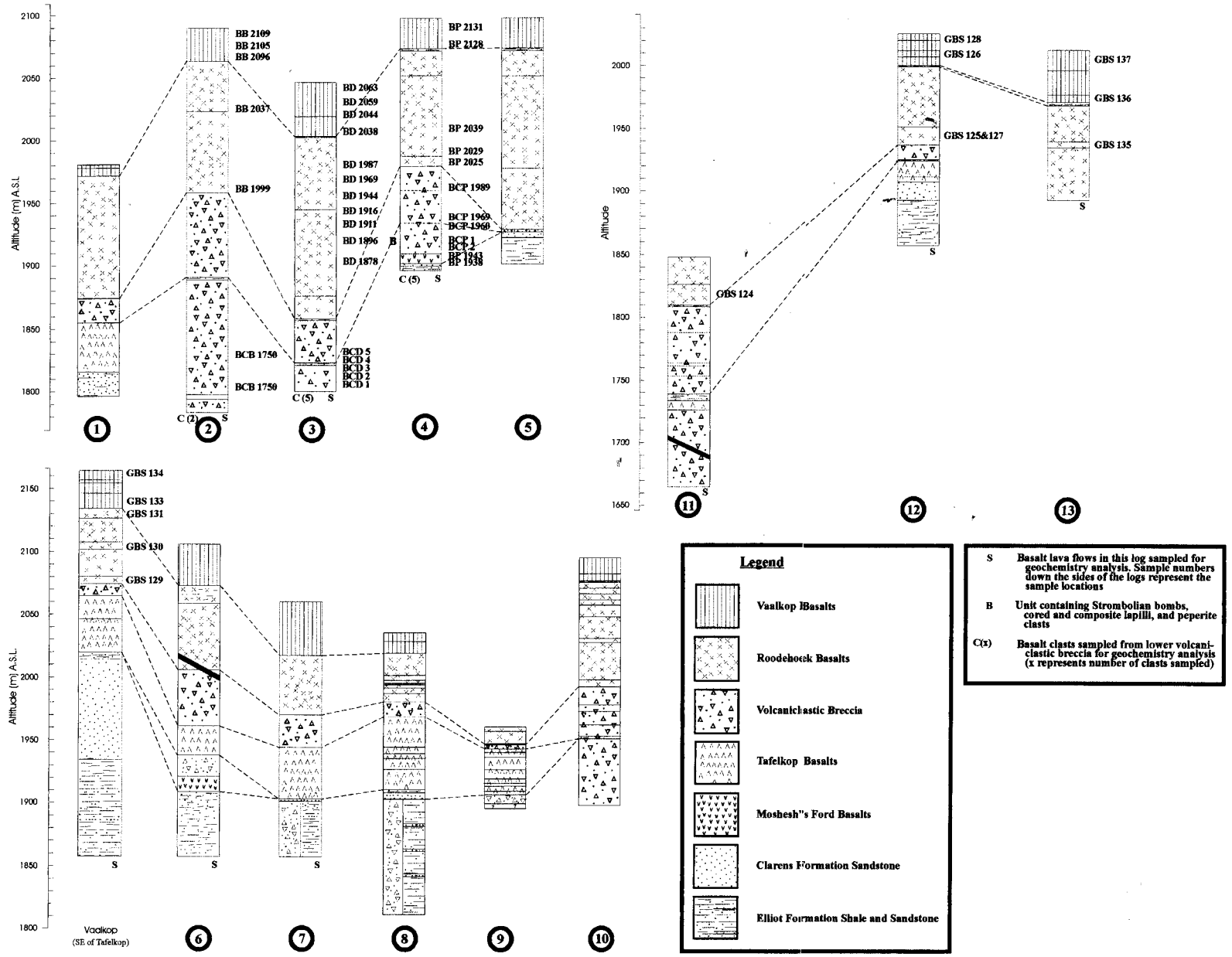

Figure 6: Main stratigraphic logs constructed through the study area. Logs are correlated using a number of thinly-laminated, muddy sandstone (lacustrine) units, and geochemistry analyses conducted on the flood basalt packages. Flood basalts and basalt clasts in the volcaniclastic breccias sampled for geochemical study are marked. Letters and numbers next to logs are sample numbers and represent the locations that the samples were taken from (see Appendix A). Logs are arranged in similar positions to geographical positions of log sites in the field from north to south and west to east. Altitude is in meters above sea level (MASL). Logs 6 and 7 are from Marsh and Skilling (1998).

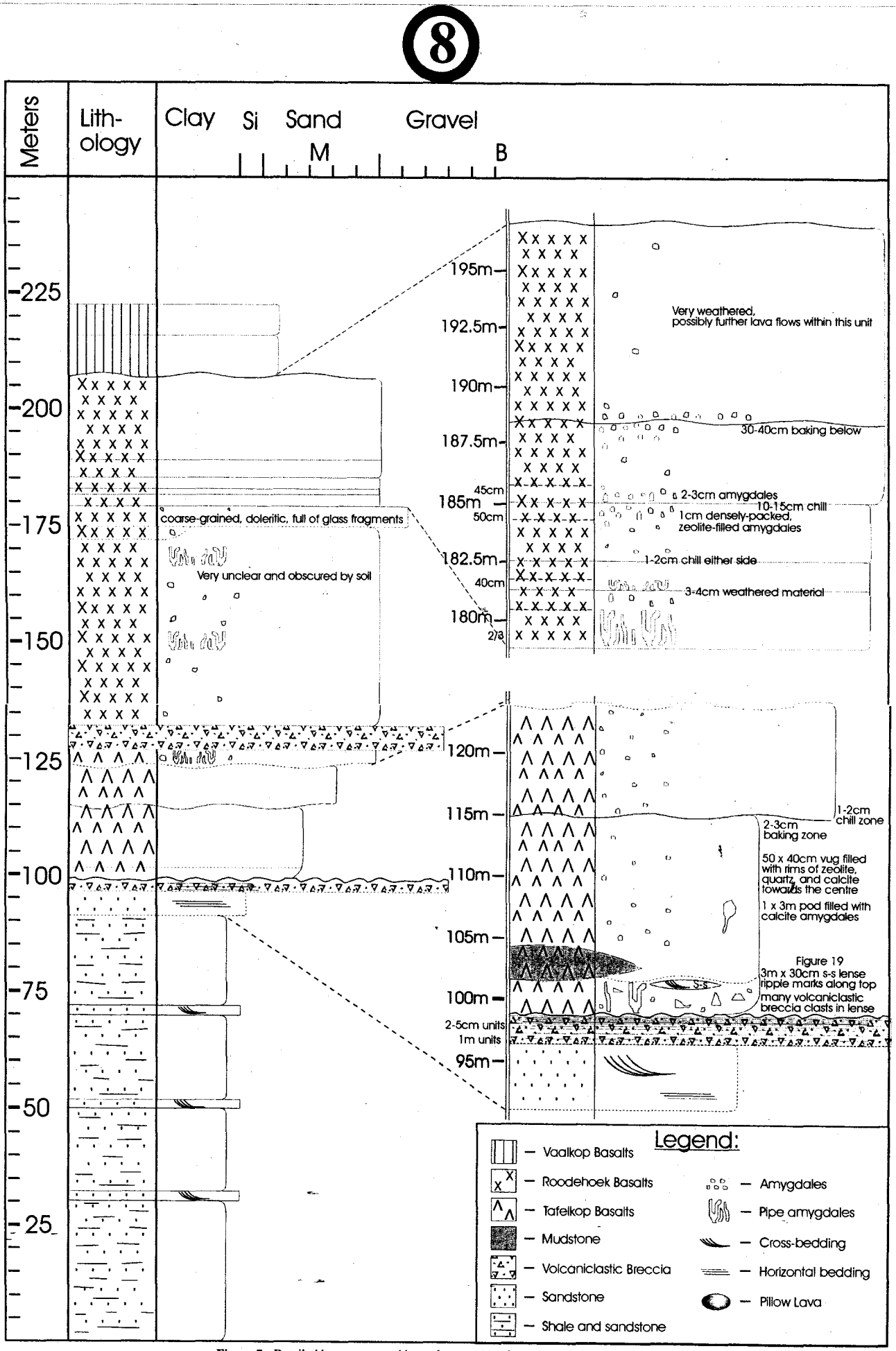

Figure 7: Detailed log constructed in study area. Number at top refers to log number on geological map (Map, Appendix B and Figure 4).

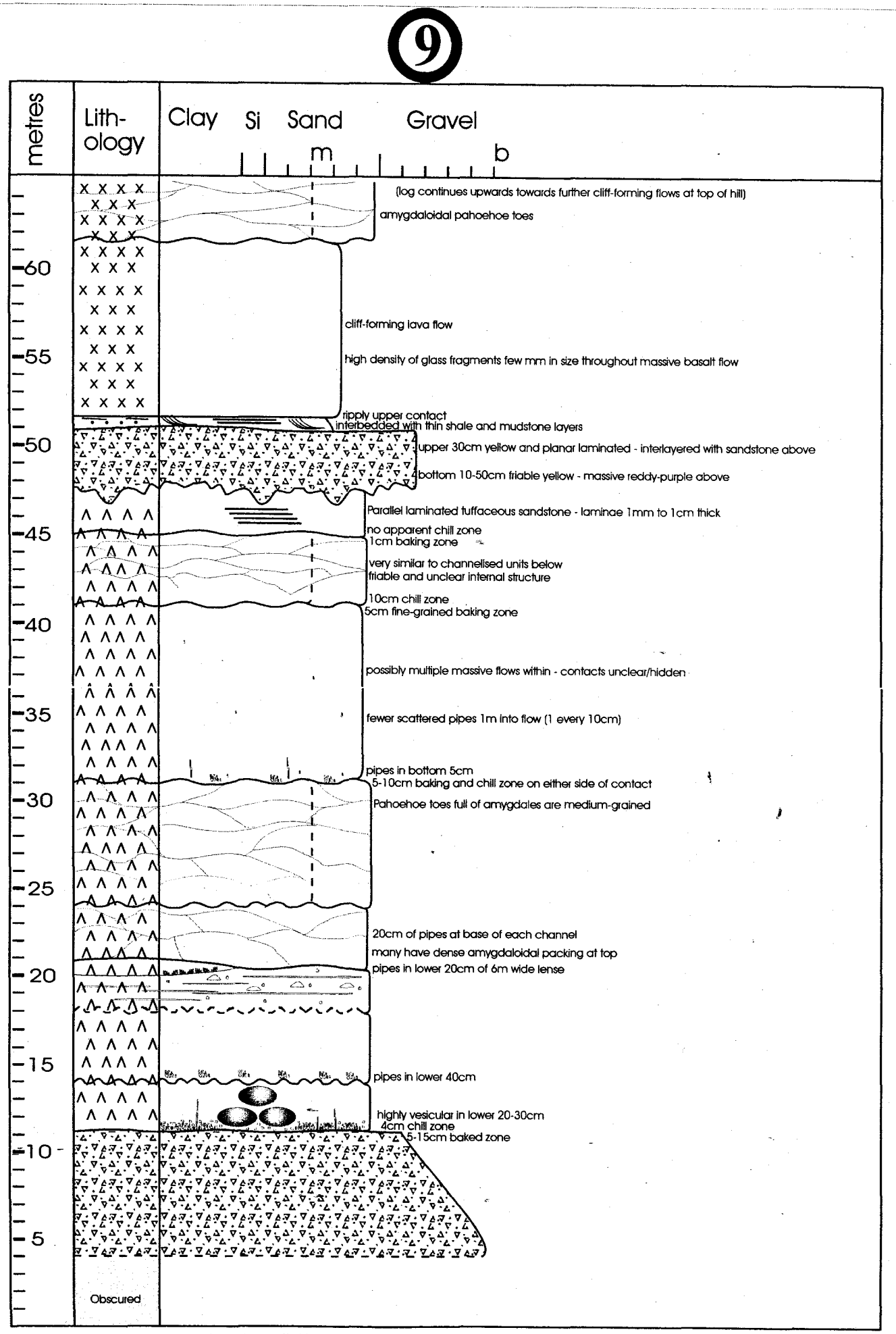

Figure 8: Detailed log constructed in study area. Number at top refers to log number on Map (Appendix B) and Figure 1. Key to symbols on Log 8 (Figure 7).

Modal Analyses: Analyses of clast type and distribution in the volcaniclastic breccias were conducted to aid in characterisation, classification and correlation of the breccias. At each site a 1x1m area was divided into 20x20cm grid blocks (Figure 9). The a- and c-axes of the exposed surfaces of clasts were measured and the clasts were grouped according to their lithology. Assuming an elliptical clast shape, the area occupied by each lithology in the 20x20cm grid, and thus the total area covered in the 1x1m grid, could be calculated.

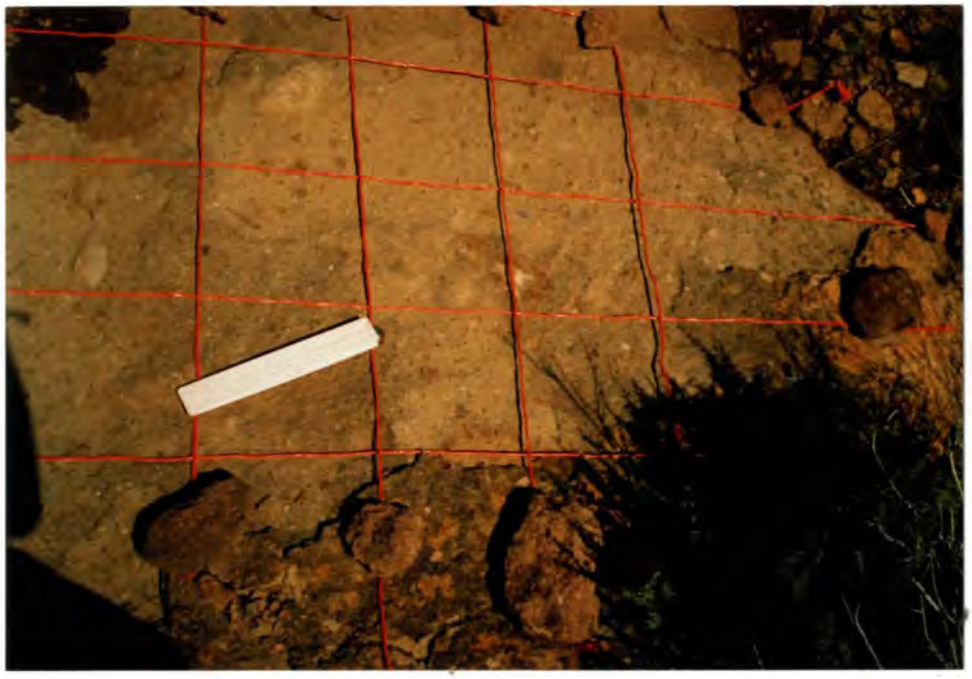

Figure 9: Photograph of a 20cm x 20cm grid constructed for the modal analyses of the volcaniclastic breccias.

Particularly large clasts (~ over 0.5m) were avoided when positioning the grid so as not to cover a large part of the grid which would result in a much smaller sampling of the clasts in the unit. To keep the grid analyses accurate, all clasts below 5mm were similarly ignored. This helped eliminate many tiny clast fragments that would have been difficult to identify and measure accurately, and would have introduced an element of error. The larger clasts (>0.5m) were noted

and described in the field description of the different lithologies and units, and the smaller clasts and clast fragments (<5mm) were observed on a far more detailed level in thin-section study. This reduced any bias towards breccia outcrops with fewer large clasts compared to breccia outcrops with many large clasts.

Cross-Sections: Much of the present study area is covered by flood basalt, and the underlying geology is obscured. Cross-sections were constructed using an altimeter and outcrops were correlated to provide a projected view of the geology below the cover of lava flows. The accuracy of the cross-sections drawn decreases towards the east where important detail may be hidden below the flood basalts. Thus, the cross-sections only provide a simplistic view of the structure of the complex. The contour interval on the topographical maps is large (20m) and so an accurate topography was not possible. Sketches drawn of contacts and outcrops in the field helped to improve the accuracy of contact positions and topography.

Geochemistry: The existence of a geochemical stratigraphy in the Karoo basalt sequence has been demonstrated by Pemberton (1978), Marsh and Eales (1984), and Marsh *et al.* (1997). Geochemical data from basalt samples taken from several sections through the regional volcanic sequence were plotted and compared to graphs produced by Mitchell (1980), Masokwane (1997), and Makadzange (1998). The geochemical fields defined by Mitchell (1980) were used to separate basalt flows into the magma types Vaalkop, Roodehoek, Tafelkop, and Moshesh's Ford (Figure 6).

Basalt clasts from the volcaniclastic breccias in the Brosterlea Volcanic Complex were also analysed. Their composition can give insight into their source area and can help to identify

which basalt types were present at the time of the formation and emplacement of the breccias, and which were emplaced afterwards. Basalt clasts were sampled from the volcaniclastic breccias at Perdekop, Bakenkop and Driehoek (Figure 4 and Map, Appendix B).

5.0 FIELD RELATIONSHIPS

The stratigraphy in the study area is shown in Figure 1. Only the Elliot and Clarens formations of the "Stormberg Group" outcrop in the study area. The term "Stormberg Group" is an informal but widely used name, grouping the Molteno, Elliot, and Clarens formations together. According to the South African Committee of Stratigraphy (SACS, 1980), there is no formal grouping of these formations. However, for ease of reference the term shall be used in this study. The Molteno Formation and the overlying Elliot Formation are both of fluvial origin. They contain mudstones and shales and fine-grained sandstones. The Molteno Formation also contains a number of coal-bearing units that were mined in the early- to mid-1900's.

The Elliot Formation was originally referred to as the "Red Beds" owing to the characteristic purple-red colour of the sediment. As well as the purple-red mudstones, shales and fine-grained sandstones, thick beds of yellow and white, fine-grained, feldspathic sandstones are very common in places (Rogers and Du Toit, 1909; Botha, 1968; Eriksson, 1984, 1985) where the red colour is not as clear as in others. The Clarens Formation comprises varying thicknesses of pale yellow, fine-grained, feldspathic, aeolian sandstones that form resistant cliff outcrops (Du Toit, 1954; Eriksson, 1981, 1986; Eriksson *et al.*, 1994). In the study area the Clarens and Elliot formations are horizontally-bedded, but begin to dip towards the volcanic complex from approximately 1km away (Figure 10). The Map (Appendix B) displays the dips of many of the sandstone units. The dipping sandstone is most noticeable along the northern and western edge of the volcanic complex where extensive units of yellow sandstone within the Elliot Formation are evident. The Elliot and Clarens formations within the volcanic complex have been tilted and fragmented, and

outcrop as megablocks (blocks between 20 and 300m in length) in the volcaniclastic breccia. This is most noticeable along the southwestern margin of the volcanic complex where one sandstone blocks over 250m in length dips into, and another, similar-sized block dips out of, the complex. The blocks are inferred to have collapsed into the complex either towards the end of, or immediately after the emplacement of the lower volcaniclastic breccia, due to their position in the breccia. Most of the blocks dip towards the centre of the volcanic complex, displaying simple tilting while those which dip away from the centre of the complex display an element of rotation in the horizontal plane during the tilting so that the edge of the block furthest from the centre of the complex tilted lower than the edge nearest the centre of the complex. The Map (Appendix B) shows the tilted nature of these blocks in the southwestern corner of the structure.

The volcanic lithologies in the study area can be divided into two main groups; an upper, horizontally-bedded sequence of lava flows and interbedded volcaniclastic breccias forming the regional flood basalt succession, and an underlying, topographically-controlled volcaniclastic breccia and sequence of basalts. The lowest breccia, termed the lower volcaniclastic breccia, is restricted to the volcanic complex, and its formation may be related to the formation of the volcanic complex. The horizontal basalts post-date most of the volcaniclastic breccia-forming eruptions, except for one volcaniclastic breccia unit interbedded with the flood basalts in the volcanic complex and a second one which outcrops on Tafelkop to the south, but not in the volcanic complex. The horizontally-bedded, interbedded volcaniclastic breccia in the volcanic complex is referred to as the upper volcaniclastic breccia. These relationships are illustrated in Figure 6 (particularly Log 6 from Tafelkop, and Log 7 from Noordhoek to the north of Tafelkop). Although unrelated to the volcanic complex which was formed before their emplacement, the two horizontally-bedded volcaniclastic breccias presumably came from similar complexes

outside the study area, that postdate the Brosterlea Volcanic Complex. Detailed analysis of the horizontally-bedded breccia outside the volcanic complex was not conducted, although it is discussed by Masokwane (1997). The sedimentary lithologies and a few basalt flows were emplaced prior to the eruptions which formed the lower volcaniclastic breccia, and have been fractured and fragmented by those eruptions.

Geochemical analyses on the basalts have allowed individual flows to be grouped into units of similar geochemical characteristics. These units are shown in Figures 6 and 12 as the Vaalkop, Roodehoek, Tafelkop, and Moshesh's Ford Basalts, which are the names used in the literature (eg. Mitchell, 1980; Masokwane, 1997; Makadzange, 1998) to describe these magma types. Mitchell (1980) was the first author to use these names for the basalt units encountered in the present study area.

Faulting is evident along the northwestern boundary of the study area and although partly obscured, appears to extend down the western border to the southwest. The fault is downthrown to the east, forming a depression, and it is inferred that the lower volcaniclastic breccia ponded in the volcanic complex. The sandstone units in the Elliot Formation around the northern and western edge of the structure appear to dip under the lower volcaniclastic breccia (Figure 10 a and b). Dips of sandstone units are marked on the Map (Appendix B).

Figure 10 (a)

Figure 10, a and b: Tilted sandstone units in the Elliot Formation along the northern edge of the volcanic complex. Sandstone units appear to dip south towards and under the lower volcaniclastic breccia. The dips of the sandstone units decrease away from the edge of the volcanic complex and the units are horizontal within 1km from the lower volcaniclastic breccia. Photographs were taken from the northwest corner of the study area, Figure 10a looking east, and Figure 10b looking north.

The Clarens Formation outcrops at a higher elevation (2070m) just north of the northernmost extent of the lower volcaniclastic breccia than to the west and south (1840m) of the breccia. Clearly some sagging and/or faulting has occurred along the northern edge of the study area as the Clarens Formation to the south is at least 230m lower than to the north. This is inferred to be due to the downthrow of the fault, outcropping between the lower volcaniclastic breccia in the north of the volcanic complex, and the Clarens Formation outcropping at 2070m A.S.L..

6.0 VOLCANIC COMPLEX

The volcaniclastic breccia-filled volcanic complex is roughly circular and exhibits a variety of structural relationships with its wall rocks. To the west and northwest the lower volcaniclastic breccia within the volcanic complex lies in direct contact with a dolerite sheet. No mixing between the two lithologies is observed, and the breccia does not outcrop west of the dolerite, suggesting the dolerite marks the western boundary of the complex. Along the southwestern margin the lower volcaniclastic breccia has a steep contact against strata of the Clarens and Elliot formations (Figure 11). These steep contacts are interpreted as fault scarps. The lower volcaniclastic breccia thins towards the east, and only a very thin (~1m) outcrop of breccia is present along the eastern edge of the Perdekop hill. No faulting is apparent along the eastern boundary of the volcanic complex, although some may exist below the horizontally-bedded basalt flows.

Figure 12 contains a group of stratigraphic logs which have been correlated using a single thinly-laminated, muddy sandstone unit used as a datum line. The datum line defines a palaeotopographic surface which was at a common altitude for all logs during the deposition of the muddy sandstone. Thus the relative, post-depositional movement of these sections of the volcanic complex with respect to each other, can be compared. Figures 7 and 8 are examples of the detailed logs constructed throughout the present study area.

Figure 11: South-western wall of the volcanic complex on the farm Noordhoek. The wall is defined by the contact between the lower volcaniclastic breccia and the Elliot and Clarens Formation strata. This is the only clear exposure of the fault scarp along the western margin of the volcanic complex.

Outcrops along the south-western fault scarp clearly display the relationship between the lower volcaniclastic breccia and the Elliot and Clarens Formation host lithologies. Although the presence of heavy shearing and/or fault gangue is not evident along the boundary of the volcanic complex, evidence for the existence of a fault scarp around the western boundary of the structure is recognised in the steep and planar contact between the Clarens and Elliot formations and the lower volcaniclastic breccia in the south-west (Figure 11 and 13). Along the plane of contact is a 1.5 x 0.5m block of Elliot sandstone which has slumped downwards presumably during the formation of the contact, and lies directly along the contact plane (Figure 14). The offset in altitude of the Clarens Formation on either side of the dolerite sheet in the northwest, as described above, provides further evidence for the existence of a fault scarp.

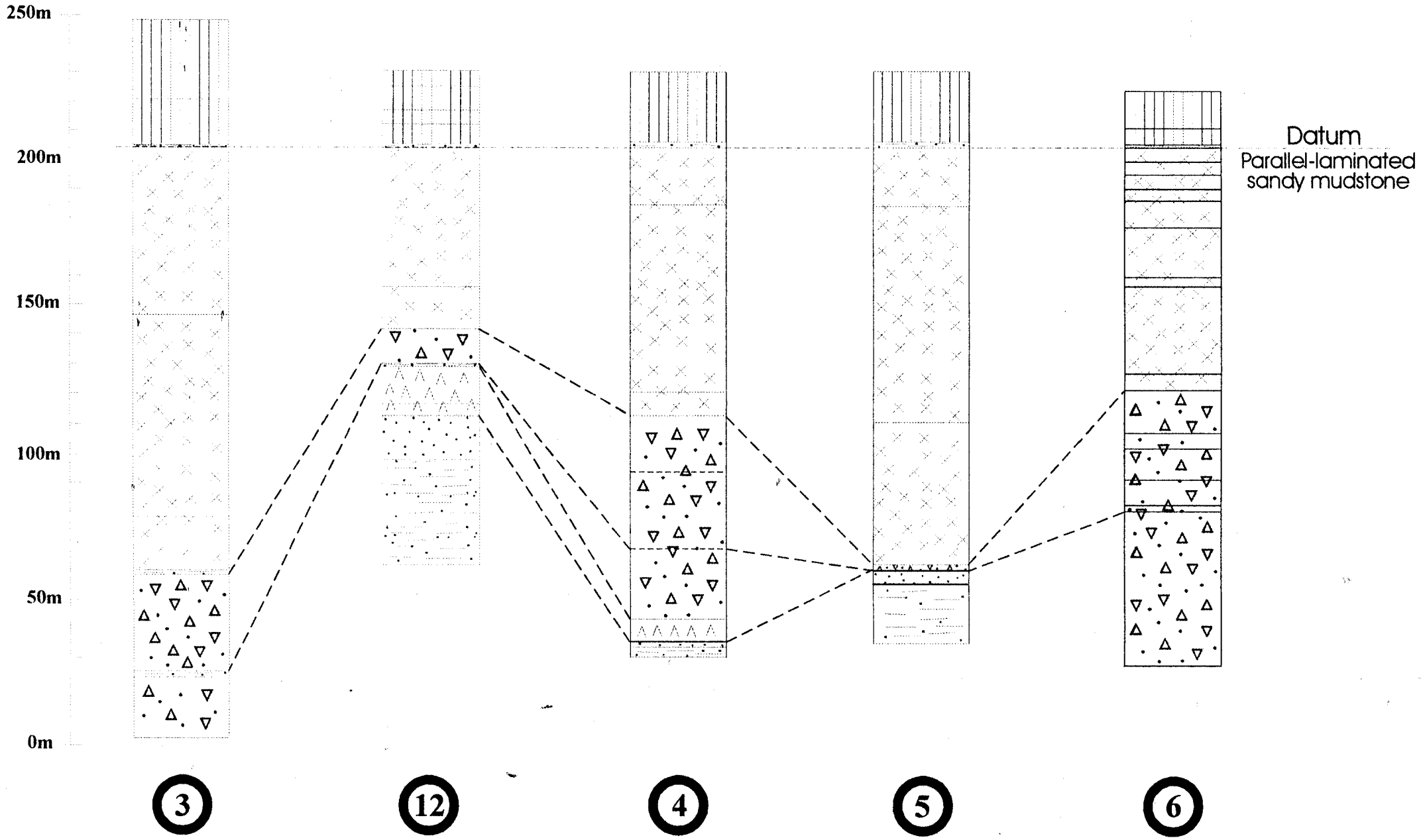

Figure 12: Stratigraphic logs with a common parallel-laminated sandy mudstone unit, inferred to have formed from a lacustrine environment, used as a datum to visualise relative post-emplacement, vertical movement of different parts of the study area. Log numbers correlate to numbers on the geological map (Appendix B).

Figure 13: A view of the fault scarp in the south-west of the study area viewed from the north. Note the angle of dip of the contact towards the east, into the volcanic complex. The volcaniclastic breccia outcrops to the left (east) of the contact, and the Elliot and Clarens formations outcrop to the west of the contact. Trees in centre of photograph are approximately 20m high. Scale bar on the side represents 200m.

Figure 14: Detail of contact shown in Figure 13. The sandstone block (3m x 0.5m) has slumped from its original horizontal position and now lies along the contact plane of the lower volcaniclastic breccia and the Elliot Formation.

In addition to the dolerite intrusion along the western boundary, a number of dolerite dykes are exposed throughout the study area. These are clearly younger than the volcaniclastic material as they intrude the deposits within the volcanic complex and also the surrounding host lithologies. Dykes also intrude the lowermost flood basalt units and the upper volcaniclastic breccia.

Overlying the lower volcaniclastic and Clarens Formation deposits is a sequence of basalt lava flows, now preserved as remnant plateau, forming high peaks and ridges. A number of basalt flows, and one interbedded volcaniclastic breccia appear to pinch out in a northern direction from Tafelkop (Figure 6, Logs 6-7). Flows are missing across the road on the Noordhoek slope and there appear to be more missing flows on the hill to the north of the Noordhoek farmhouse. To the north of this area the basalt between the volcaniclastic breccias disappears completely and the upper volcaniclastic breccia lies directly above the lower volcaniclastic breccia. Towards Bakenkop, Perdekop and the two hills south of Perdekop the breccias are separated in places by a 1m thick lacustrine deposit of thinly laminated, muddy sandstone.

7.0 LITHOLOGY

Detailed descriptions of the lithologies (Figure 1) outcropping in the study area are presented below. Only the Elliot and Clarens formations of the "Stormberg Group" outcrop in the study area. The Molteno Formation only outcrops 10-15km to the south of the volcanic complex, and so a detailed description is not included here.

7.1 LITHOLOGY OF ELLIOT FORMATION

The Elliot Formation has an estimated maximum thickness of about 500m in the Eastern Cape (Visser, 1984; Eriksson, 1985), and contains Norian/Rhaetian fossil fauna, as well as Jurassic dinosaur bone. The palaeocurrent direction is mainly towards the north, northwest and west (Visser and Botha, 1980; Tankard *et al.*, 1982).

The Elliot Formation lies disconformably over the Molteno Formation, and the boundary marks a time period during which a change in the palaeoenvironment occurred so that the deposits of the Elliot Formation display a reduction in fluvial energy and proportion of bedload from the underlying Molteno Formation.

The Elliot Formation consists of shales and mudstones with interbedded fine-grained sandstone units. The shales and mudstones are characteristically structureless (Eriksson, 1985), particularly towards the top of the sequence, and purple-red in colour (Rogers and Du Toit, 1909; Du Toit, 1954; Botha, 1968; Visser and Botha, 1980; Tankard *et al.*, 1982). The red colour of the finer-

grained sediment is due to finely-divided haematitic mineralisation (Botha, 1968; Visser and Botha, 1980). Tabular to lenticular bodies of yellow and white fine- to medium-grained, channel-fill feldspathic sandstones are interbedded with the red beds (Rogers and Du Toit, 1909; Botha, 1968; Visser and Botha, 1980; Tankard *et al.*, 1982). The sandstone channels or lenses contain planar and trough cross-bedding (Eriksson, 1985). The increase in feldspar upwards within the Elliot Formation sandstones may reflect the increased aridity of their depositional environment (Visser and Botha, 1980; Visser, 1984; Turner, 1986; Smith *et al.*, 1993).

The descriptions of the characteristics of the Elliot Formation above apply equally to the area around the Brosterlea Volcanic Complex. Only the upper part of the Elliot Formation outcrops in the study area, so very little variation in the formation is actually observed.

7.2 Lithology of Clarens Formation

The Clarens Formation in the Stormberg-Lesotho region outcrops in a curved north-south-trending belt from the Eastern Cape, through Lesotho, to Natal. It is varies around 100m thick (du Toit, 1954). In few areas the contact between the Elliot Formation and the Clarens Formation appears abrupt, planar and clear, but this is not a common characteristic. Du Toit (1954) and Beukes (1970) note that although the contact between the Elliot Formation and the Clarens Formation is usually abrupt at any locality (within a few metres), the overall, gradational nature of this facies change, both laterally and vertically, means that it is almost certainly an "irregularly diachronous junction on a regional scale" (Dingle *et al.*, 1983). The facies change is described as either thick beds of creamy white to yellow sandstone appearing at the top of the Elliot Formation, or laminated, fine-grained, red sandstone appearing at the base of the Clarens

Formation. According to SACS (1980), the descriptions of distinguishing features and boundaries have not changed since du Toit's description (1954). Eriksson (1981) described a general gradational contact between the Elliot and the Clarens Formations, and suggested that it represents a gradual environmental change from fluvial to aeolian.

In the study area, just outside the volcanic complex, the contact between the Elliot and Clarens formations is gradational and unclear. The pink-coloured sandstones and shales of the Elliot Formation and ~1m thick units of yellow, fine-grained sandstone of the Clarens Formation are interbedded with each other over at least 5m in the southern part of the study area. On Tafelkop in the south of the study area the contact appears to be sharper, and the Clarens sandstone unit is thicker (up to 80m). The contact between the Clarens Formation and the Drakensberg lava flows is sharp. Occasional lenses of sandstone within the basalt sequence indicate that sandstone deposition persisted after the start of the volcanics.

In the study area (see Figure 15), the Clarens sandstones resemble descriptions by Rogers and Du Toit (1909), Du Toit (1954), Eriksson (1981; 1986), Smith *et al.* (1993), and Eriksson *et al.* (1994). The sandstones are, on the whole, light yellowish-brown (locally reddy-pink), massive, fine- to medium-grained, poorly-sorted, quartz-rich, feldspathic wackes, commonly containing calcareous concretions and cement. In Kwazulu-Natal where the Clarens Formation is thickest, Eriksson *et al.* (1994) describe an upward increase in the clay and feldspar content suggesting an increasingly immature character. This was not observed in the present study area. Where in contact with basalt, the baked sandstones have a pale blue colour, and in one outcrop adjacent to the stream north-east of sites ***d*** and ***e*** (Figure 16) flame structures along the sandstone - basalt

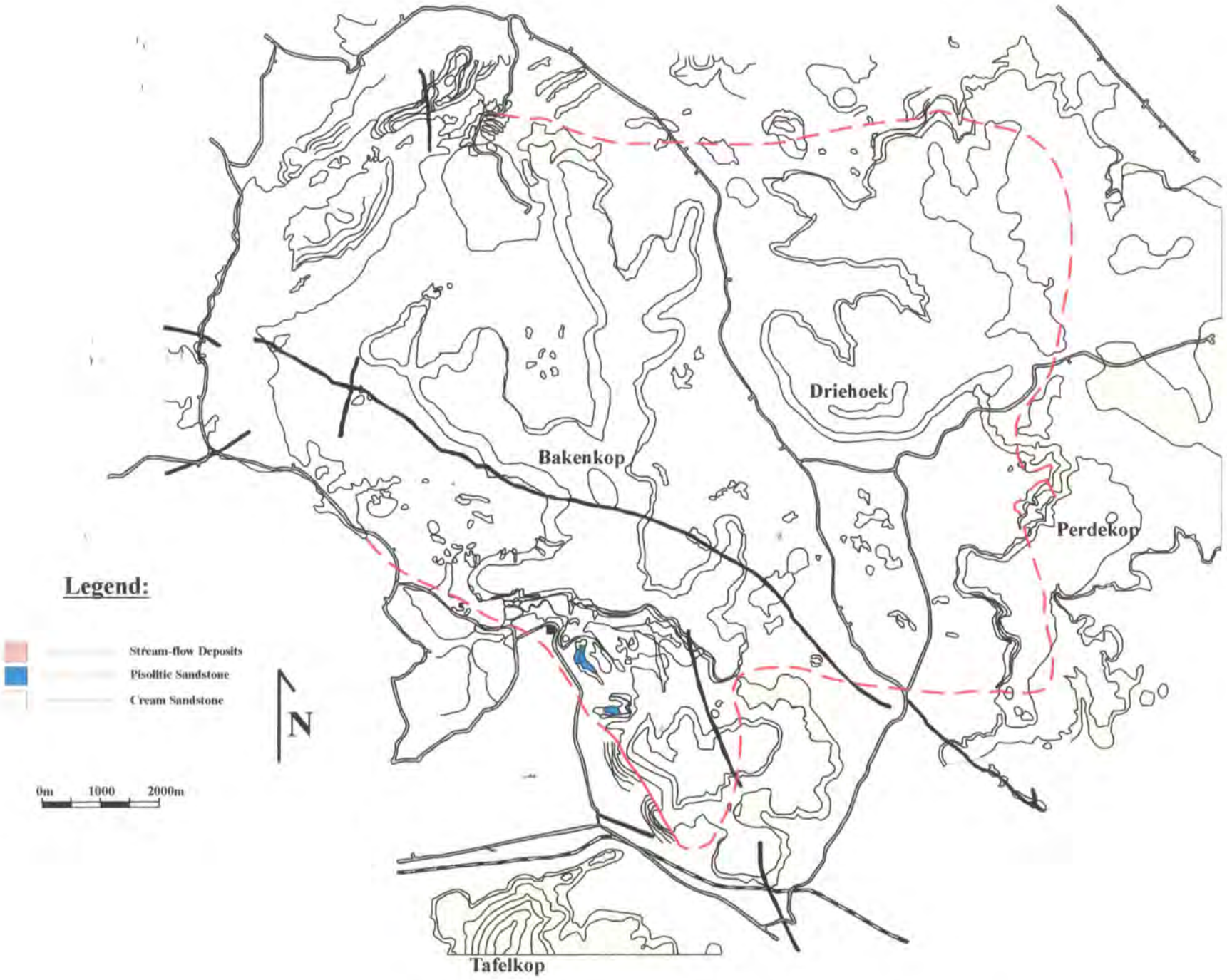

Figure 15: Map of study area with boundary of volcanic complex outlined in red. The areas filled in with solid yellow define the outcrops of Clarens Formation sandstone.

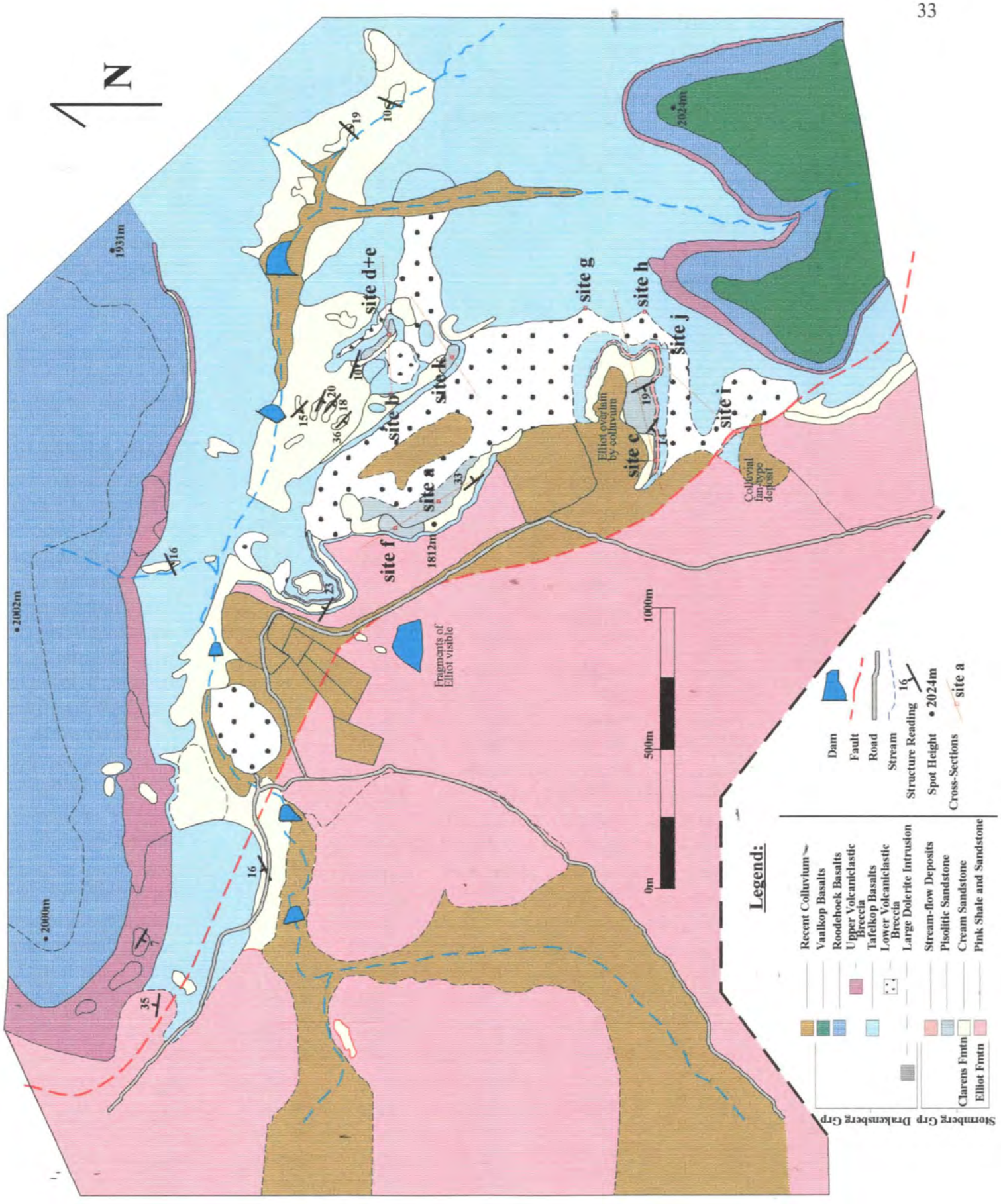

Figure 16: Geological map of the southwestern area of the volcanic complex. The boundary of the volcanic complex is outlined in red. This area is delineated in Figure 4.

contact (Figure 17) are evident where unconsolidated, wet sand has been forced up into fractures in the overlying basalt.

Although the sandstones are predominantly comprised of quartz and feldspar grains, very fine-grained, argillaceous material is also present in varying quantities. Thin sections of rocks from the study area reveal the presence of tourmaline, zircon, hornblende, sphene and white mica in accessory amounts. Rogers and Du Toit (1909), Eriksson (1981, 1986), and Eriksson *et al.* (1994) also recorded spinel and garnet as accessory minerals in the sandstone.

Figure 17: Flame structures indicating unconsolidated sediment forced up cooling fractures in basalt flow. This provides evidence that many areas of the Clarens Formation sandstone were unconsolidated during the eruptions forming the lower volcaniclastic breccia and flood basalt emplacement. Location of the outcrop is described in the text.

In thin section the quartz, plagioclase and microcline grains of the Clarens Formation sandstones in the field area are angular to subrounded, and many display undulose extinction. Grain boundaries are often sutured. Angular basalt glass fragments, present only in some sandstone specimens, do not exceed 10% by volume, and their presence implies that some local volcanic activity occurred prior to, or contemporaneously with sedimentation. Some small sandstone clasts with palagonitised glass fragments are found in the Clarens sandstone. Some thin sections display areas of sandstone which have been affected by localised pore fluid alteration. Interstitial carbonate precipitation is more common here, and Fe-oxides in the fluids have given rise to reddy-brown, dendritic, interstitial, haematitic or goethitic accumulations.

The sandstones exhibit well-developed cross-bedding in places with dips of no more than 20° (Figure 18, a and b) and parallel laminations towards the upper contact in a number of outcrops. This suggests that fluvial activity became the dominant mode of deposition, and that water was present in the field area at the time of the phreatomagmatic eruptions. The horizontally-bedded lithologies higher up in the stratigraphy also display characteristics such as muddy-sandstone sediments which suggest the presence of surface water.

Figure 18 (a)

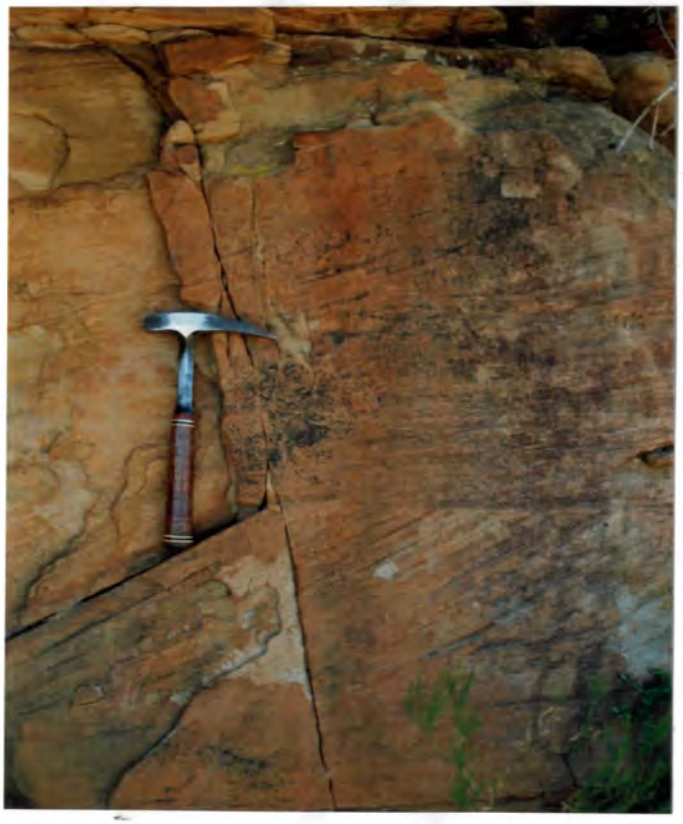

Figure 18, a and b: Large-scale cross-bedding in the Clarens sandstone. These outcrops are found approximately 150m north of Site ***b*** (see Figure 16).

Figure 19: Trace fossils like these ~500m NE of Log 9 (see Figure 4) are rarely observed in sandstone outcrops in the field area.

Along the northern boundary of the volcanic complex outcrops of sandstone containing tiny (<0.5cm) fragments of basaltic glass are observed. The sandstone is cream-coloured, and appears to be sediment from the Clarens Formation. Bedding is evident in most of the outcrops, but is folded and disrupted and in many cases, suggesting that the sandstone has been disturbed. It is inferred that the sediment was unconsolidated and was disrupted by intruding magma, and mixing between the sediment and the magma introduced the glass fragments to the deposit. The sandstone in these outcrops is referred to as "chaotic sandstone" in Figures 4,5,21, and Map, Appendix B.

7.3 LITHOLOGY OF PISOLITIC SANDSTONE

Pisoliths have been observed in Clarens Formation sandstone blocks within the lower volcaniclastic breccia (Map, Appendix B and Figure 16). Their presence is of sedimentological importance as their association with basalt intrusions and lava flows is rare (eg. Friedman, 1969; Friedman and Sanders, 1978; Blatt, 1982; Greensmith, 1989).

Pisoliths are round, accretionary grains of non-specific origin. They are larger than 2mm in diameter, and have a concentric or radial structure (Friedman, 1969; Friedman and Sanders, 1978; Blatt, 1982; Greensmith, 1989). They are not necessarily oversized ooliths (Friedman and Sanders, 1978; Blatt *et al.*, 1980), which are defined by North (1930), Blatt *et al.* (1980), Tucker (1981), Boggs (1987), and Greensmith (1989) as spherical to sub-spherical grains consisting of one or more regular, concentric lamellae around a nucleus which is most commonly a carbonate particle or a quartz grain. Although similar in appearance to ooliths, they tend to be less spherical and are crenulated (Boggs, 1987). Ooliths are less than 2mm in diameter, and usually average 0.2 to 1mm in size (North, 1930; Greensmith, 1989).

By far the most important environment for pisolith formation is the vadose zone (Greensmith, 1989). The vadose zone includes the section of ground above the water table in the aerated section. This zone contains water and air-filled pores around the sediment grains, as well as complex variability such as changes between cementation, leaching, compaction, non-tectonic fracturing and internal sedimentation (Füchtbauer and Peryt, 1980). Water moves rapidly enough to transport silt and deposit it as inclusions in the pisoliths (Friedman, 1969). Pisoliths can be

formed from a variety of minerals, although carbonate and iron-rich minerals appear to be the most common.

The concretions encountered in the study area are termed "pisoliths" based on their size and shape. The pisoliths are rarely larger than 3cm, and usually 1-2cm in diameter. They are observed more commonly in sandstone blocks around the edge of the volcanic complex, closely associated with the volcaniclastic deposit and doleritic intrusions. Pisoliths are not very clear in thin-section, and only a very general concentric structure is observed (Figure 20).

Figure 20: A plane polarised light (ppl) view of the interstitial material forming a pisolith in sandstone. The darker material is opaque minerals, probably tiny haematite grains, in the rings of interstitial calcite. Tiny haematite crystals are also common without calcite as the interstitial material in some pisoliths. Sample from pisoliths at Sites ***d*** and ***e***. (Magnification: 10x)

In all the outcrops of pisolitic sandstone the pisoliths display different stages of development. Some are merely a small staining of the sandstone while others are clear concentric structures still part of the sandstone, and others are loose and almost free of the sandstone host. Figures 21 to 23 show pisoliths in the different stages of development. The development of pisoliths is discussed later in section 10.3.

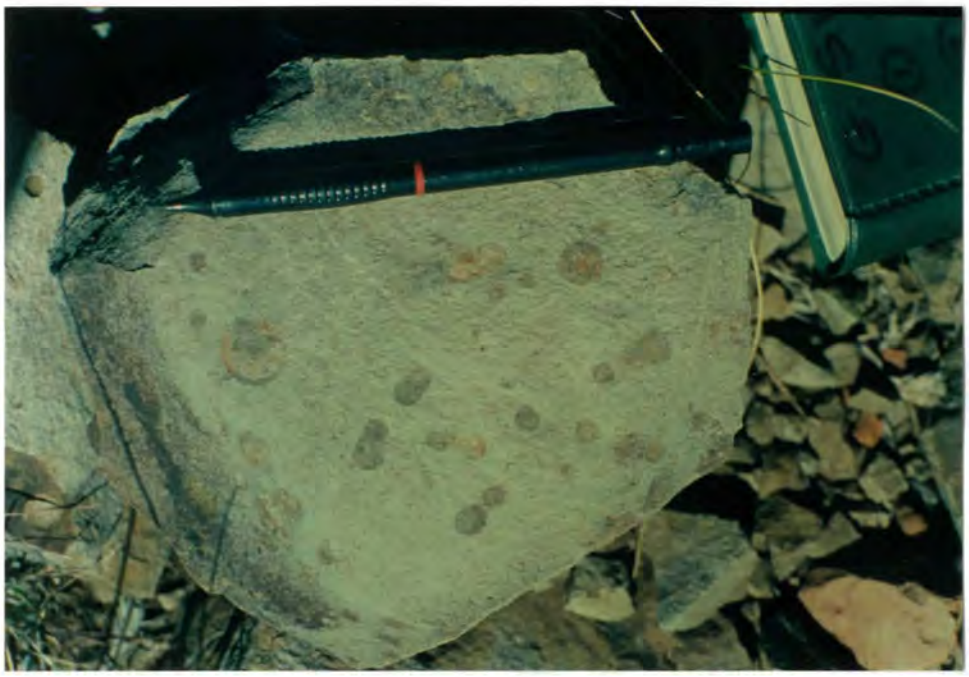

Figure 21 (a)

Figure 21, a and b: The precipitation of haematite forms a staining in the sandstone. These photos represent the first stage in the development of pisoliths. Sample from Site **c** (see section 7.3.1).

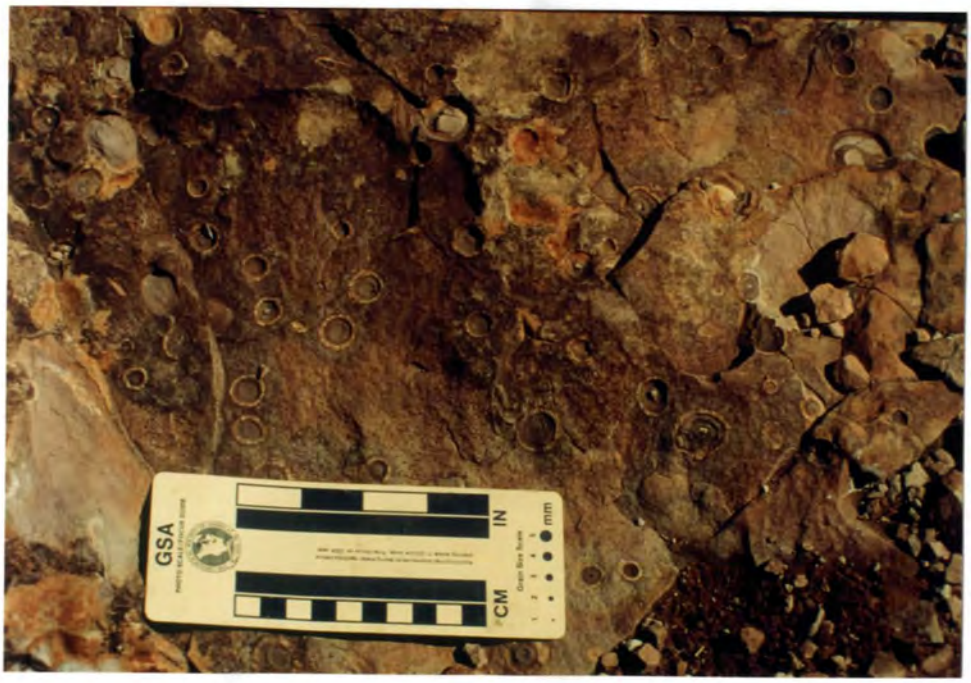

Figure 22: Better developed pisoliths, where the minerals making the pisolith have precipitated in a concentric pattern. Sample from Site **d** and **e** (section 7.3.1).

Figure 23: An almost completely developed pisolith. The pisolith is now more resistant to fracturing than the host sandstone. Rings of the precipitated mineral and the sandstone fragment nucleus are evident. Sample from Site **a** (section 7.3.1).

The pisolith descriptions below are separated into sample sites. These sample sites are shown on a smaller map area (Figure 16) where the majority of the pisoliths encountered in the volcanic complex outcrop.

7.3.1 Pisolith Sample Sites

As there are a limited number of sites where pisoliths are found within the volcanic complex, and because the pisoliths at each site vary slightly in appearance, size, distribution and chemistry, each site is described separately below. Cross-sections through the rocks at sites ***a*** to ***k*** are shown in Figure 24 and their orientations marked in Figure 16.

Site ***a*** is situated towards the edge of a massive, unbaked, pink sandstone block, close to where the sandstone is covered by the lower volcaniclastic breccia to the immediate north-east (Figure 16). The sandstone has been altered to a pale turquoise-blue colour, and the area of pisolith development is between 3 and 20m wide. The outcrop contains pisoliths up to 2.6cm in diameter, and in various stages of development, from a red to purple colouration of the sandstone. Some pisoliths have been completely separated from the sandstone, leaving spherical pits.

The sandstone at Site ***a*** contains a little interstitial carbonate but with high concentration rings of interstitial carbonate forming the pisoliths. The fine-grained sandstone (~0.13mm) is matrix-supported and has very fine-grained quartz and feldspar as well as the carbonate in the interstices.

Site ***b*** lies approximately 400m to the north-east of Site ***a***, and displays similar characteristics. The sandstone has a pale turquoise-grey colour on fresh surface, but is reddy-brown on weathered surface. All the pisoliths are 0.5-1.8cm in diameter. The pisolitic sandstone outcrop is between 1 and 2.5m wide, and extends for 400m along the length of the sandstone block adjacent to the contact with the lower volcaniclastic breccia. Site ***b*** has less pervasive carbonate throughout the sandstone than Site ***a***. The carbonate is concentrated mainly where the pisoliths have formed and

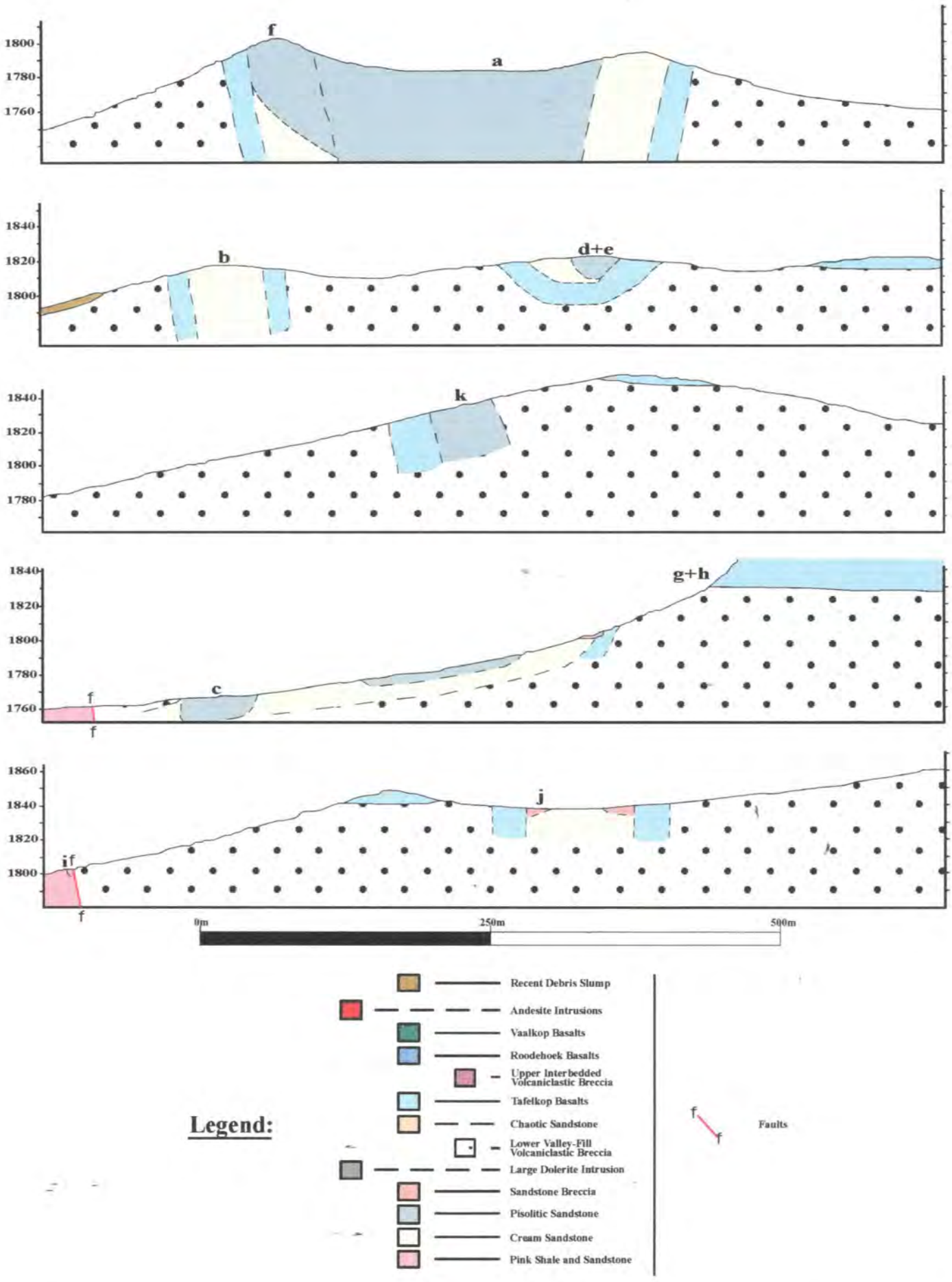

Figure 24: Cross-sections through the sandstone blocks and stream-flow deposits containing pisoliths. Thin-section and hand specimen sample sites are numbered **a** to **k**.

is not very common in the matrix outside these areas. The sandstone is clast- to matrix-supported, and has an average grain size of 0.15mm.

The pisoliths at Site *c* occur close to the southern contact between the basalt and the sandstone block. The sandstone in the centre of the block is creamy yellow and unaltered, but approximately 5m from the basalt the sandstone becomes pale turquoise in colour and pisoliths are observed. A roughly spherical zone (~ 250m in diameter) in the centre of the sandstone block also contains pisoliths of the same characteristics as the ones on the outer margin. The pisoliths are very similar in colour and size to the ones at sites ***a*** and ***b***.

At Site *c* the pisoliths are hosted by sandstone consisting predominantly of angular quartz and feldspar sand grains (< 0.125mm), and a matrix of very fine-grained quartz and feldspar with scattered patches of alteration material with first order interference colours, inferred to be zeolites. These zeolites surround some minerals and small vugs in the sandstone. Accessory haematite, zircon, sphene, and sericite exist in the matrix of the sandstone. The central zone of the pisoliths has a pale grey colour, and contain sand grains with interstitial very fine-grained quartz and feldspar coexisting with minerals with a low interference colour, also inferred to be zeolites. The rings of the pisoliths are very similar in mineralogy to the host sandstone except that the concentration of zeolite is greater in these rings than in the rest of the sandstone. The main ring in all the pisoliths is the first one from the central zone outwards, and has the greatest concentration of zeolite. It can be up to 1.2mm in thickness, but does not maintain a constant thickness around the pisolith core. Further rings outside the first ring are evident, but are not as well defined, nor as concentric as the first ring. The pisoliths have diameters of between 0.4 and 0.7mm.

The pisoliths at Site ***d*** occur in a rose-coloured sandstone. They are small (under 1cm) and are raised from the weathered surface of the sandstone, being more resistant to weathering than the sandstone. The pisoliths are a rusty orange colour, contrasting with the more pinky-coloured sandstone. A fresh surface reveals lighter pink-coloured pisoliths contrasting with the darker brown, unaltered sandstone. Rings in the pisoliths are visible as alternating bands of lighter and darker pinky-brown sandstone. In thin-section the matrix of the pisoliths is more yellow-coloured, lighter and less red than the rest of the sandstone. There is a high concentration of pisoliths in the rock, ranging in size from 0.4 to 3.3cm. The average pisolith diameter is approximately 1cm. The sandstone containing pisoliths appears to be more matrix-supported than the non-pisolitic sandstone, containing more argillaceous material than in sites ***a*** or ***b***. The sand grains also appear smaller in size, providing more room for interstitial material as the smaller grains do not appear to have allowed a tighter packing. The largest sand grains are ~ 0.3mm while the average size is between 0.18 and 0.2mm. No carbonate material is present in the sandstone.

A few metres northwest along the sandstone outcrop, a second sample site, Site ***e***, contains pisoliths with different characteristics to those at Site ***d***. The Site ***e*** pisoliths have developed in a grey-blue, very fine-grained sandstone with an orangy-brown alteration surface. The pisoliths are a lighter grey-white colour in fresh surface, getting darker towards the centre of the pisoliths until they almost reach the same dull blue-grey colour as the sandstone outside the pisoliths. The rings of the pisoliths are clearly seen on weathered surfaces and range in weathered colouration from dark brown, through yellow-brown, to an oxidised-looking orangy-brown.

In thin-section the pisoliths at Site ***e*** are defined by bands of carbonate concentration. Added to the carbonate bands are bands of minerals with a low interference colour, inferred to be zeolite. The interstitial spaces within the pisoliths appear to be more quartzose and feldspathic than argillaceous. The pisoliths are more clast-supported and slightly larger (average diameter of 1.6cm) than those at Site ***d*** while the average sandstone grain size is ~ 0.2mm.

Site ***f*** differs slightly in appearance as the *nodules* retrieved from the sandstone block do not appear to have concentric rings typical of pisoliths, but rather a spherical form of massive sandstone. These features are found in the upper 1m of the small sandstone outcrop. The nodules range in size from 0.7 to 2.3cm, the majority approximately 1.8cm in diameter. The matrix of the sandstone at Site ***f*** is full of zeolite. Very little other interstitial material is observed with only accessory amounts of zircon, palagonite and sericite.

7.3.2 Stream-Flow Deposits of Brecciated, Pisolitic Sandstone

Outcrops of brecciated and redeposited sandstone are closely associated with the pisolitic sandstone outcrops, particularly those at sites ***g***, ***h***, ***I***, ***j*** and ***k*** (Figure 16). These deposits appear to consist almost entirely of pisoliths and sandstone fragments, and are observed in fairly narrow outcrops (Figures 25 and 26). They are stratigraphically positioned between the Clarens Formation and a few thin lava flows prior to the emplacement of the lower volcaniclastic breccia. Figure 25(a) also shows the only outcrop where cross-bedding can be inferred. Although not very clear, trough cross-beds can be observed in the centre of the block.

Figure 25 (a)

Figure 25, a and b: Stream-flow deposits of brecciated, pisolitic sandstone. The deposits are horizontally-bedded, and can fine- or coarsen-upwards. Cross-bedding is evident in Figure 25(a). Very little basaltic glass is encountered in these deposits. Sample from Site **j** (Figure 16).

Figure 26: Horizontally-bedded stream-flow deposit full of angular fragments of sandstone and spherical, concentric pisoliths. The matrix consists predominantly of sand grains. Sample from Site **I** (Figure 16).

Very little variation exists between the outcrops of stream-flow deposits as the mineral composition is almost identical in each deposit. The deposits consist almost completely of angular sandstone fragments and spherical pisoliths in a sandstone matrix.

Most of the deposits are composed of quartz and feldspar grains approximately 0.1mm in size. Patches of ultra-fine-grained unknown material is also very common, although carbonate is discernible throughout these patches. The sandstone in these patches appears to have been baked and the grains welded together. The coarser-grained sandstone surrounding the patches has a carbonate matrix and with distance from the ultra-fine-grained material, grades into a sandstone with a sericitic matrix. The coarser-grained sandstone areas are fairly dirty in parts, containing much argillaceous material.

A number of angular fragments (~ 0.8-2mm) of palagonitised basaltic glass are present in the stream-flow deposits. These fragments are full of amygdales of fibrous zeolite. Many fragments are fractured and the fractures and other spaces are filled with coarse-grained, greeny-yellow fibrous palagonite. In a number of amygdales or vugs, a radial fabric of palagonite surrounds a finer-grained, zeolite core. The palagonite fibres are 0.3mm and less in length.

A few pisoliths around 1-2cm in diameter are present and have a 1-3mm core of sandstone with a dark, ultra fine-grained matrix of unknown composition. The pisolith also contains bands of sandstone with many tiny haematite grains in the matrix. Accessory minerals in the stream-flow deposits include zircon, sphene and opaque minerals.

Debris-flows of sand and brecciated sandstone slumped into streams from the banks. These were reworked by stream-flows, concentrating the coarser constituents together in bands (Reading, 1996). These stream-flows appear to be the most likely mechanism for the formation of the brecciated sandstone deposits outcropping in the study area. It is inferred that the fine material is removed, leaving the coarser-grained sand and larger pisoliths and sandstone fragments as a lag deposit. Cross-bedding in the deposits (Figure 25) suggests that the material was deposited during brief periods of high energy stream flow. The deposits accumulated in small depressions, or as small stream channels and were baked when covered by subsequent lava flows.

The unit at Site ***g*** for example, is a breccia composed of angular fragments of sandstone in a crude, upward coarsening sequence. A small amount of angular basaltic glass is present in the breccia. The sandstone fragments consist predominantly of fine-grained sandstone, and appear to be fragments from the Clarens Formation. Some fragments could possibly be Elliot

sandstones, but due to their size and the slight colour change through baking from the adjacent basalt flows, this is not clear. The unit at Site ***g*** contains alternating layers, 1 - 10cm thick, of very fine-grained sandstone, coarse-grained sandstone, and sandstone fragments. It is in association with these sandstone fragments that pisoliths are found in high concentration. The pisoliths are small (< 1cm) and are packed together with sandstone fragments. No evidence of compaction exists.

Within 1.5 and 1m of the contact between the southern edge of the sandstone block and basalt at Site ***c***, the pale turquoise, pisolitic sandstone gives way to a baked stream-flow deposit of a dull greeny-yellow colour with a creamy yellow surface. The stream-flow deposit contains creamy yellow sandstone clasts, as well as scattered pisoliths, in a dull, glassy-looking matrix. The pisolitic stream-flow deposit overlies the *in situ* pisolitic sandstone, and is itself overlain by basalt. The thickness of the stream-flow deposit varies, and pinches out in places along the sandstone block so that the bleached, pisolitic sandstone lies disconformably against the basalt. Site ***j*** is further east along the same sandstone block as Site ***c***, and displays a pisolitic sandstone and stream-flow deposit of similar characteristics to those at Site ***c***.

Many veins and fractures are present in the deposit, most filled with glassy quartz, and these have zeolite and oxidation alteration minerals along their lengths. Zeolites also surround small vugs as well as some sand grains. Palagonitised glass fragments containing sand grains are also observed.

The stream-flow deposits at Sites ***h*** and ***I***, east of Site ***j*** and along the southern fault exposure respectively, are small outcrops with the same characteristics as Site ***c***. Each outcrop is only approximately 2-3m long, and no pisoliths were observed in either of the exposures.

Site ***k*** is located on the southeastern side of a long, thin sandstone outcrop, 300m from Site ***b***. Both sites are located along the same sandstone unit. The stream-flow unit at Site ***k*** contains mixed sandstone clasts of different colours from creamy-yellow, through turquoise, to reddy-yellow. Turquoise, glassy-looking veinlets are present. There are also many small vugs, or air spaces between fragments. The baked sandstone has a sugary, translucent, glassy appearance, and weathers to an orangy-brown colour. Resistant sandstone fragments and pisoliths protrude from the stream-flow deposit and often have a more rusty orange colour than the rest of the deposit. At this site the flow is not as organised and layered as at Site ***g***, and no size grading is evident. The zones of sandstone fragments, pisoliths and sandstone matrix are disturbed and deformed around each other.

Thin sections of the pisoliths occurring at Site ***k*** reveal an inner core of sandstone with many very tiny, interstitial haematite grains. The grains are too small to measure and are barely visible, but in high concentrations provide an overall reddy-pink colour to the sandstone. Moving outwards from the core of the pisoliths, the sandstone matrix becomes far less concentrated with haematite grains and the rock appears clearer, but is isotropic in cross-polarised light. This contrasts strongly with the non-pisolitic, host sandstone which contains interstitial clays and fine-grained quartz and feldspar, all of which are clearly discernible in cross-polarised light. The pisoliths are between 0.8 and 2cm in diameter.

7.4 LITHOLOGY OF SEDIMENTS INTERBEDDED WITH BASALT LAVA FLOWS

Pahoehoe tholeiitic lava flows of the flood basalt sequence, and the upper volcaniclastic breccia horizons overlie the Clarens Formation. Generally the base of this volcanic sequence is marked by lava flows overlying the Clarens sandstone. The supply of Clarens detritus and the depositional environment associated with it persisted after the start of lava flow volcanism. Sandstone interbeds between lava flows are common within the lower hundred metres of the volcanic sequence (du Toit, 1904, 1954; Lock *et al.*, 1974). As observed in the study area, some of these are persistent over wide areas and Lock *et al.* (1974) used sandstone interbeds in the Barkly East area to subdivide the volcanic sequence.

In the study area lenses of sandstone interbedded with lava flows are common and indistinguishable from typical Clarens sandstones, although these lenses are not very laterally persistent, seldom wider than a few hundred metres, and are thus not useful as stratigraphic markers. One lens displays well-developed trough cross-lamination, and has a blue centre with a browny-red outer rim (0.5-1.5cm). Other lenses of sandstone are channel-shaped, and range from 10-20cm wide by 10-15cm thick to many metres wide and up to 0.5m thick. The palaeoflow direction in these deposits, indicated by trough cross-bedding, is predominantly to the south-east. Symmetrical ripple marks (Figure 27) are preserved along the upper surfaces of some thin sandstone outcrops.

Figure 27: Symmetrical ripple marks preserved on the upper surface of a thin, planar cross-laminated sandstone unit interbedded with lava flows adjacent to Log 7, implying a shallow, waterlain depositional environment with a bidirectional palaeocurrent as would occur along the edges of a lake.

Directly adjacent to the fault exposure in the southwest of the study area, overlying the lower volcaniclastic breccia, is a 1m sequence of cyclic, upward-fining beds only a few millimetres thick. This sequence is inferred to represent reworking of the underlying volcaniclastic breccia and redeposition as a number of thin, graded sheetwash deposits. The outcrop is localised, overlain by basalt, and lateral continuity could not be determined.

7.5 Lithology of Lacustrine Units

Interbedded with the lava flows within the volcanic complex are a number of thinly-laminated, laterally extensive, reworked yellow-green, silty sandstone units, seldom thicker than 1m (Figure 28, a and b). These units contain a few (<5%) basaltic glass fragments (<5mm). There are three clearly defined units of at least a kilometre in length, and possibly also smaller units which may just be wide, shallow channels of silty-muddy sand material. The deposits are inferred to represent a low energy, depositional environment, and perhaps a large, shallow lake or playa which formed on the surface of the underlying basalt or breccia units during periods of quiescence in the emplacement of the volcaniclastic breccias and flood basalts. These units are easily traced laterally and are thus good marker horizons which can be used as datums for restoring the original stratigraphic position of sequences.

Figure 28 (a)

Figure 28, a and b: Parallel laminated and less commonly cross-laminated, silty sandstone units up to 1m thick, but laterally extensive for kilometres. The unit in Figure 28a outcrops adjacent to Log 9 between the upper volcaniclastic breccia and a lava flow. The unit in Figure 28b outcrops towards the top of Perdekop (Log 4) between two flood basalt units.

The lowest of the three silty sandstone units is interbedded between the lower and upper volcaniclastic breccia (Map, Appendix B), clearly marking the boundary between the two. The lacustrine deposit is still present between the two volcaniclastic breccias where they lie almost in contact with one another on the western slope of Perdekop (Map, Appendix B). It is a critical marker horizon allowing the separation of the two breccias into an upper and lower unit. Without this unit the separation would be difficult because of the very similar appearance between the two breccias. This deposit demonstrates a break in the eruptions and the development of a low energy, shallow lake environment.

A second lacustrine deposit outcrops along the upper contact of the upper volcaniclastic breccia. A further deposit is interbedded with the basalt flows near the top of the highest peaks of exposed rock, separating the Roodehoek basalts from the Vaalkop basalts. In some areas the deposits have a mudcracked upper surface (Figure 29) and some have clearly defined water escape structures which have subsequently been filled in with a slightly coarser, brown-coloured, muddy sand (Figure 30).

Figure 29: Thin, mudcracked upper surface of a parallel-laminated, silty sandstone unit near the top of Perdekop implies periods of desiccation of an otherwise ephemeral, wet environment.

Figure 30: Water escape structures in a thin, parallel-laminated, silty sandstone formed during the compaction and diagenesis of the hydrated sediment. Spaces are later filled with sediment, or collapse. These structures outcrop near the top of the Perdekop peak.

7.6 Lithology of Volcaniclastic Breccia

The volcaniclastic breccias in the study area (Figure 31) are poorly-sorted deposits containing angular rock fragments less than 1mm to over a few metres in size (Figure 32 a and b, and Figure 41). The breccias are divided into clasts (≥2cm) and matrix (<2cm). The clasts are predominantly Clarens Formation sandstone and basalt, with fewer Elliot Formation sandstone and shale, basaltic glass and peperite clasts. The matrix consists predominantly of smaller clasts of shale, sandstone and basalt, as well as glass fragments and sand grains (Figure 33). Fragments from the Molteno Formation may also be present, although due to the similarity of the Elliot and

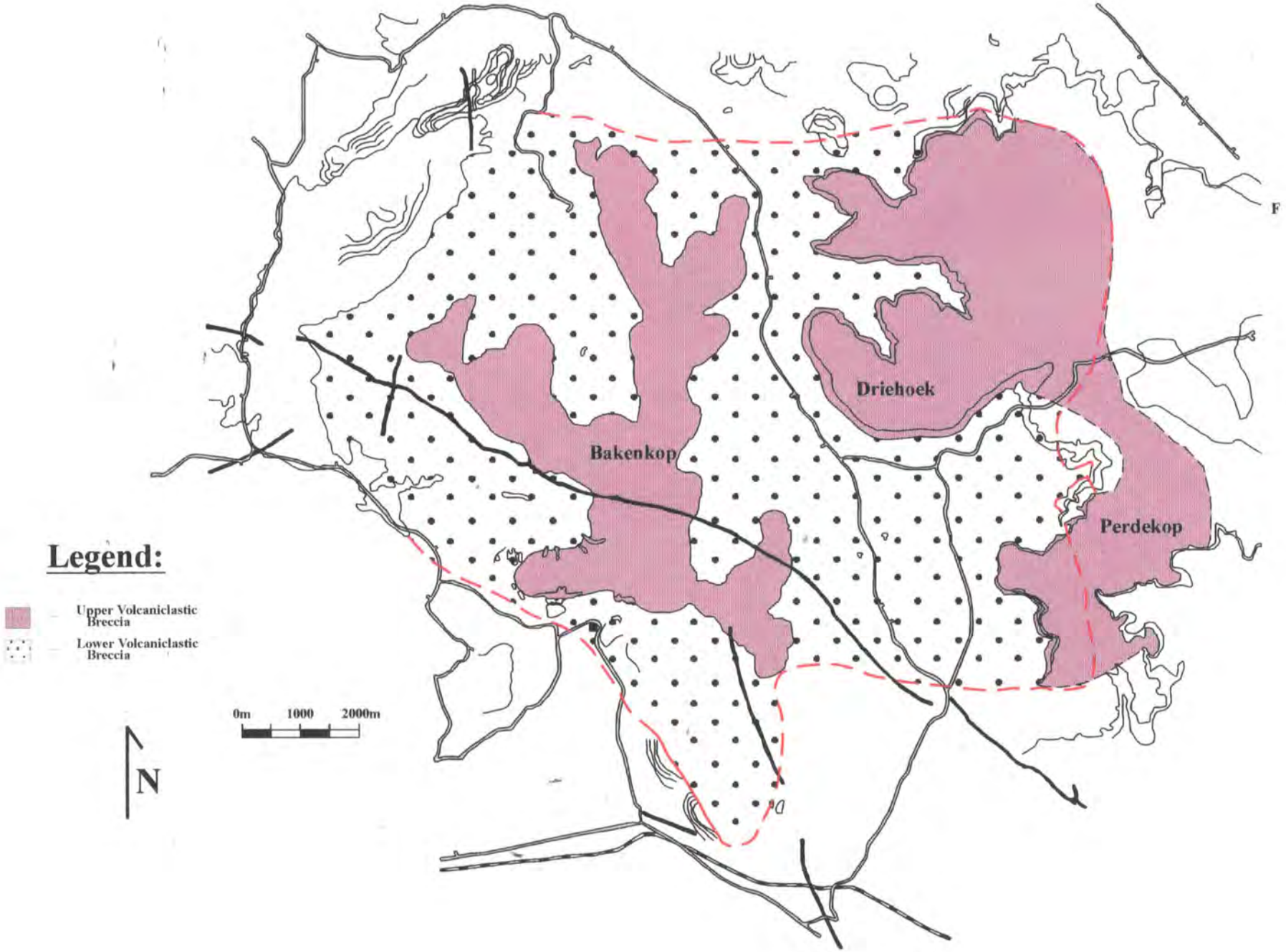

Figure 31: Map of study area with boundary of volcanic complex outlined in red. The areas filled in with black dots and solid purple define the areal extent of the lower and upper volcaniclastic breccias respectively.

Molteno Formations in many areas, this cannot be determined with certainty. The volcaniclastic breccias show diversity in terms of colour, degree of alteration and clast lithology within individual units, both vertically and laterally. They are dominantly clast- or matrix-supported, poorly sorted and ungraded.

Figure 32 (a)

Figure 32: Field photos of volcaniclastic breccia. The lower volcaniclastic breccia adjacent to Site ***a*** (Figure 16) is depicted in (a), while (b) shows a sample of the upper breccia upslope from Site ***h***. The clasts present in both photos include pale yellow sandstone, pinky-red shale and sandstone, grey mudstone and basalt clasts, and green basaltic glass fragments. The matrix consists of smaller clasts of sandstone, shale, mudstone, and basalt, as well as small basalt glass fragments. The matrix also includes individual sand grains.

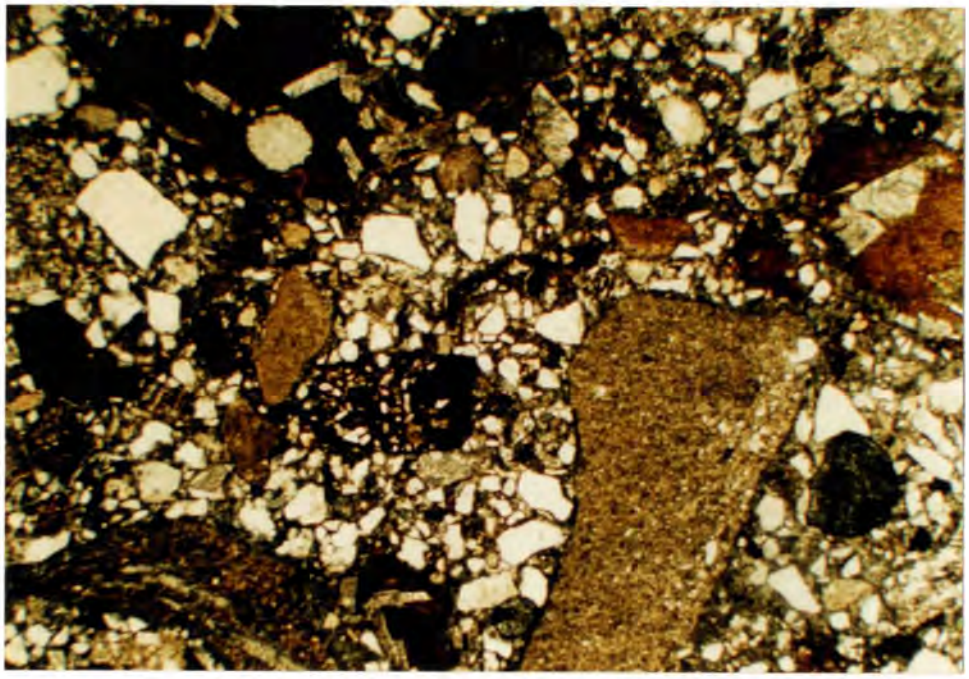

Figure 33: A typical example of volcaniclastic breccia (ppl, 25x magnification). The yellow clast in the bottom right quadrant is fine-grained sandstone, the dark brown fragment in the upper left corner with plagioclase laths and an amygdale within it is palagonitised basaltic glass. Both tachylite (eg. dark material containing sand grains in the centre) and more commonly sideromelane glass fragments (red-orange fragment just below top right corner) are observed in the breccias. The white grains in the matrix are quartz and feldspar. Sample from lower breccia just west of Site *g*.

7.6.1 Appearance of Lower Volcaniclastic Breccia

The lower volcaniclastic breccia appears to fill the volcanic complex, with an approximate area of 270km^2, and has an estimated minimum volume of 27km^3. This volume is based on the observation that the breccia has an exposed thickness of at least 100m in most outcrops. Like the upper volcaniclastic breccia, the lower breccia ranges in colour from a yellow-blue-grey to a pinky-white depending on the degree of zeolite alteration in the matrix. The clasts in the lower breccia, many up to 3-5m in diameter are, on average, larger than the clasts in the upper breccia.

Yellow and pink sandstone clasts are more common in the lower volcaniclastic breccia than the upper breccia, while basalt clasts are far less common in the lower breccia. Fewer red shale, and pink and yellow sandstone fragments are observed in the matrix of the lower volcaniclastic breccia than in the upper breccia. Sedimentary lithics comprise approximately 25 vol% of the lower breccia, while the proportion of unconsolidated sediment in the lower breccia is ~ 30 vol%. Cored bombs (fine-grained to glassy basalt rind surrounding basalt clasts) and peperite clasts (wet sandstone mixed with basalt) are common in certain localities within the lower volcaniclastic breccia (discussed later), but are not present in the upper breccia. In this study the term "peperite" describes the deposit formed when wet, unconsolidated sand is intruded by and mixed with basalt without an explosive eruption.

In the outcrop on the western edge of the slope behind the Noordhoek farmhouse (Figure 4), a number of larger glass fragments up to 15cm are observed (Figure 34). This is a rare size for juvenile, basaltic glass fragments in the study area, given that they are extremely brittle and are usually broken up if transported any distance. Glass fragments this size are not observed at all in the upper volcaniclastic breccia, and are rare in the lower breccia.

An estimated 25 vol% of the lower volcaniclastic breccia is juvenile glass ($6.8km^3$). This represents the volume of intrusive material which interacted with approximately 30 vol% unconsolidated sediment ($8.1km^3$), ~25 vol% lithic sediment, and ~20 vol% lithic basalt ($5.4km^3$).

Figure 34: Large glass fragment on the western edge of the slope behind the Noordhoek farmhouse, preserved in the lower volcaniclastic breccia. Although heavily altered, the fragment is clearly basaltic, and might possibly be an altered Strombolian bomb. No internal structure has been preserved in these fragments due to subsequent alteration.

7.6.2 Internal Structure and Variations within Lower Volcaniclastic Breccia

Along the western slope of Perdekop (Map, Appendix B and Figure 4) the lower volcaniclastic breccia can be subdivided into three subunits. The basis for the subdivision is the variation and distribution of certain clast types. The subdivision is not noticeably present anywhere else in the study area. The lowest subunit contains a concentration of peperite clasts (Figure 35, a and b) and larger general clast sizes (up to 3m) compared with the rest of the lower volcaniclastic breccia. This subunit is overlain by a subunit with far fewer peperite clasts and a high proportion of cored and ribbon bombs with a few spindle bombs (Figure 36, a, b, c, d, and e). This in turn is overlain by a subunit almost devoid of peperite clasts and cored or ribbon bombs and is finer-

grained with clasts seldom exceeding 5cm in diameter. This change from peperite clasts to Strombolian bombs higher up represents an increase in explosive energy. This may have been as a result of an increase in the rate of magma intrusion and/or a drying out of the sediment that the magma interacted with. Initially a non-explosive interaction between the magma and unconsolidated, wet sediment formed peperite. With an increase in the amount of magma intruding the unconsolidated, wet sediment, and/or a local reduction in the amount of wet sediment input, a more explosive interaction between the sediment and the magma occurred. Strombolian eruptions formed the bombs encountered in the subunit overlying the subunit containing peperite clasts. No sediment is present in the rinds of the cored bombs, implying that the bombs originated from a Strombolian eruption, rather than from the same eruptions which produced the lower volcaniclastic breccia. This is discussed in greater detail in section 10.7.

Figure 35 (a)

Figure 35, a and b: Clasts of peperite within the lower volcaniclastic breccia on the Perdekop slope (Map, Appendix B, Figure 4). Clasts are predominantly subrounded to angular and vary in size from a few centimetres to 3m. The paler material in the clasts is hydrothermally altered basalt, and the darker material is baked sandstone.

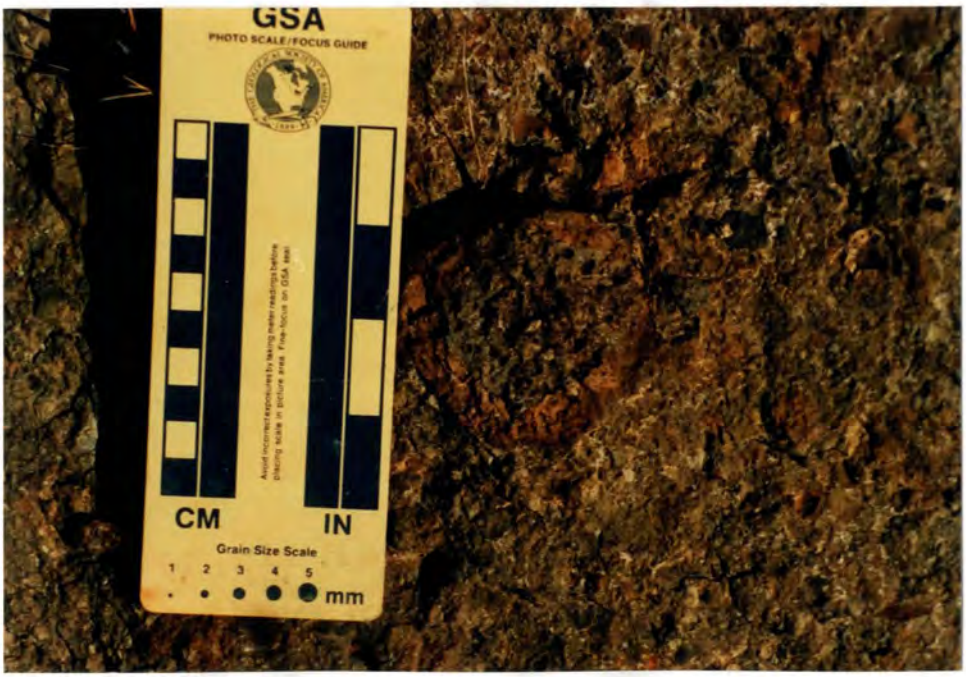

Figure 36 (a)

Figure 36 (b)

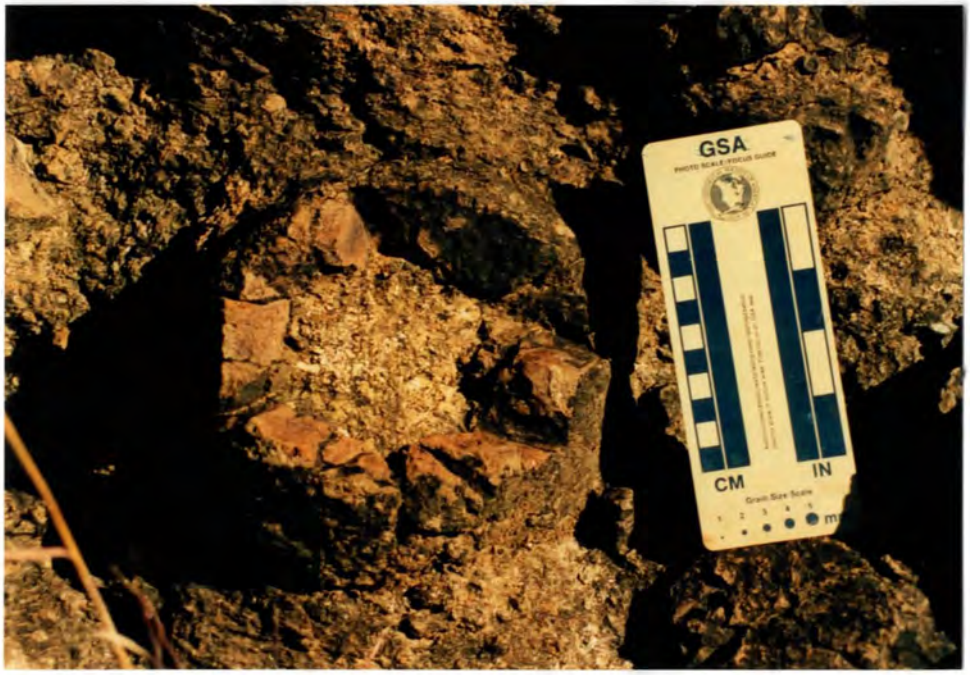

Figure 36 (c)

Figure 36 (d)

Figure 36, a,b,c and d: Cored bombs within the lower volcaniclastic breccia on the slope of Perdekop. Rinds range from a few millimetres to 6-7cm; **e:** A ribbon bomb of basalt from the same locality within the lower volcaniclastic breccia.

Radially-fractured mudstone clasts are present in the lower of the three subunits in the lower volcaniclastic breccia (Figure 37). According to Lock (1978), radial fractures in shale clasts are indicative of rapid cooling after heating. This implies that the shale clasts were hot (500-800°C) when emplaced and that they were incorporated into a colder lahar. The source of the heat is unclear, however, and how the shale clasts could be preferentially heated while the volcaniclastic breccia remained cold is also not clear. It is possible and, the author feels, more likely, that the radial fractures in the shale clasts are a result of fracturing from loading of the above material or from dewatering. The reason why only a few shale clasts are fractured remains uncertain.

Figure 37: A 15x20cm radially-fractured mudstone clast in the lower volcaniclastic breccia on the western Perdekop slope. The clast is well-rounded.

A sandstone block in the valley to the west of the Bakenkop peak (Map, Appendix A and Figure 4) is comprised almost entirely of fine-grained sand. It contains some small clasts of fine-grained yellow, pink, and greeny-yellow shale and sandstone, as well as a few clasts of coarser-grained, laminated yellow sandstone (2-4cm). A few coarse-grained basalt clasts up to 0.5m are evident, but very few basaltic glass fragments are observed. Thin section examination reveals far fewer glass fragments in the clast than in any of the volcaniclastic samples. The block most likely represents unconsolidated sand that incorporated basaltic and lithic fragments before undergoing diagenesis. A 5m fluidal peperite clast is observed in the lower volcaniclastic breccia to the south of the sandstone block, and an isolated exposure of basalt is encountered within 1.5m to the west of the block. Fluidal peperite is the term used to describe peperite that forms when the magma and the wet sediment mix as two immiscible fluids without any brittle fracturing of the magma occurring.

7.6.3 Appearance of Upper Volcaniclastic Breccia

The upper volcaniclastic breccia ranges in colour from a yellow-grey to a pinky-white. Many glass fragments, no greater than 1.5cm, as well as larger (~5cm) basalt clasts and red shale and sandstone clasts, more common than the basaltic clasts, are present in the matrix of this unit. The largest clasts are up to 50cm in size and are usually massive or amygdaloidal basalt. The upper volcaniclastic breccia intersected by Log 8 (see Map, Appendix B) contains very large basalt clasts up to 3m in diameter in contrast to an average clast size at this outcrop of 30cm. The upper volcaniclastic breccia is almost exclusively finer-grained than the lower volcaniclastic breccia.

In places the upper volcaniclastic breccia displays localised alteration, particularly of the matrix. One such locality lies between log sites 8 and 9 and displays a white zeolitised matrix. The breccia contains many clasts of green shale, red Elliot shale and sandstone, and Clarens sandstone. A few metres south, the matrix of the volcaniclastic breccia changes to a creamy-pink colour and is less altered. This implies that alteration is often very localised.

Clasts of volcaniclastic breccia are observed within the upper volcaniclastic breccia around the western edge of the hill behind the Noordhoek farmhouse. Although very similar to their host in appearance, they are clearly clasts within the unit. Towards the bottom of the upper volcaniclastic breccia a few patches or blocks exist (one of which is ~20x15m) where the normal, creamy volcaniclastic breccia grades over approximately 10cm into basalt-rich, dark-blue zones. These patches are full of vesicular and massive basalt (clasts 1m and less), and contain few sandstone clasts. As the creamy breccia unit is more devoid of basalt clasts, this transition is particularly clear. It is inferred that these large patches define an irregular upper surface of the lower volcaniclastic breccia, and erosion has exposed areas of lower breccia through remnants of the upper breccia.

7.6.4 Internal Structure and Variations within Upper Volcaniclastic Breccia

There are few outcrops where large vertical sections through the volcaniclastic breccias are exposed. However, one of these outcrops just east of sites ***h*** and ***j*** (Figure 16) reveals a crude upward fining sequence within the upper volcaniclastic breccia. Here large basalt clasts are concentrated at the contact with the lower volcaniclastic breccia. On the western side of the hill behind the Noordhoek farmhouse (Figure 4), the upper unit is particularly well exposed, and

larger sandstone and basalt clasts are more concentrated in the centre of the unit than in the lower and upper parts. The zone of coarsening hosts numerous very coarse-grained, heavily zeolitised basalt fragments. Other noticeable features of the unit include the lack of red sandstone clasts near the base, but an increase in their concentration towards the top. Angularity of sandstone and basalt clast fragments also appears to increase towards the top.

The presence of features which allow internal subdivision of the upper volcaniclastic breccia are uncommon. At one locality on the western face of Perdekop, a number of well-defined ridges occur, accentuated by weathering. The more resistant subunits form well-defined ridges that are laterally continuous along the length of the western face of Perdekop (Figure 38). The softer subunits between them are more weathered, and protrude less than the resistant subunits. Except for the noticeable resistance to weathering of some of the subunits, there are no apparent visible, lithological differences between them, either in hand specimen or thin section. They are all pale yellow, and have clasts seldom exceeding 5-10cm in diameter.

In the valley just south of the farm Modena, in the northeast of the study area, a lense 1.5m deep and 15m wide occurs in the upper volcaniclastic breccia (Figure 39). The lense is filled by angular (conchoidally-fractured) clasts of basalt and baked sandstone. The clasts average 30cm, but some are as large as 60cm in diameter, and the ratio of sandstone to basalt clasts is 60:40. Above and below the lense the volcaniclastic breccia is the same as in the rest of the unit, with clasts averaging 2-3cm and up to a maximum of 6-7cm (Figure 40). The matrix in the lense (below 2cm) is identical to that of the rest of the unit. It comprises angular to subrounded, red to creamy-blue shale, green to blue to cream sandstone, and basalts clasts. Many glass fragments are also present in the matrix.

Figure 38: View of the western face of the slope below the two hilltops south of Perdekop on the eastern margin of the volcanic complex. Note the thin, pale yellow-coloured ridges of upper volcaniclastic breccia in the middle of the slope.

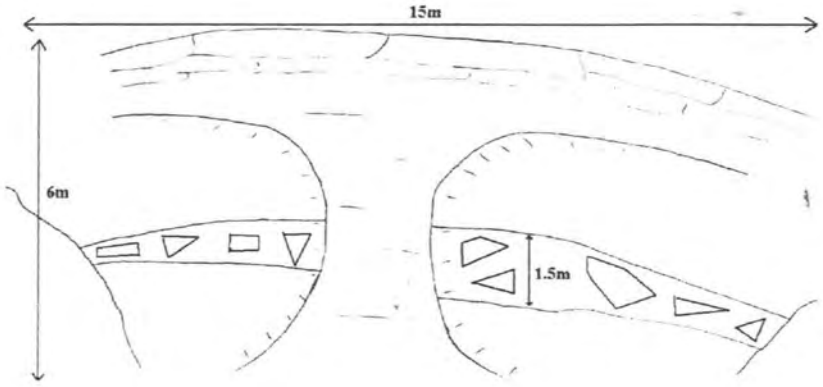

Figure 39: Sketch of exposure of volcaniclastic breccia lense south of the farm Modena. The coarser lense is exposed in two depressions in the outcrop face, separated by a raised middle section where water has obscured all features. The edges of the lense are obscured by soil and plant cover to the sides. The entire exposure is volcaniclastic breccia; only the lense with larger clasts (predominantly basalt, few sandstone) than the rest of the breccia is detailed here.

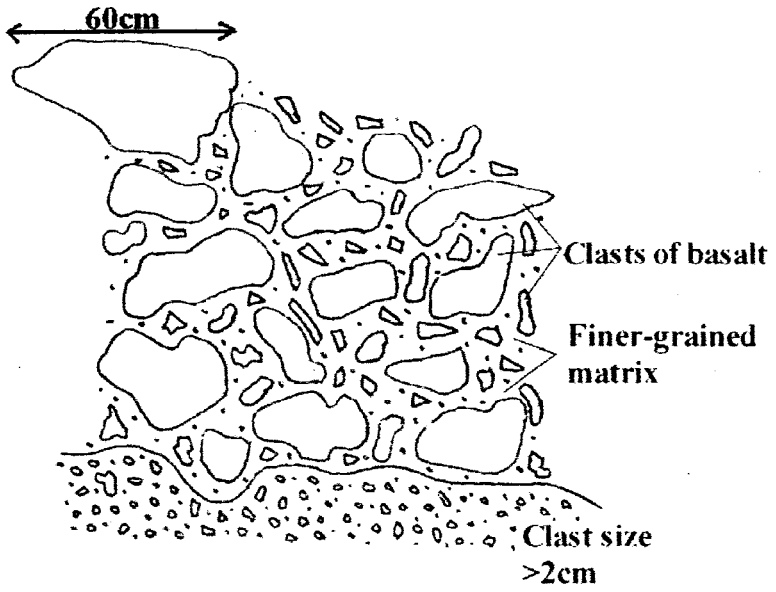

Figure 40: Close-up sketch of the volcaniclastic breccia with large clasts in the lense. This figure demonstrates the relationships and size variations between the breccia within the lense and the host breccia. The matrix of the breccia in the lense is the same as the matrix in the rest of the upper volcaniclastic breccia. The basal contact of the lense is uneven.

7.6.5 Volcaniclastic Breccia Contacts

The upper contact of the lower volcaniclastic breccia, and the upper and lower contacts of the upper volcaniclastic breccia are all very similar in appearance and characteristics. They are sharp and planar, although some undulations do occur in places due to the uneven surface of the underlying lithology. The upper contacts of both the upper and lower volcaniclastic breccias with basalt do exhibit some mixing between the units on either side in a few areas. Here the hot lava has either plucked fragments of breccia off the surfaces of the breccia units, or heating of fluids within the breccias caused fracturing of the upper surfaces, allowing basalt to penetrate downwards.

Figure 41: Sharp contact between dull yellow breccia above and grey-blue breccia below (upper and lower parts of the upper volcaniclastic breccia respectively). Possibly an alteration or weathering feature within the same unit.

Figure 42: Similar-looking contact plane to Figure 41 between a dull, yellow-grey breccia above and a pink-red breccia below. This outcrop occurs to the southeast of the outcrop in Figure 41, across the valley.

On the slope behind the Noordhoek farmhouse, the upper volcaniclastic breccia appears to have thickened rather dramatically from 20-30m to almost 100m. It is also positioned lower in altitude than the outcrop across the valley to the southeast. A contact between a yellow-coloured unit above and a blue-grey unit below is observed (Figure 41). The contact is sharp, appears planar, dips to the south at 7°, and may separate a more weathered or altered part of the upper breccia from the rest of the breccia. A similar contact plane occurs at the same elevation across the valley to the southeast (Figure 42). This contact plane has a less pronounced colour change than the contact on the hill behind the Noordhoek farm.

7.6.6 Petrography of volcaniclastic breccias

In thin-section both volcaniclastic breccias are very similar in terms of size and type of clast within the matrix, and as a result, the petrography of the upper and lower volcaniclastic breccias are described together. The proportions of individual clast types vary between the upper and lower volcaniclastic breccia. This is discussed later in the section on modal analyses.

Sedimentary Clasts in Volcaniclastic Breccias

Fine-grained (0.2-0.4mm), subrounded sandstone clasts are common in the volcaniclastic breccias. They contain varying amounts of clay and so classify as sandstone to greywacke. Fewer clasts of dark siltstone, very fine-grained, grey mudstone/shale and red sandstone and red shale occur in the volcaniclastic breccias than occur in the sandstone clasts. The unaltered sandstone clasts are colourless to slightly yellow, and have a colourless to grey, argillaceous matrix. Some sandstone clasts have a slight pinky-brownish colour caused by many 1μm-sized haematite grains in the matrix.

In one section two matrix-supported, medium-grained sandstone clasts contain calcite in the matrix which has totally replaced the previous interstitial material. Due to the complete replacement by carbonate, compared to the relative lack of carbonate replacement of adjacent clasts, these clasts appear to have undergone alteration and secondary replacement before the eruption which incorporated them into the lower volcaniclastic breccia.

No gas or water escape structures, which may have formed from unconsolidated sandstone being heated by intruding basalt, are evident in any of the sandstone clasts. The lack of such structures

in the sandstone does not imply that heating of the sandstone did not occur. The sand could have been dry, already lithified, and the structures may not be clear in outcrop, or may not even have formed. The sandstone is also more likely to have fractured around these structures. The matrix of the sandy clasts is dominated by very fine-grained quartz and feldspar, muscovite and sericite, with accessory amounts of chlorite, sphene, amphibole and zircon. The sericite in one section exhibits a localised preferred orientation of crystals in bundles, with each bundle either lying parallel, or perpendicular to adjacent bundles.

Basalt Clasts in Volcaniclastic Breccias

Many of the largest clasts in the volcaniclastic breccias are basalt due to their resistance to weathering. The porphyritic basalt clasts are angular to subrounded. Large plagioclase laths, up to 1.9mm in size are clouded with numerous tiny inclusions. The laths range from fibrous or acicular, to tabular (1:4 width:length). Pyroxene grains (predominantly clinopyroxene) with a similar size to the plagioclase are also evident in many basalt clasts, and accessory amounts of orthopyroxene are found. No preferred orientation of the phenocrysts is evident in any of the basalt clasts. Most clasts have a fine-grained matrix which has altered to a dull yellow-brown colour, and contains a large number of micrometer-sized, red haematite and cubic magnetite grains. The rest of the matrix consists of varying proportions of small plagioclase and clinopyroxene grains, and fragments of glass. In some of the finer-grained basalt clasts parts of the interstitial matrix consist of glass. Calcite occurs as a secondary phase in the matrix and in some amygdales. Angular quartz grains less than 2mm are evident in the basalt clasts. This is not unlikely as many basalts were intruded through and extruded over sandstones.

Evidence of slight palagonitisation of the edges of basalt clasts in the volcaniclastic breccias also exists where the clast boundaries are somewhat corroded and uneven. This suggests the alteration occurred after the basalt was incorporated in the volcaniclastic breccias. Amygdales in one section contain very fine-grained palagonite around the rims, while the centres are filled with calcite.

Patches of acicular, intergrown plagioclase laths are present in the matrix in parts of the upper volcaniclastic breccia. The largest patch is 3.5mm, the smallest, 2.5mm, and all contain some fragments of acicular glass and blebs of carbonate. There is no preferred orientation of the laths, and there is some evidence of a feature resembling granophyric texture in places. However, the minerals are too fine-grained for identification. These patches may be remnants of very coarse-grained doleritic fragments which crystallised lower down and were brought to the surface during the explosive eruptions, producing the volcaniclastic breccias, as is the case for the plagioclase patches described earlier.

Glass Fragments in Volcaniclastic Breccias

Angular glass fragments are abundant in the volcaniclastic breccias and range up to 7mm in size. They are highly palagonitised (yellow-brown in colour) and the alteration is concentrically banded (Figure 43, a and b). Some shards have well-developed, cuspate edges (Figure 44) but most are straight-sided and angular. Many of the larger shards contain phenocrysts of plagioclase and/or pyroxene, and rarely olivine. In a few of the larger fragments, calcite has filled the vesicles (Figure 45). Part of the glass is broken off, leaving the remaining glass on one end of the phenocryst. In some sections glass fragments appear laminated or banded.

Figure 43 (a)

Figure 43, a and b: Highly palagonitised basaltic glass fragments common in both volcaniclastic breccias. Note the many plagioclase laths within the fragment and the banded nature of the fibrous palagonite. The glass fragments are angular due to the rapidly-cooled basalt being fractured. The breccias must either have been transported as a solid mass, or over a short distance for the glass fragments to have remained angular and not have been rounded. Samples from lower volcaniclastic breccia ~150m northwest of Site *g* (Figure 16). (Magnification: 25x and 100x)

Figure 44: Cuspate boundaries of a glass shard. Sample from lower volcaniclastic breccia outcrop on slope behind Noordhoek farmhouse. (Magnification: 100x)

Glass fragments are sometimes amygdaloidal and the amygdales are predominantly filled with fibrous zeolites. Few amygdales contain very fine-grained quartz and feldspar. This could result from interstitial or matrix sand grains entering open vesicles anytime from initial mixing of the magma and sediment to after the emplacement of the breccias. The orientation of the thin-section slice may also cause the vesicle to appear as though it completely encloses the sand grains.

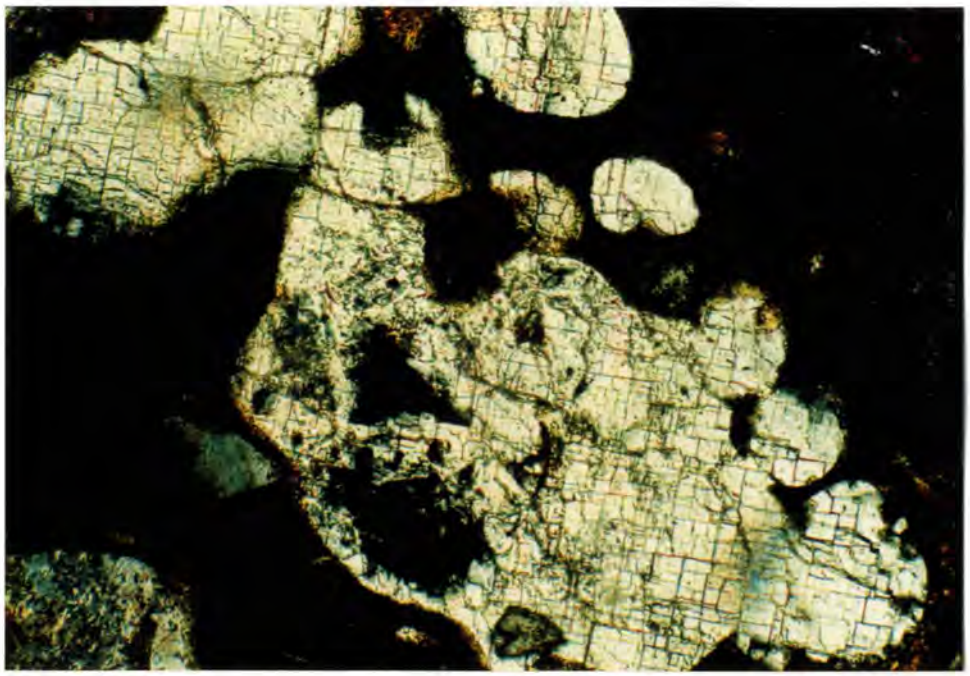

Figure 45: Calcite in vesicles in a basalt sample from the lower volcaniclastic breccia on the western slope of Perdekop. (Magnification: 100x)

Matrix of Volcaniclastic Breccias

The poorly-sorted matrix of the volcaniclastic breccias contains predominantly angular quartz and feldspar grains with a moderate sphericity, although some grains are rounded with a high sphericity, as well as tiny clasts and argillaceous material. Some clinopyroxene grains, the same size as the quartz and feldspar, occurs in the matrix material. The finer-grained material consists of very fine-grained clays, quartz, feldspar, and palagonitised basaltic glass. Sphene, zircon, chlorite, muscovite, and opaques are present as accessory minerals in the volcaniclastic breccias. Carbonate, which is evident in some sections but not others, has crystallised as a secondary alteration of plagioclase or argillaceous matrix. It fills pore spaces or replaces matrix material in the volcaniclastic breccias, displaying euhedral crystal shapes.

The matrix in the volcaniclastic breccias is often altered, the colour changing from an unaltered, generally light yellow-green to a dark orange-brown depending on the degree of alteration. Devitrified glass, most commonly present rimming the basalt vesicles, has generally been altered to a fibrous palagonite. Usually the order of alteration from the edge of the vesicle towards the centre is palagonite, zeolite, carbonate, but very few clasts have all three, and only some have two. Palagonite and zeolite are mostly seen with a fibrous habit as a replacement of basaltic glass fragments or filling amygdales or small vugs respectively. Calcite fills the interstices around clasts, crystals or grains, sometimes replacing the matrix, and also fills fractures in the volcaniclastic breccias.

7.6.7 Porphyritic Basalt Clasts in Volcaniclastic Breccias

Fragments of a porphyritic basalt contain plagioclase laths up to 1cm in length which occupy approximately 60% of the fragments. These have been found predominantly in the upper volcaniclastic breccia. No outcrop of this rock type is found anywhere in the field area, and it is assumed that the upper flow must have brought fragments of this unit from further afield. It does, however, have a different petrography to the finer-grained basalt lava flows within the field area, and is described separately below.

Plagioclase

The plagioclase laths are coarser-grained (average 3.5mm up to 10mm in length) and more tabular or rectangular (1:3 width: length) than those in the lava flows. They are also far more corroded (still rectangular in shape, but boundaries less sharp and clear) and altered (grey-brown,

cloudy appearance), presumably due to the larger surface area of the crystals. Both unclear crystal boundaries, and twinning are indistinct.

The finer-grained (1.5mm and less), interstitial plagioclase might possibly coexist with alkali feldspar and/or quartz, but due to the size of the laths it is not clear if this is the case. Marsh (pers.comm., 1998) states that alkali feldspar, although present in the Karoo basalts, is not very abundant. Sutured contacts are very evident between the plagioclase phenocrysts and the interstitial plagioclase. The interstitial plagioclase laths contain inclusions of heavily altered material of unknown composition. Possibilities include amphibole and clay minerals. The laths are inferred to be the product of a late-crystallising phase of granophyric intergrowth with quartz.

Amphibole

Hornblende commonly occurs interstitially between the plagioclase and clinopyroxene grains, commonly as fibrous crystals, and as an alteration product of original augite phenocrysts. Few original clinopyroxene grains remain. Those that have remained unaltered are up to 4.5mm in size, and in most cases, fractured. A high concentration of opaques are present in the amphibole; as magnetite and translucent, red haematite.

Carbonate

A moderate amount of alteration or replacement calcite is present in the section, where calcite fills interstices, surrounding clasts in patches. Much calcite has crystallised in a botryoidal form, apparently filling small vesicles, although this is not particularly clear. The calcite contains a high concentration of tiny opaques which have red margins. The carbonate fluids could have originated from the melt, altering what had just been crystallised, but judging by the large amount

of carbonate throughout the thin section, the carbonate is more likely to be the product of later hydrothermal fluids permeating through the rock.

Accessory Phases

An abnormally high concentration (~ 2%) of accessory apatite is present as tiny needles with a high relief and anomalous birefringence. Sphene, haematite, magnetite, chlorite, quartz, and very few zircon grains are also present throughout the section.

7.7 PEPERITE

Peperites may form by a process of sediment fluidisation (Kokelaar, 1982) where large volumes of wet sediment can be replaced by igneous material with minimal disturbance of the remaining host. The terms fluidal or globular and blocky peperite (Busby-Spera and White, 1987) describe the appearance of the peperite after it has been formed. Fluidal peperite is the result of a mixing of basalt with wet sediment where the basalt has cooled and solidified slowly enough to avoid fracturing. When the basalt is cooled too quickly, it fractures, forming a breccia of basalt fragments in sediment and this is termed blocky peperite.

Within the lower volcaniclastic breccia peperite clasts are common. Both blocky and fluidal types occur. Along the north-eastern edge of the dolerite intrusion in the west of the study area, fluidal peperite outcrops along the basal contact of the dolerite and the underlying sandstone. It is identical in appearance to the peperite clasts in the lower volcaniclastic breccia, suggesting a possible source for the peperite clasts.

Although fluidal peperite is predominantly observed as clasts within the lower volcaniclastic breccias, blocky peperite is observed *in situ* where the Moshesh's Ford basalt has extruded over consolidated and unconsolidated Clarens sandstone. This results in the preservation of a thin veneer of peperite along the contact (Figure 46). This demonstrates that the Clarens sandstone was at least partly unconsolidated and/or wet in parts.

Figure 46: Blocky peperite exposed in an outcrop approximately 250m east of sites ***d*** and ***e***. This implies a wet sediment rapidly cooling a thin veneer of basalt above. The chilled basalt fractures as it cools, forming the blocky appearance.

Figure 47 has the appearance of blocky peperite, but may only represent the sole of a basalt flow which fractured when chilled by wet sediment below, allowing the penetration of fluidised sediment (Figure 48). The basalt sole thus remains intact and non-brecciated. In Figure 47 it does not seem likely that the basalt fragments have completely detached and rotated. Basalt

clasts containing angular quartz grains occur in the volcaniclastic breccias and provide more evidence for basalt-sediment mixing.

Figure 47: Contact between sandstone and overlying basalt which appears to be brecciated, approximately 600m east of sites ***d*** and ***e***.

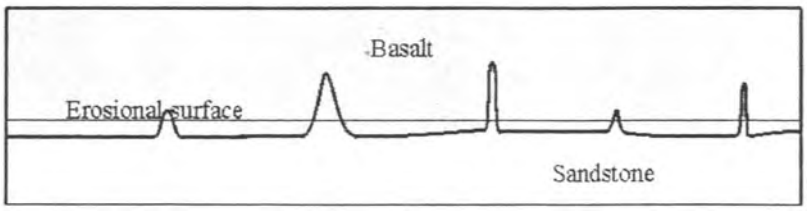

Figure 48: Sketch of the basalt-sandstone contact of Figure 47 where recent erosion has exposed sandstone in the cooling fractures at the base of the overlying basalt flow.

7.8 LITHOLOGY OF BASALT LAVA FLOWS

The explosive eruptions that produced the volcaniclastic breccias occurred due to the movement of intruding magma towards the surface. The lower volcaniclastic breccia was produced after the emplacement of the Moshesh's Ford lava flows in the volcanic complex. This is evident because the Moshesh's Ford lava flows are present outside the volcanic complex, but absent within the complex. This suggests that the Moshesh's Ford lava flows were erupted from the volcanic complex when the lower volcaniclastic breccia was produced. Subsequent lava flows began to cover the breccia, building up into a thick pile of flood basalt. All the lava flows are inferred to have originated outside the study area, because no source vent is present in the study area, and because they are laterally persistent outside the volcanic complex, and the same magma types are observed throughout most of southern Africa (Figure 2) and Antarctica. Further explosive activity outside the study area and during the emplacement of the lava flows produced the upper volcaniclastic breccia. The quiet extrusion of the flood basalts presumably reflects a depletion of available groundwater near the vent, while the source areas of the volcaniclastic breccias had more groundwater and/or a higher rate of magma supply which caused explosive eruptions which produced the breccias.

Owing to the great variation in thickness of the Clarens sandstone over distances as short as 300-400m, the thicknesses of the first few basalt flows vary considerably compared to the upper basalt flows due to their filling topographic irregularities. The upper basalt units extruded onto a horizontal substrate, forming fairly laterally continuous, horizontal, compound, pahoehoe lava flows.

There is considerable textural variation through individual basalt flows, so coarse-grained and fine-grained basalt can be observed within the same flow. Some flows have an overall finer-grained appearance to others in the study area, and these are commonly the more resistant basalt flows capping the hilltops. The coarser-grained areas of a basalt flow commonly possess a small amount of residual glass, and the feldspar occurs either as porphyritic crystals (up to 8mm) between which small grains of augite and feldspar lie, or as small laths which are partially or wholly enclosed by masses of augite. The centre of the basalt flows is commonly bluey-grey when fresh, but alters to a dull browny-purple when weathered. Undulose extinction is evident in most crystals, indicating a period of stress either during emplacement or after. The majority of the thin-sections display minerals that have a hazy appearance created by the presence of tiny inclusions in the crystals. Slightly larger inclusions of zeolite, a little chlorite, and occasional apatite are also present. Further alteration, mainly zeolite, ranging from fairly light, pale yellow-coloured to heavy, dark brown-yellow-coloured has affected most of the crystals in the basalt. Under heavy alteration many of the crystal boundaries are very indistinct, and the identification of the minerals is more difficult.

Plagioclase

The plagioclase laths are subhedral to euhedral, acicular or prolate to almost square, and equant. There is no preferred orientation of the crystals in the basalt flows with some laths displaying a radial habit (Figure 49). The laths range in size from 1.25mm and less in length (averaging ~0.35mm). The plagioclase displays a variety of twinning; the main types being simple, pericline and polysynthetic. Alteration of the plagioclase often takes the form of tiny inclusions throughout the plagioclase crystals, giving them a cloudy appearance. In some areas the

alteration appears to be more sericitic, while in others the inclusions are predominantly zeolite, and chlorite.

Figure 49: Radial habit of plagioclase laths which is often a result of rapid cooling. Sample from basalt ~100m south of Site ***h*** (Figure 16). (Magnification: 100x)

A number of patches (from ~1mm to 6mm x 2.5mm) of closely-packed, intergrown plagioclase laths exhibiting a trachytoid to glomeroporphyritic texture exist (Figure 50). The majority of the phenocrysts have undergone sericitic alteration, manifested as tiny, angular, elongate crystals of mica and sericite. These patches could possibly be fragments ripped from the neck of the magma conduit. Some of the patches contain variolitic laths, but the majority show straight laths in a radial splay. These slightly curved laths are a common product of a fairly fast-cooling melt.

Figure 50: Trachytoid to glomeroporphyritic texture of short, broad plagioclase laths. Sample from basalt ~500m northwest of Site ***f***, and adjacent to circular sandstone block (Figure 16). (Magnification: 25x)

Most of the larger pyroxene crystals exhibit ophitic textures with the inclusion of many plagioclase laths. These laths often fragment the crystals, accelerating the rate of alteration by providing a larger surface area of the crystal.

In a number of thin sections, large amygdales exist which are filled with zeolites and a thin rim of fibrous zeolite. Adjacent to these amygdales the plagioclase laths in the main body of the unit appear particularly clear and unaltered with very few alteration inclusions or other evidence of alteration.

Olivine

Little olivine is found in the basalts, and in many specimens examined, only small amounts of highly altered olivine were encountered. The olivine appears to be closely related to the

accessory opaque minerals in the matrix, but this could be an association with the serpentinisation surrounding the olivine. This suggests that if the opaques are magnetite, and thus Fe-rich, the source of that Fe could be the olivine grains themselves. However, the magnetite could be subsolidus, having crystallised as a late-stage primary phase in the basalts.

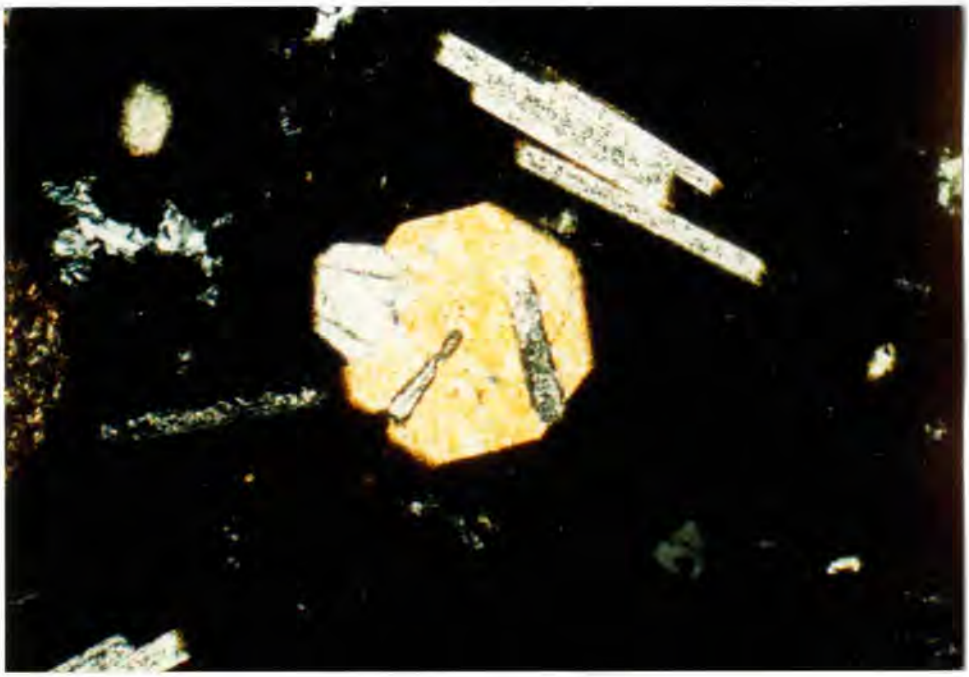

Figure 51: Euhedral clinopyroxene crystal. Sample from basalt clast in large volcaniclastic breccia outcrop northwest of large dam almost in centre of Figure 16. (Magnification: 100x)

Pyroxene

Both augite and pigeonite were identified in the basalts, and are anhedral to subhedral in shape. Very rarely, a euhedral pyroxene crystal is observed (Figure 51). The original crystals are inferred to have been approximately 1.5mm or larger in diameter, but now the largest unaltered pyroxene grain is about 0.75mm. They are noticeably larger than the olivine grains and generally far less altered. The unaltered crystals commonly display an ophitic texture due to the inclusions

of plagioclase laths. Marsh (pers.comm., 1998) states that pigeonite is a very common mineral in the Karoo basalts and dolerites. In some sections in the study area, it is observed as small grains surrounding the larger augite grains.

Matrix

In most basalt flows, the unaltered matrix is a darker brown than the palagonite and zeolite. The dark colour is probably caused by the ultra-fine-grained (cryptocrystalline) interstitial crystallites of pyroxene, and/or dendritic oxides as a result of quench crystallisation. The cooling of the melt, although rapid, was slow enough for tiny crystallites to form. In many areas, the glassy matrix has been altered to palagonite or less commonly, zeolites.

In a few sections, "microphenocrysts" of plagioclase and clinopyroxene are noted in the matrix. These were most likely quench-crystallised from the residual fluid in the magma chamber, after eruption. This quenching resulted in the formation of thin, curved, inter-grown crystals of both plagioclase and clinopyroxene.

Alteration

Zeolite appears to be more common in the basalts than palagonite, as an alteration product, although in certain sections they are equally represented, or one may exist without the other. The palagonite and zeolite can be either fine-grained and fibrous or cryptocrystalline.

It seems that in almost all cases fibrous palagonite surrounds the rim of glass fragments or vesicles, and zeolite (also predominantly fibrous) continues in a banded fashion from the palagonite towards the centre (Figure 52, a and b). In some cases calcite occurs in the centre of

the vesicles. This suggests that palagonite was the first alteration product after the crystallisation of the melt, followed by zeolite alteration, and lastly by calcite precipitation.

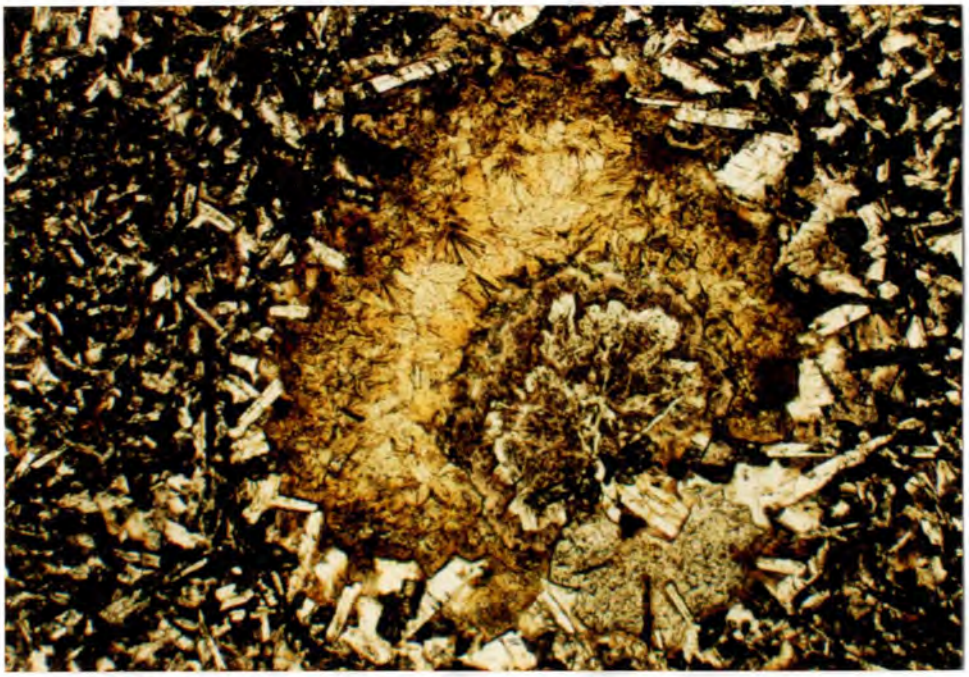

Figure 52 (a)

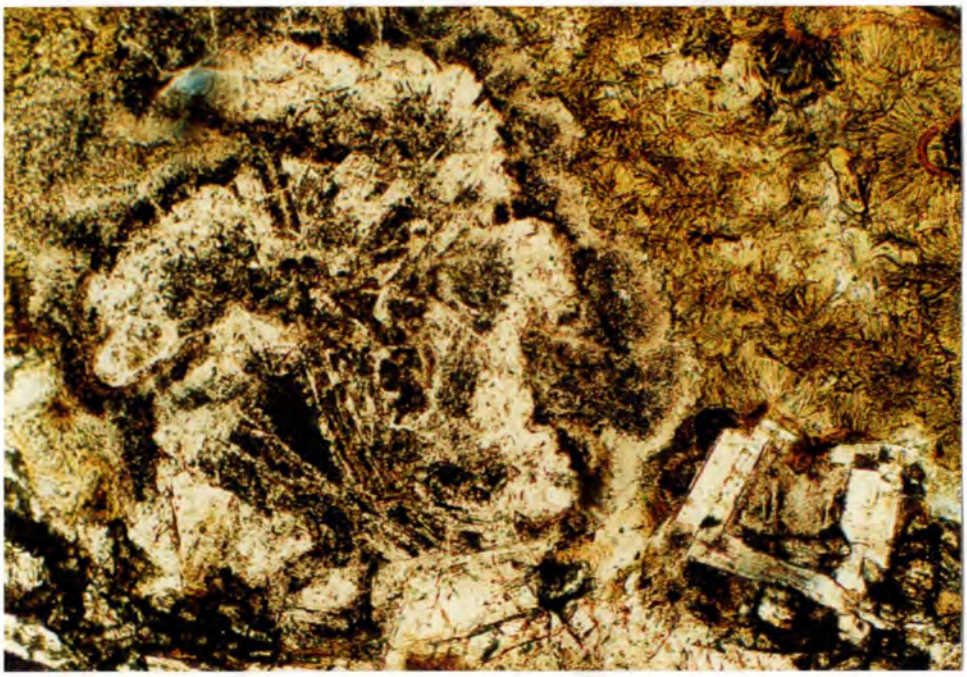

Figure 52, a and b: Banded fibrous palagonite on the outside, changing to banded zeolite towards the centre of the glass fragment. The palagonite alteration occurred prior to zeolite alteration as the glass fragment was altered from the outside in. Sample from Roodehoek basalts north of altitude marker in southeast of Figure 16. (Magnification: 100x)

The main conduits for the movement of the fluids which cause the alteration of the rock are the vesicles, because in many cases the palagonitisation appears to have begun around the edges of the vesicles (where glass is in contact with hydrous fluid), and then spread into the rest of the rock.

The alteration contains a high concentration of cubic opaques which, according to Gevers (1928), are most probably magnetite, and small, red, translucent, anhedral to rounded grains of haematite. The cubic magnetite crystals are 0.3mm and less in size, averaging 0.17mm, while the haematite grains are far smaller. In many cases the cubic opaques are intergrown with each other in dendritic bunches, still retaining the euhedral shape (Figure 53). This dendritic pattern is also due to quench crystallisation which is very common in fast-cooling magmas.

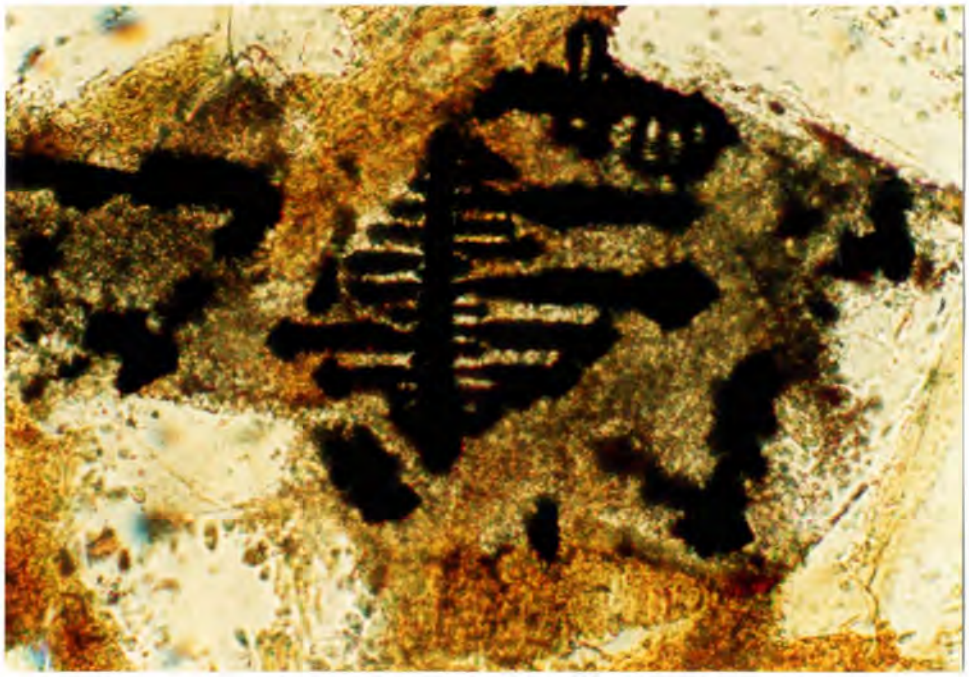

Figure 53: Euhedral, cubic dendrites of magnetite grains caused by rapid cooling of the basalt flow. Sample from western-most Tafelkop basalt type outcrop in Figure 16. (Magnification: 100x)

Carbonate has crystallised in the interstices of some rocks, in the core of some vesicles, and in many veins or fractures. This appears to be the last stage of hydrothermal fluid permeation, where carbonate has been precipitated in spaces throughout the rock. In some places the carbonate is the sole alteration product for the section.

Nearly all of the flows have a lower zone (2-60cm from the lower contact) with a high concentration of amygdales, and an upper zone of similar size with fewer amygdales. These amygdales are filled with either quartz, calcite or zeolites, and in some cases the zoning of all three in the same amygdale is evident (zeolites to calcite to quartz in the centre). Pipe amygdales are also very common in the lower zones of the flows, and have the same secondary mineralisation. The pipes are usually perpendicular to the base of the flow, although in rare cases, curved pipes are observed. One of the lava flows on Tafelkop contains pillows, and some of the flows capping the hills in other parts of the study area display columnar jointing (Figure 54). In one locality, near the top of the Perdekop peak, a flow top displays a well-developed pahoehoe surface (Figure 55).

Figure 54: Columnar jointing in an aphanitic basalt flow forming the capping of the hill at the top of Log 8.

Figure 55: Exposed upper surface of a pahoehoe basalt flow near the top of Perdekop.

Basalt lava flows generally overlie the volcaniclastic breccias with a regular planar contact but in places the contact may be very irregular and disrupted. No peperitic contacts are observed between the basalt flows and either of the volcaniclastic breccias, presumably due to a lack of water and/or a coarseness of the breccias which would prevent fluidisation occurring. Sandstone lenses are interbedded within the flow sequence, providing evidence for periods of continued sand deposition between lava flows. The low-angle (10-20°), cross-bedded nature of the sandstone, as well as ripple marks observed on the surfaces of some lenses suggest a fluvial depositional regime. Although ripples are also observed in marine environments, no evidence exists in the study area for a marine environment. Some contacts between sandstone and basalt, and volcaniclastic breccia and basalt are complex, with fragments of the one lithology in the other (Figure 56). The time period between one lava flow and the next one was always too short for a palaeosol to have developed.

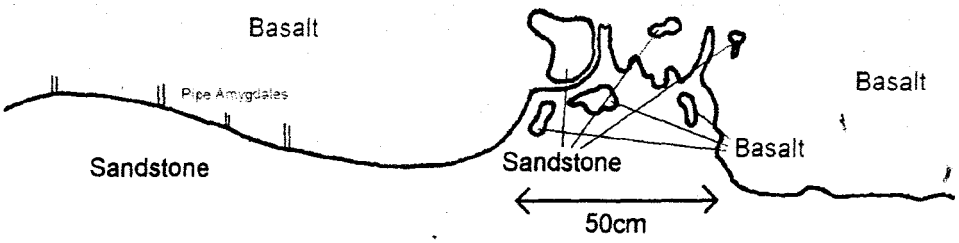

Figure 56: Sketch illustrating the irregular contact between sandstone and basalt. In many areas the flowing basalt appears to have eroded or "ripped up" the upper surface of the sandstone and incorporated sandstone fragments into the flow, although this may be a fluidisation peperite-forming process.

7.8.1 Petrography of Basalt Geochemical Types

The basalt lava flows in the study area can be subdivided into five distinct basalt types (Mitchell, 1980), based on petrographical characteristics and geochemical signatures. The geochemical characteristics are discussed later in section 10.2 (Geochemistry of Lava Flows), but a brief summary of the petrographical characteristics of the five basalt types is outlined here.

Vaalkop

The Vaalkop basalts in the study area are hypocrystalline and porphyritic, tending towards glomeroporphyritic. The main phenocrysts are labradorite and augite with a ratio of 9:1 respectively. Olivine occupies less than 2% of the rock, while the phenocrysts occupy 20-30%. The groundmass is plagioclase, clinopyroxene, and acicular opaque oxides (Mitchell, 1980).

Roodehoek

According to Mitchell (1980) the Roodehoek basalts are divided into two types. Type A is hypocrystalline, and phaneritic with seriate texture. Augite occupies 30-40% of the rock, and the augite crystals often contain cores of pigeonite. Plagioclase exhibits normal compositional zoning in the range An_{50} - An_{80}. Olivine occupies less than 5% of the rock, although proportions of up to 20% have been noted in some outcrops. This basalt in the study area exhibits evidence of rapid cooling, indicated by the highly zoned nature of the mineral grains and a glassy mesostasis. Type B has a glomeroporphyritic texture. Labradorite phenocrysts occupy 15-20% of the rock, while olivine only occupies 5% (Mitchell, 1980). The groundmass of the basalt in the study area consists of microcrystalline plagioclase and clinopyroxene.

Tafelkop

The Tafelkop basalts in the study area are hypocrystalline and phaneritic fine-grained basalts. They contain acicular and anhedral opaque oxides, and also exhibit evidence of rapid cooling with a glassy mesostasis occupying 20% of the rock, and zoned plagioclase phenocrysts.

Moshesh's Ford

The Moshesh's Ford basalts in the study area are hypocrystalline and phaneritic. Plagioclase is present as zoned, subhedral laths ophitically intergrown with intersetal augite. The plagioclase has a compositional range from An_{40} to An_{60} (Mitchell, 1980). Pigeonite commonly occurs as cores to the augite. Mitchell (1980) observed that olivine is almost entirely altered to iddingsite, serpentine and bowlingite, and that glassy mesostasis occupies 15% of the rock and crystallites of K-feldspar, quartz, apatite as well as Fe-Ti oxides occur in the mesostasis.

7.9 INTRUSIONS

A number of dykes, frequently varying in width from 1-2m to 5-6m, outcrop throughout the study area (Figure 57). These exhibit well developed columnar jointing perpendicular to the walls of the dyke. The chilled margins of the dykes are frequently more resistant to weathering than the central zone, and some dykes exhibit a "train-track" appearance in the field.

Figure 57: An example, 800m south along the dyke at Log 9, of the many dykes encountered in the study area. Note the cooling fractures perpendicular to the walls of the dyke.

Andesite intrusions are fairly common in the Karoo volcanics as intrusions, veins and/or interbeds (Mountain, 1960). Gevers (1928) first identified the "highly compact, light andesitic type of basalt" surrounded by lower volcaniclastic breccia on the farm Roodehoek (in the north-western corner of the study area). He believes it to be a source of the lower volcaniclastic breccia. This theory is discussed in section 10.6. Rumble (1979) claims that the andesite intrudes the Elliot Formation and has a faulted and brecciated contact along the western edge. The andesite intrusion is not in contact with or near to the Elliot Formation at any point along its margin. It does, however, intrude the lower volcaniclastic breccia. The sharply-defined contact of which is best seen along the western margin of the andesite. No fault is evident along the western contact as stated by Rumble (1979).

A large dolerite intrusion marks the northwestern and western boundary of the volcanic complex (Figure 4 and Map, Appendix B) and its southern extension terminates against the fault marking the southwestern boundary of the complex. The exact relationship between the dolerite and the fault is not observed, and it is inferred from the orientation and position of the dolerite intrusion that the intrusion exploited the fault plane and thus marks the western boundary of the complex.

Figure 58: A megablock of Elliot sandstone units presumably incorporated into the large dolerite intrusion in the west, and tilted at approximately 25°. The 2.4km x 1km block is completely surrounded by dolerite which forms the lower-lying ground in this figure.

No volcaniclastic breccia outcrops on the western side of the dolerite intrusion, and no mixing between the intrusion and the lower volcaniclastic breccia is observed except for possibly a small area at the northern edge of the main body of dolerite. This implies that the dolerite intruded after the faulting of the western edge of the volcanic complex, but might have been instrumental in the emplacement of at least some of the lower volcaniclastic breccia outcropping in the valley

to the east. Gevers (1928) believes this intrusion to be a volcanic vent, from which he suggested the lower breccia was erupted. This theory is discussed later in section 10.6.

A megablock of Elliot Formation sandstone and shale is surrounded on all sides by the doleritic intrusion, and has been tilted by the dolerite so that it now dips to the west at ~25° (Figure 58).

8.0 Comparison between the Volcaniclastic Breccias in the Study Area and Stratigraphically-Equivalent Deposits in the Central Transantarctic Mountains, Antarctica

Pyroclastic deposits, interpreted as lahar deposits, in the central Transantarctic Mountains closely resemble the volcaniclastic breccias encountered in the present study area. They represent the Antarctic equivalent of the explosive eruptions occurring on the African continent prior to the break-up of Gondwana during the mid-Jurassic (Hanson and Elliot, 1996). By comparing the lahar deposits in the Transantarctic Mountains to the volcaniclastic breccias in the present study area, similarities and differences between the types of deposits can be described on a continental scale.

The tholeiitic Kirkpatrick basalts of the Transantarctic Mountains overlie the widespread tholeiitic pyroclastic deposits, called the Prebble Formation (Figure 59), in much the same way as the Drakensberg basalts overly the volcaniclastic breccias in the present study area. The Prebble Formation has a thickness >360m (compared with ~100m in the study area) which suggests that it may have been confined by topography and forced to thicken vertically, rather than spread out over a larger area. The Prebble Formation is part of an extensive phreatomagmatic field estimated to have covered an area $\geq$7500km^2 (compared to an approximate 8400km^2 in the Karoo Basin). No visible vents for either the Kirkpatrick flood basalts or the Prebble Formation lahar deposits were observed in the field area along the Queen Alexandra Range of the Transantarctic Mountains (Hanson and Elliot, 1996). Neither were any dykes extending from the Prebble Formation into the basalt flows.

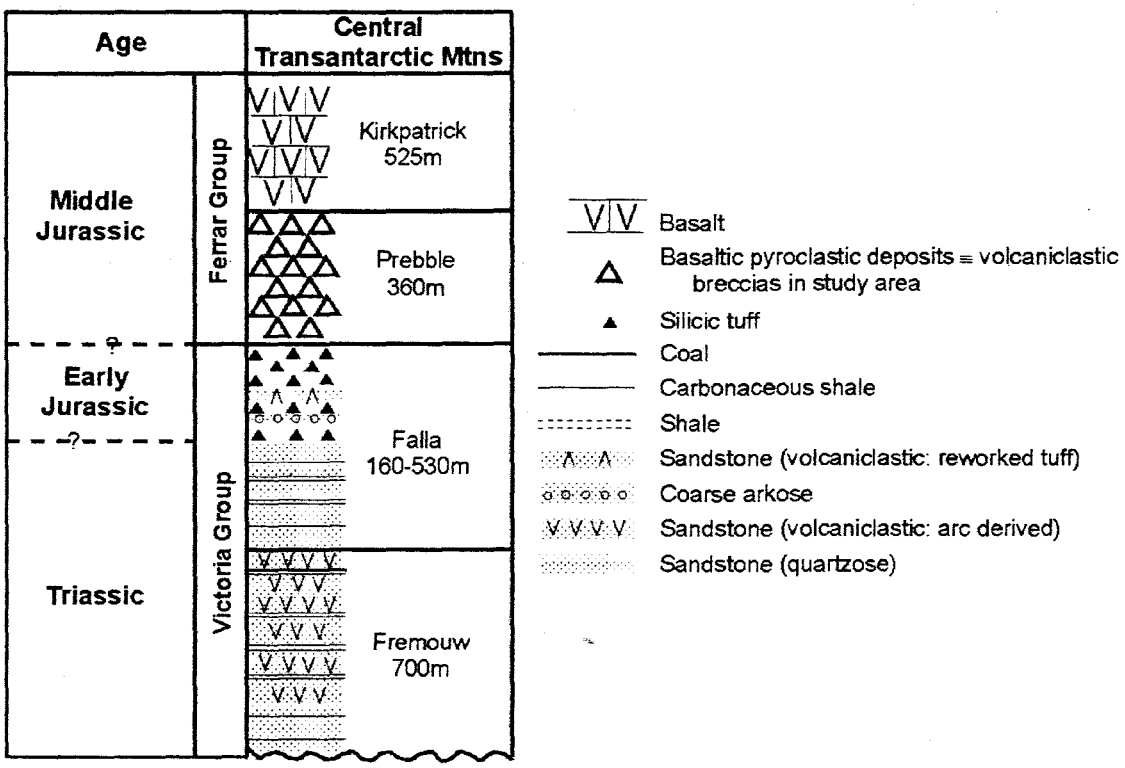

Figure 59: Simplified stratigraphic column for Victoria and Ferrar groups in the central Transantarctic Mountains (after Hanson and Elliot, 1996). The Prebble Formation is equivalent to the volcaniclastic breccias in the study area.

The Prebble Formation consists of 50-60% accidental lithic fragments and sand grains from the underlying strata. This is very similar to the abundance of Elliot and Clarens Formation fragments in the volcaniclastic breccias in the study area (Section 7.6.1). Hanson and Elliot (1996) believe this suggests an explosive phreatomagmatic interaction of basaltic magma with wet sediment. Some clasts are scoriaceous to vesicular with elongate forms, and have vesicles aligned parallel to the clasts' long axes. This suggests that these clasts were formed in a vesiculating magma during upward flow in a conduit. Such clasts were not observed in the volcaniclastic breccias of the Brosterlea Volcanic Complex, and neither was there any evidence for direction of flow in the matrix of the breccias. Other pyroclasts described by Hanson and

Elliot (1996) were droplet-shaped, and were believed to have been generated from a magma which was still fluid when blasted apart during explosive magma-water interactions. These droplet-shaped pyroclasts were not observed in the Brosterlea area, although ribbon bombs and cored bombs were. Droplet-shaped pyroclasts are observed in equivalent breccias in the Sterkspruit valley near Rhodes, in the Barkly East area (Skilling, pers. com., 1999). Hanson and Elliot (1996) also described armoured lapilli in some of their deposits indicating the cohesive nature of wet ash.

The petrography of the deposits in Antarctica is very similar to the petrography of the deposits in the Brosterlea Volcanic Complex. The abundance of sideromelane and palagonite in the Prebble lahars is consistent with a hydrovolcanic origin (Hanson and Elliot, 1996). Palagonite is also very common in the volcaniclastic breccias in the Brosterlea Volcanic Complex. In the Prebble Formation, as in the volcaniclastic breccias, secondary mineralisation occurs as pore-filling cements and as alteration products of glass and primary igneous minerals. Zeolites are very common throughout the Prebble Formation, and smectitic clays, very fine-grained, disseminated haematite, leucoxene, and calcite are present in smaller amounts.

The bedding contacts in the Prebble Formation are diffuse, and are defined by gradational changes in clast size and abundance, indicating rapid emplacement of several lahars, or a series of pulses during a single lahar event. Most of the units are coarser at the base, some have erosional basal contacts, and channels were also identified in some units. The volcaniclastic breccias in the Brosterlea Volcanic Complex were almost entirely massive, poorly sorted and ungraded, although the outcrop on the western slope of Perdekop (Map, Appendix B and

Figure 4) does display a general subdivision into three subunits. However, the subunits are not as clearly defined as the units described in the Prebble Formation.

Planar-bedded deposits ≤60cm thick and containing tuff, lapilli-tuff, abundant accretionary lapilli and pyroclasts, typically better sorted and finer-grained than the lahar pyroclasts, are described by Hanson and Elliot (1996). These are not observed in the Brosterlea Complex.

There is no sedimentological evidence for the presence of large lakes at the time of the emplacement of the Prebble Formation. Therefore the formation is inferred to have occurred in a rift basin with aquifers in the Falla Formation sandstone, underlying the Prebble Formation, supplying water to the system. Lacustrine units, cross-bedding and ripple marks described in the Brosterlea Volcanic Complex suggest the presence of water and wet sediment needed for the eruption and emplacement of the lower volcaniclastic breccia.

The Prebble Formation lahar deposits closely relate to the volcaniclastic breccias in the Brosterlea Volcanic Complex petrographically and lithologically. It appears that these pyroclastic deposits throughout southern Africa and Antarctica vary little on a regional scale. Although their palaeoenvironments are interpreted as having been slightly different, the formation mechanism, that of phreatomagmatism due to the interaction of basalt with wet sediment, is the same for both deposits. Since the continents were joined at the time of the explosive eruptions, it is likely that their palaeoenvironments were similar enough for the deposits to have formed in the same way.

9.0 Comparison between the Volcaniclastic Breccias in the Study Area and similar breccias in the Stac Fada Member in the lower Torridonian succession, Scotland

The volcaniclastic breccias in the study area might be referred to as erupted peperite deposits due to their mechanism of formation by magma intruding wet, consolidated and unconsolidated sediment. The Stac Fada Member is the only example in the literature of similar rocks to the Karoo-Ferrar breccias. The Stac Fada Member within the Lower Torridonian succession of the Stoer Group is inferred to have been generated by phreatomagmatic activity and transported to the surface as a "buoyant peperitic slurry" (Sanders and Johnston, 1989).

The Stac Fada Member differs from the outcrops of volcaniclastic breccia in the study area, outcropping as a narrow (≤200m) dyke that extends for 5km N-S. Similar deposits occur in isolated exposures within the Stoer Group over a strike length of approximately 50km. The "peperite" deposit comprises a matrix of poorly-sorted, dark red sediment with a mud to sand grade. The sand-sized particles include quartz and feldspar with minor amounts of epidote, mica, opaques, and chlorite. The matrix supports many angular clasts, ≤1cm in size on average. These clasts are of a green to black, aphyric, chlorite-dominated volcanic material, many of which are microbreccias with angular quartz and feldspar grains in a green chlorite matrix. Some are micro-vesicular tephra, while others appear to be fine-grained albitite (Sanders and Johnston, 1989). Clasts of mudrock, sandstone and basement gneiss are also common in the peperite.

The slurry is inferred to have originated when magma intruded the wet, unconsolidated sediment of the Stoer Group succession. Rapid expansion of pore water caused fluidisation of the sediments, fragmentation of the volcanic material and mixing of the two. The resultant highly mobile, steam-inflated slurry possibly exploited several conduits to rise to the surface (Sanders and Johnston, 1989) (Figure 60). This mechanism appears similar to that described by Grapes *et al.* (1973) and was responsible for the generation of the volcaniclastic breccia observed in the volcanic complex of the present study area. The comparison between the Stac Fada Member and the peperite and volcaniclastic breccias in the study area is an important one due to the similarity of formation and emplacement mechanisms of the different deposits.

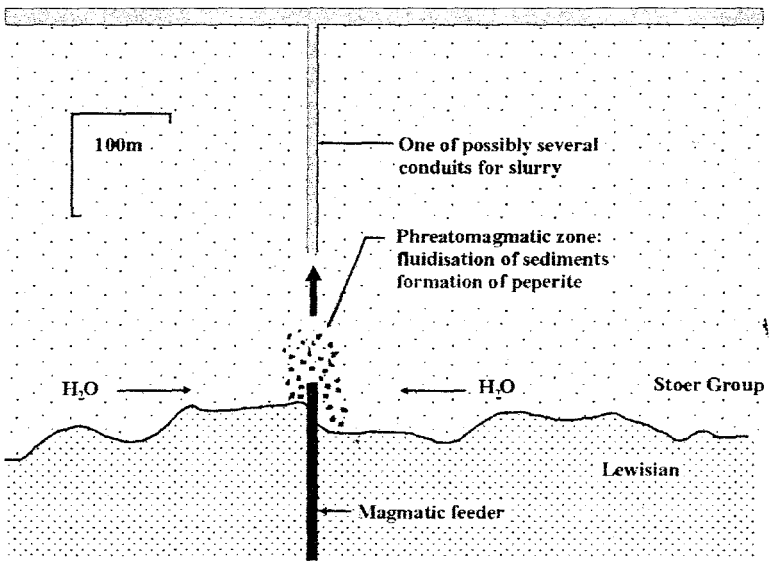

Figure 60: Cartoon showing how the peperitic slurry may have been generated some 400m below the surface in the lower Torridonian succession in Scotland, when magma rising through fractures in the "dry" gneissic basement interacted explosively with a copious supply of groundwater. After Sanders and Johnston (1989).

10.0 RESULTS AND DISCUSSION

Detailed analyses of clast and matrix type, size, colour, degree of weathering, relative proportions, and distribution in both volcaniclastic breccias were conducted in the southwestern corner of the volcanic complex. These analyses were conducted in order to determine whether characteristics of the volcaniclastic breccias remained constant throughout the same breccia unit, as well as between breccia units. The analyses of the volcaniclastic breccias are limited to a small area of the volcanic complex as the results obtained in the southwestern corner were consistent. General observations of the volcaniclastic breccias elsewhere in the complex supported the results from the southwestern corner.

10.1 MODAL ANALYSIS OF THE CLASTS IN THE VOLCANICLASTIC BRECCIAS

Graphs have been constructed from the modal analysis data of the clasts in the volcaniclastic breccias. These graphs have proved useful in identifying and displaying differences in the volcaniclastic breccias, both between breccias, and laterally within the same breccia. They quantify how heterogeneous the volcaniclastic breccias are in clast type, size, and proportions. The correlations and similarities are summarised below to try to group the outcrops and sample sites into the correct volcaniclastic breccias. As all the clasts are similar, irrespective of size, the clasts >5mm in the matrix were included in the analysis with the larger clasts. The clasts greater than 50cm were excluded from the analysis. The reasons for the minimum and maximum clast size limits have been previously discussed in the Methods section.

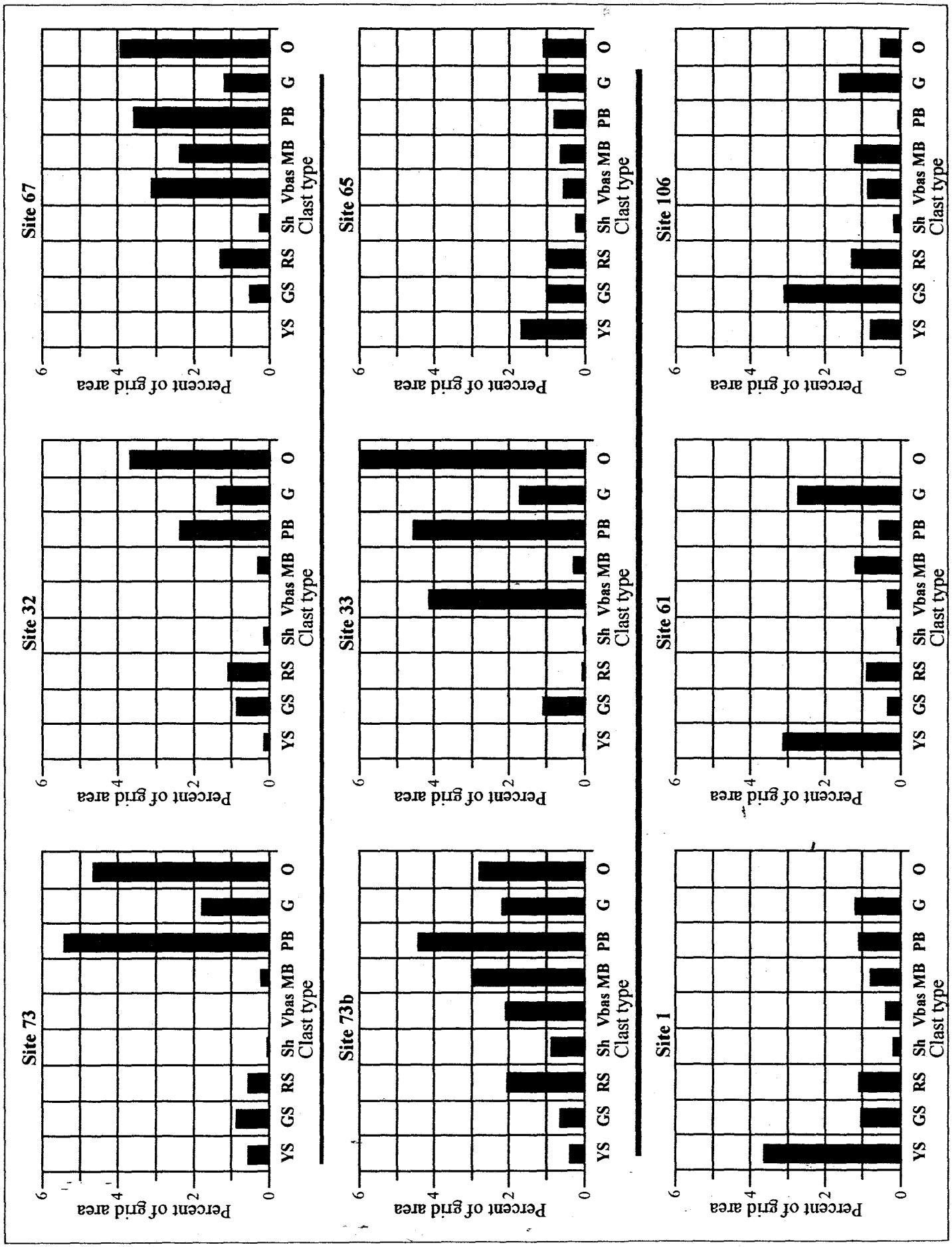

Figure 61: Histograms of percentage proportions of each clast type at numbered sample sites in the volcaniclastic breccias (southwestern area of subsidence structure, see Map, Appendix B and Figure 16). YS - Yellow Sandstone, GS - Grey Sandstone, RS - Red Sandstone, Sh - Shale, Vbas - Vesicular Basalt, MB - Massive Basalt, PB - Porphyritic Basalt, G - Glass, O - Other (usually heavily altered clasts). Histograms are arranged as upper subunit of upper, volcaniclastic breccia (upper row), lower subunit of upper volcaniclastic breccia (middle row), and lower volcaniclastic breccia (bottom row).

Histograms of clast type (Figure 61) suggest that sites 1, 61, and 106 (in the south-western part of the study area) are from the same unit, as they have similar proportions of the different clast types. They display higher proportions of sedimentary (YS, GS) and glass clasts (G), and a lower volcanic content. The upper volcaniclastic breccia (represented by histograms of sites 73, 32, and 67) appear to have a higher proportion of volcanic clasts than sandstone clasts. The bars of basalt and porphyritic basalt clasts are particularly high. The upper volcaniclastic breccia histograms also suggest that clasts >5mm are more common in the upper volcaniclastic breccia than the lower breccia. Sites 73b and 33 from the lower half of the upper volcaniclastic breccia have trends which more closely match those of the upper part of the upper volcaniclastic breccia than the lower volcaniclastic breccia. Site 65 is better correlated with the lower volcaniclastic breccia, having fewer clasts than the upper volcaniclastic breccia. However, due to its stratigraphic position in the hill slope adjacent to the fault outcrop (Figure 16), Site 65 cannot be part of the lower volcaniclastic breccia.

Figure 62 is an example of a set of histograms depicting the cumulative increase in clast area percentages from the first to the 25th 20x20cm grid of the total 1m^2 area at Site 73b. If the shapes of the smaller histograms change as more information is added it would suggest that the sampling of the clast proportions is unlikely to be representative of the whole volcaniclastic breccia outcrop in one area. Of all the histogram sets created, none show any change in histogram shape from the first 20x20cm grid, to the 25th. Thus the sample size, and the data collected seems sufficient to display the correct clast assemblage at each 1x1m grid site. Matrix:clast ratio histograms for each grid analysis site are all roughly the same. The clast proportions range from 10 to 20% of the grid area (Figure 63). Sites 32 (from the upper part of the upper volcaniclastic breccia) and 65 (from the lower part of the upper volcaniclastic breccia)

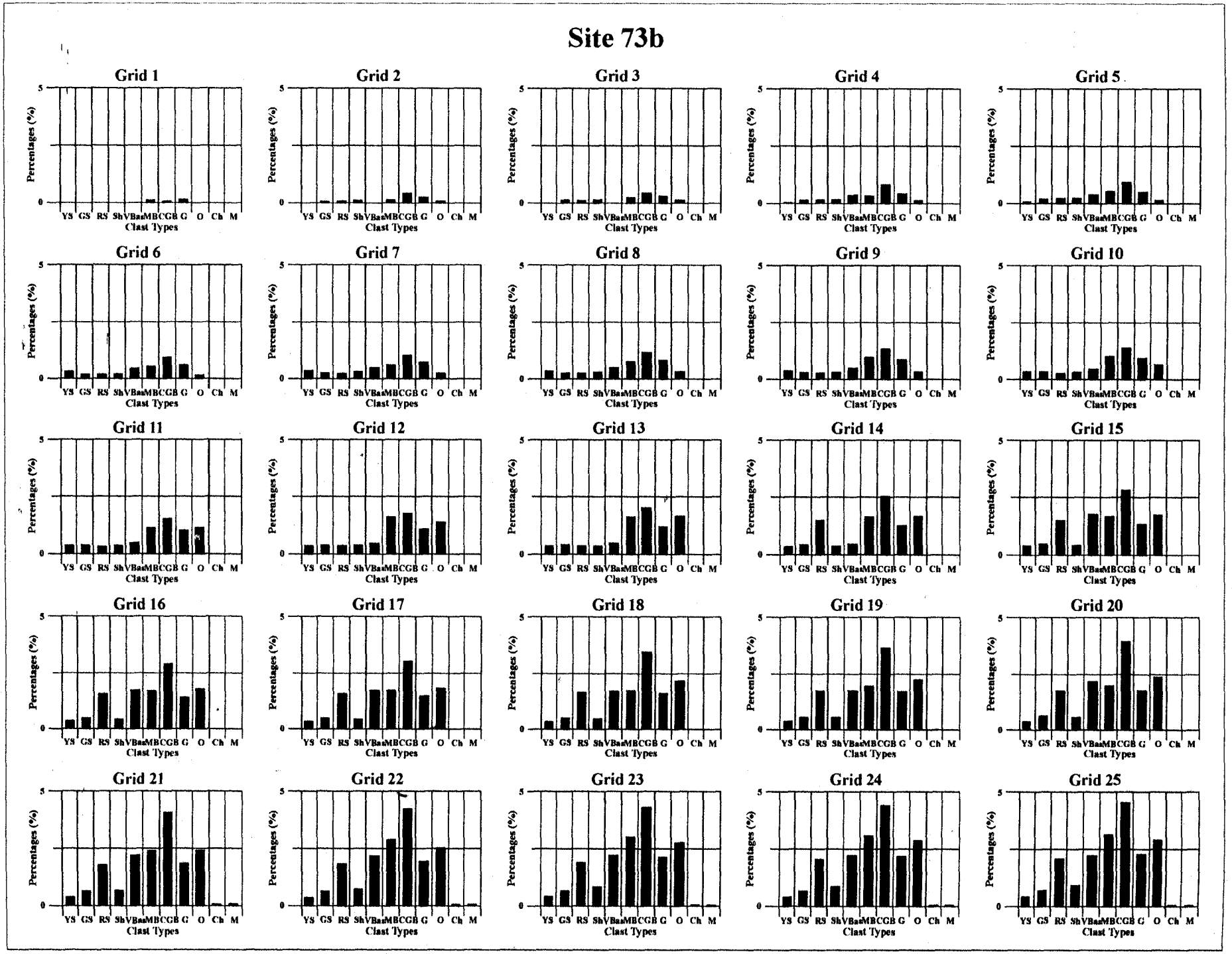

Figure 62: Cumulative histograms of 20 x 20cm squares (1 - 25) in a 1m2 grid at Site 73b. This consistency represents a homogeneity of the volcaniclastic breccia throughout the 1m2 grid. Each sample site has similar trends to these.

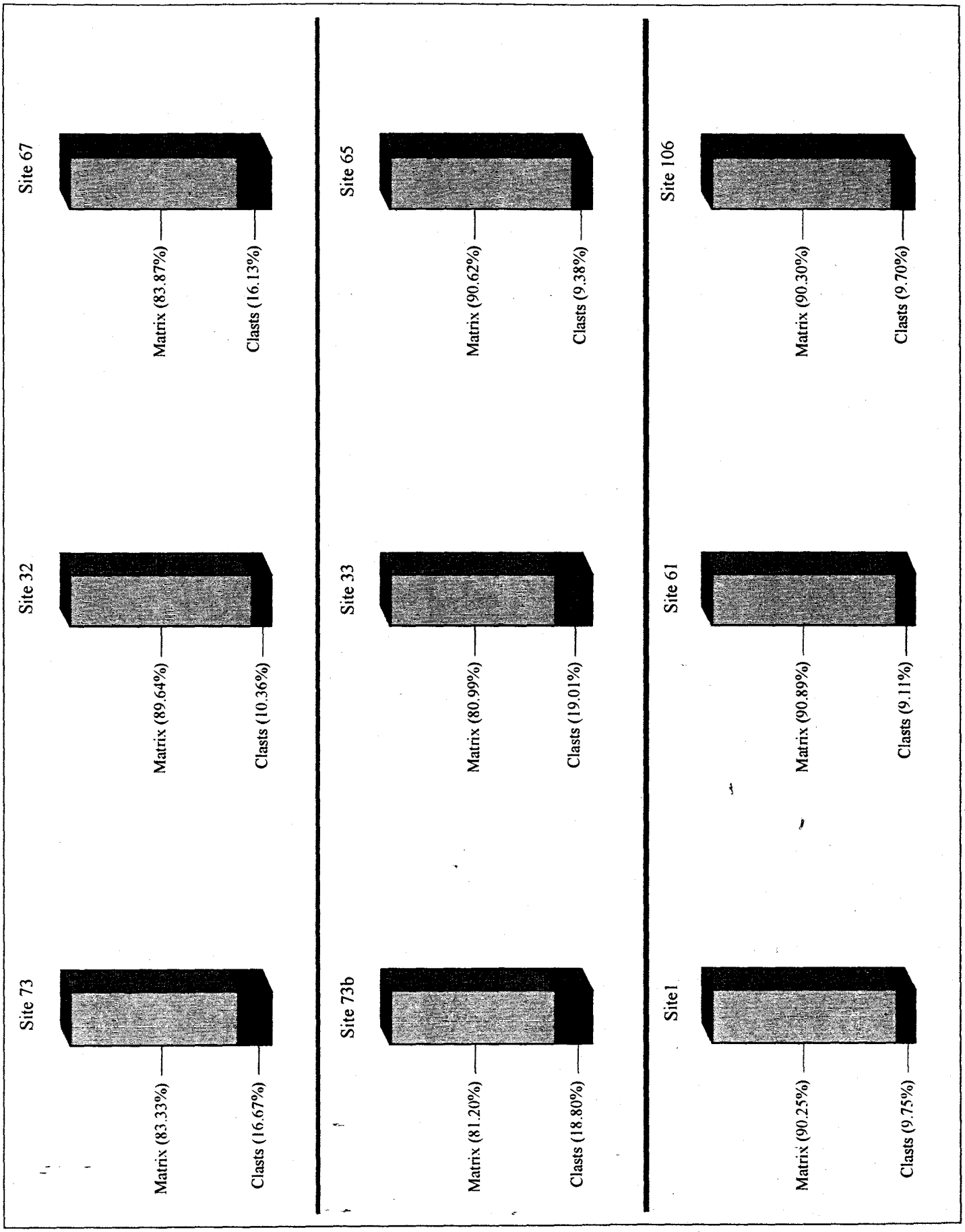

Figure 63: Graphs comparing the matrix to clast proportions for each sample site. Note that all the clast fragments below 0.5cm are included as matrix.

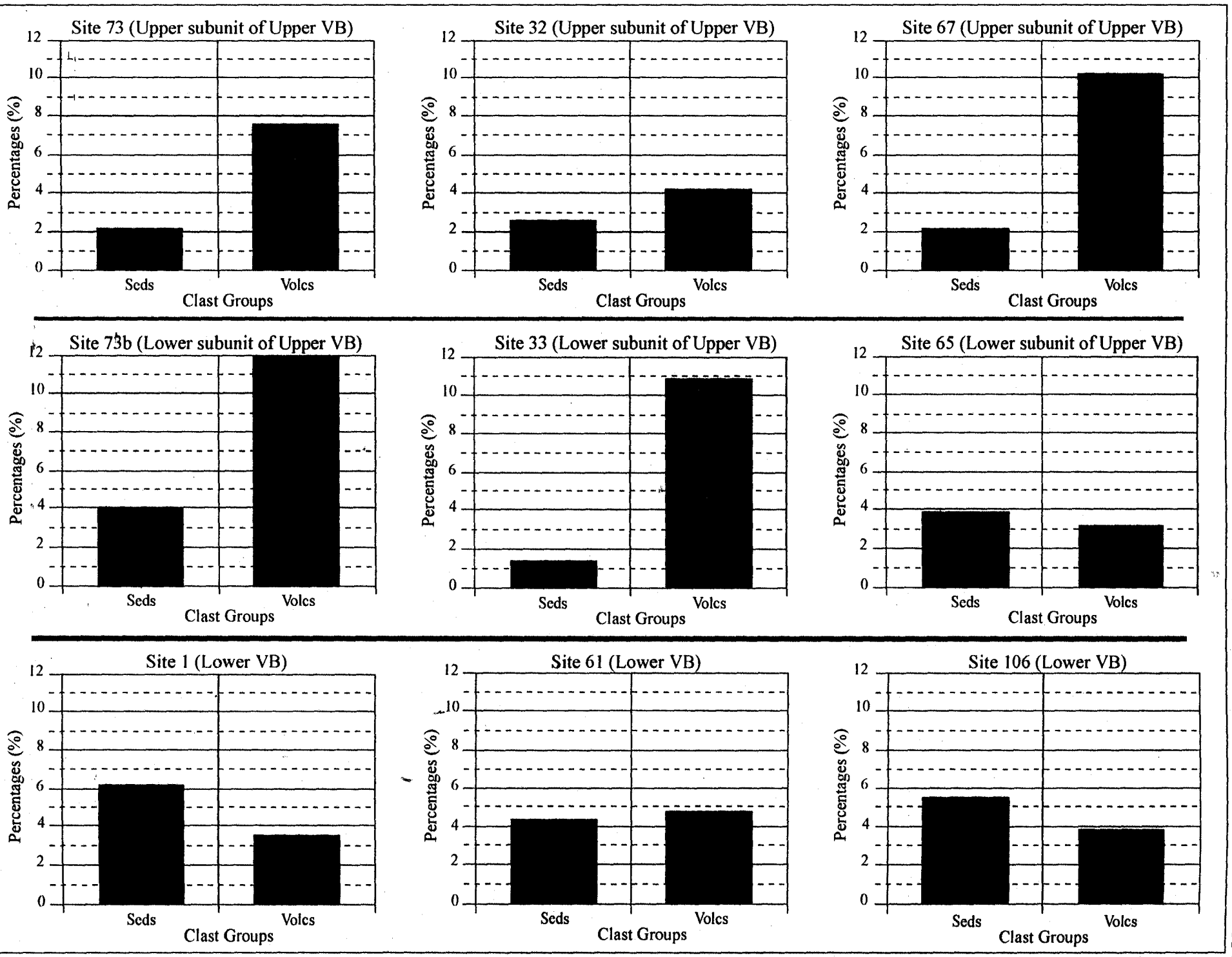

Figure 64: Graphs comparing sedimentary clast to volcanic clast proportions for each sample site.
VB - Volcaniclastic Breccia.

have clast proportions below 10.5% of the total volume, which correlates more with the lower volcaniclastic breccia (under 10%) than the combined lower and upper parts of the upper volcaniclastic breccia (between 16 and 19%).

Histograms comparing sedimentary to volcanic clast proportions (Figure 64) do reflect a variation in the proportions of sedimentary and volcanic clasts. The upper three histograms (sites 73, 32, and 67) are from the same unit (upper part of the upper volcaniclastic breccia), and although the magnitudes of the clast proportions differ, the shapes of the histograms are similar. The material outcropping at the sites in the lower part of the upper volcaniclastic breccia (sites 73b, 33, and 65) (middle row) appears to have undergone a different degree of alteration to the material in the upper part of the upper volcaniclastic breccia based on the change in colour of the outcrop from the upper part to the lower part. An important result is that the upper volcaniclastic breccia has a far greater proportion of volcanic clasts to sedimentary clasts.

The lower three histograms (sites 1, 61 and 106) represent data collected from the lower volcaniclastic breccia, and maintain a fairly constant histogram shape. The histograms from data collected from the lower volcaniclastic breccia illustrate a more equal distribution than the histograms from the upper volcaniclastic breccia. Sedimentary clasts are generally more common in the lower volcaniclastic breccia than the volcanic clasts.

The difference in overall clast-group distribution between the upper and lower volcaniclastic breccias could be due to the difference in their ages. The lower volcaniclastic breccia was formed at the start of the flood basalt effusion, and as a result, has a lower volcanic clast to sedimentary clast ratio. It seems that only the Moshesh's Ford basalts had been emplaced at this

stage. The upper volcaniclastic breccia formed subsequently, and is interbedded with the flood basalts. A greater amount of basalt had been emplaced by this stage, and more basalt was fragmented and incorporated into the upper volcaniclastic breccia. Another possibility is that the upper volcaniclastic breccia, which was transported from its eruption site nearby, "picked up" angular, fragmented material from the basalt flow tops it was moving over. However, there appears to be no increase in the proportion of vesicular basalt clasts in the upper volcaniclastic breccia which would indicate that the clasts originated from basalt flow tops.

10.2 GEOCHEMISTRY OF LAVA FLOWS

A number of magma types have previously been described in parts of the present study area (Mitchell, 1980; Masokwane, 1997). Geochemical analyses of the lava flows were conducted to separate the flows into their magma types. The data from these analyses are listed in tables in Appendix A. The sites of the samples used in the analyses are listed in Figure 65, and their geographical locations and positions within the stratigraphic logs are shown in Figure 4 and 6 respectively. Using geochemical fields delineated in Mitchell (1980), the data were grouped into the Moshesh's Ford, the Tafelkop, the Roodehoek, and the Vaalkop Basalt magma types. The variation diagrams of major elements do not yield as clear a distinction of the different magma types as the trace element variation diagrams do. Therefore, only the trace elements are represented graphically in this study. In all trace element graphs, data from Makadzange (1998), collected from the study area, was also used.

Figure 66 illustrates variation diagrams of trace elements plotted against Zr. The plots are grouped into the four different basalt types. The elements Rb, TiO_2, Nb, Sr, Ba and Y all show

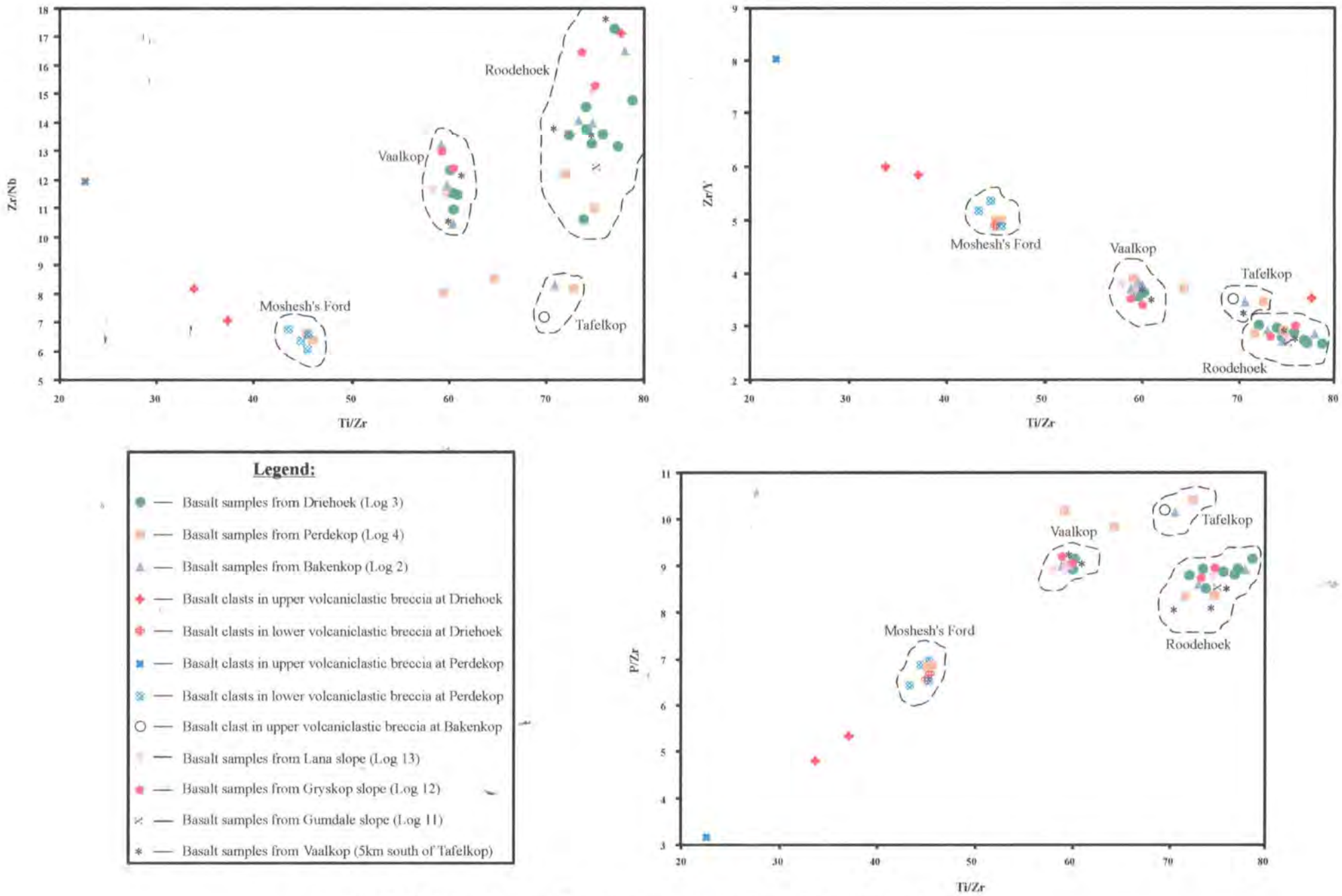

Figure 65: Variation diagrams of basalts grouping the basalt samples into separate basalt units. Two of the samples taken from the lower volcaniclastic breccia at Driehoek and one sample taken from the lower volcaniclastic breccia at Perdekop plot outside the fields in all the graphs. The significance of this is outlined in the text.

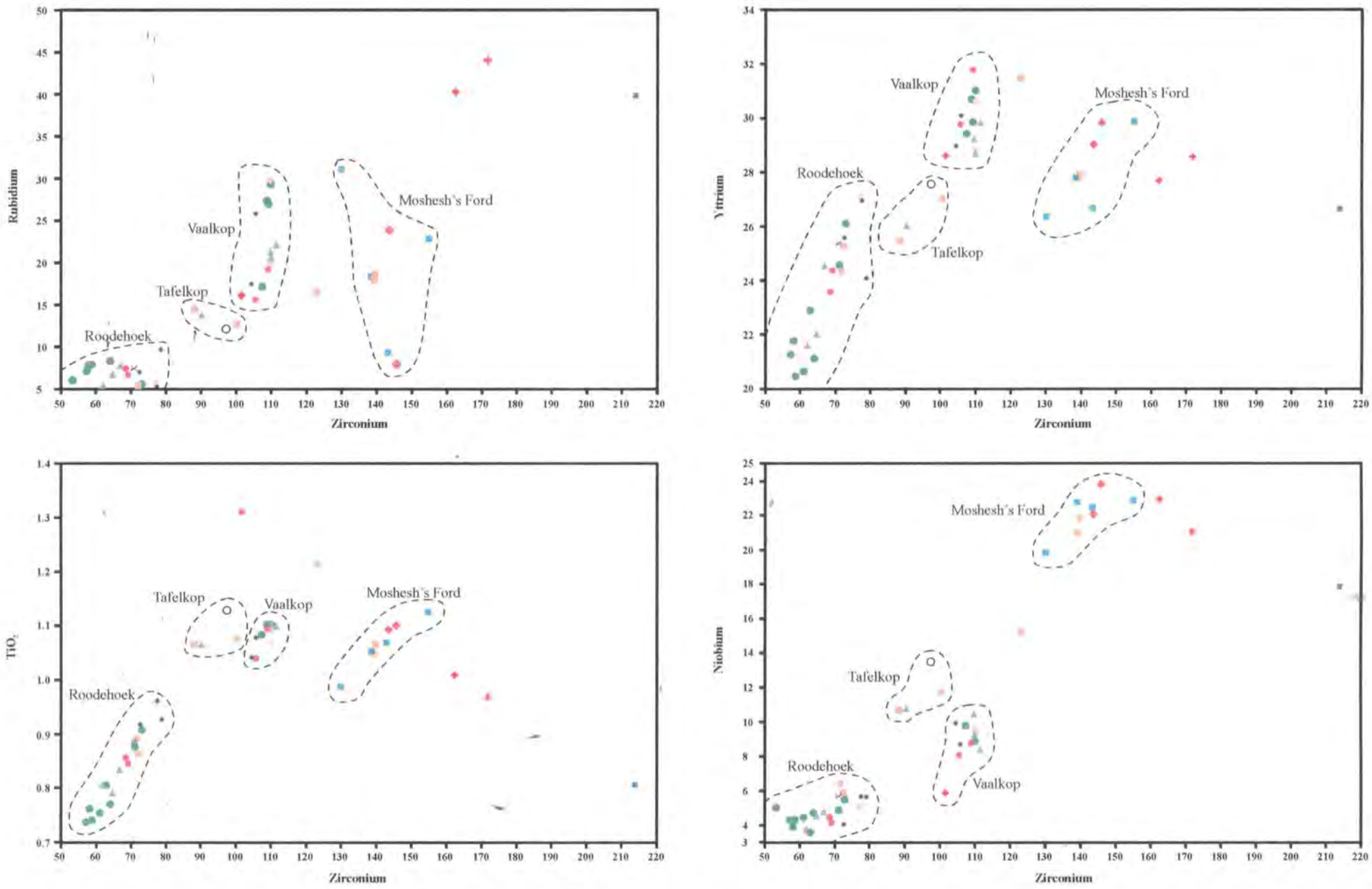

Figure 66: Variation diagrams of basalts grouping the basalt samples into separate basalt units plotting other trace elements against zirconium. These incompatible trace elements increase in concentration with an increase in incompatible zirconium. A key to the symbols is in Figure 65.

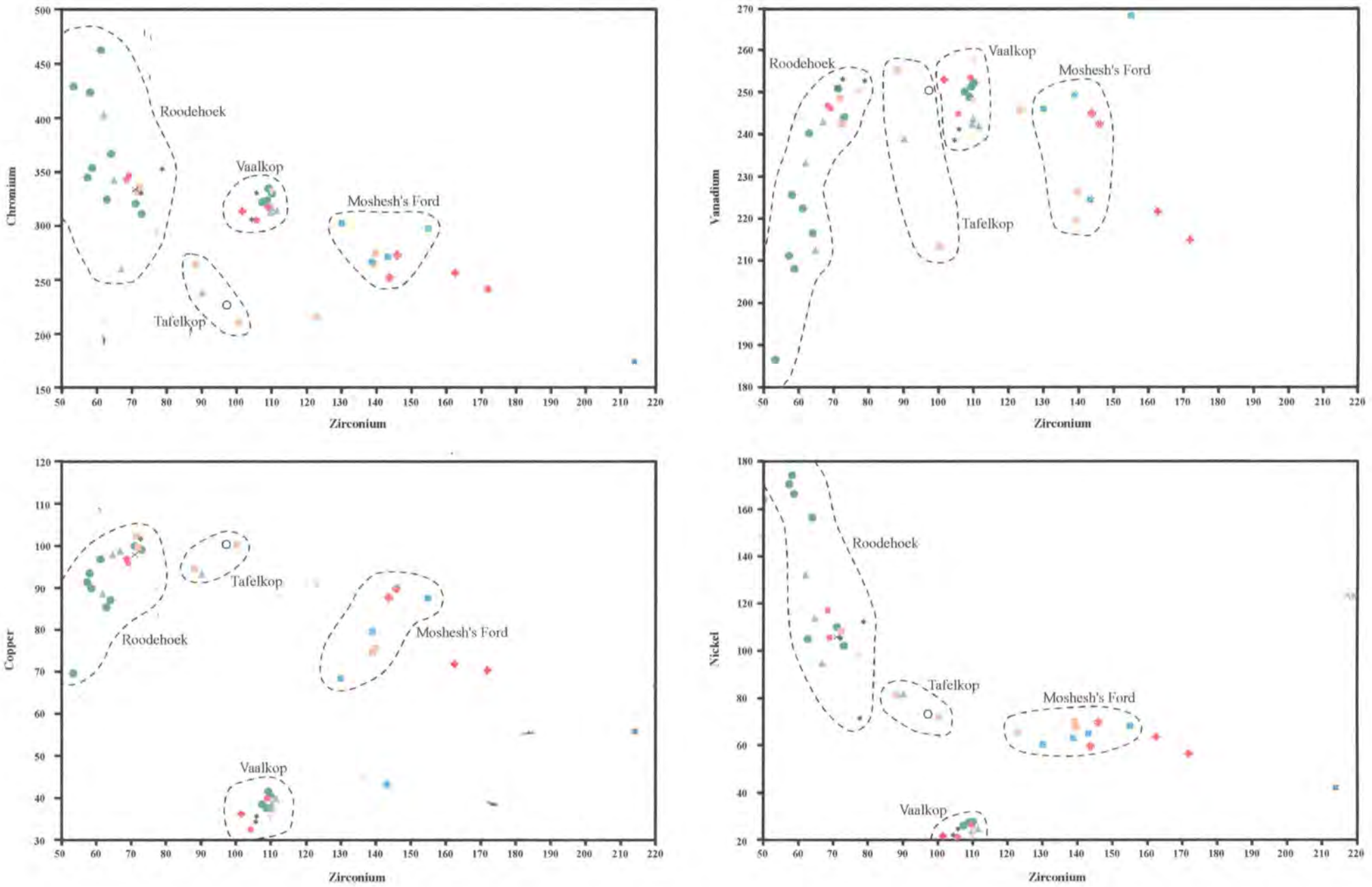

Figure 66: (cont.) Variation diagrams of basalts grouping the basalt samples into separate basalt units plotting other trace elements against zirconium. These compatible trace elements decrease in concentration with an increase in incompatible zirconium. A key to the symbols is in Figure 65.

increasing concentration with an increase in concentration of Zr, while Cr, V, Ni and Cu decrease in concentration with an increase in Zr concentration.

The trace elements plotted as ratios in the variation diagrams in Figure 65 (Zr, Ti, Nb, P, and Y) are immobile (Rollinson, 1993). In F-free systems these elements remain immobile even under hydrothermal conditions and up to medium-grade metamorphism. These elements are thus useful for geochemical correlations between basalt samples which may have been weathered or hydrothermally altered (Rollinson, 1993).

Some of the data in the variation diagrams represent samples collected from basalt clasts within the lower volcaniclastic breccia, and these plot within the Moshesh's Ford basalt field. This is significant because no *in situ* Moshesh's Ford basalt has been recorded within the volcanic complex. As discussed later, the lower volcaniclastic breccia was produced *in* the complex. Therefore, the presence of Moshesh's Ford basalt as clasts within the lower volcaniclastic breccia (~ 20 vol%) suggests that the basalt was emplaced prior to the explosive eruptions which produced the lower volcaniclastic breccia. The explosive activity fractured the Moshesh's Ford basalt, which overlay the Elliot and Clarens formations, and erupted clasts of these rocks from the volcanic complex.

Other data points in the variation diagrams represent samples collected from basalt clasts within the upper volcaniclastic breccia. These data plot within the defined basalt type fields as well as outside the fields. This indicates that some of the basalt clasts may have originated outside the study area, suggesting that the upper volcaniclastic breccia was generated outside the study area.

10.3 Pisolith Development in Clarens Formation and Deposition by Stream-Flows

Pisoliths in the study area were observed in different stages of development, outlining the manner in which they were formed, as well as how they were removed from the Clarens Formation sandstone and deposited in the stream-flows. The different stages of development are discussed here. Figure 67 shows the range of sizes and numbers of pisoliths within each size range. Evidence of deposition by stream-flows shows that some of the pisoliths have been excavated and deposited away from their point of origin; ie., they are allogenic. Although many pisoliths are still *in situ*, many are present in the stream-flow deposits.

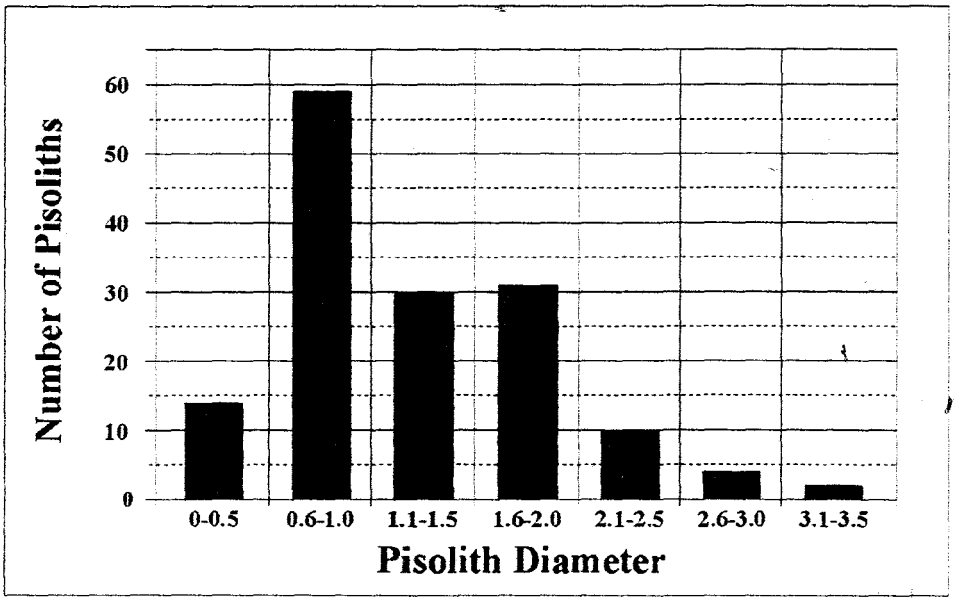

Figure 67: Histogram of pisolith diameters from 150 pisoliths sampled. Note that by far the majority are between 0.6 and 1cm in diameter. The mean diameter is 1.2cm.

Based on colour, texture and grain size, the pisoliths in the volcanic complex originated in sandstone assumed to belong to the Clarens Formation. The pisoliths usually occur on the outer edges of sandstone blocks or units, close to the basalt lavas. They are rarely larger than 3cm in

diameter, and are usually 0.5 to 2cm in diameter. From thin section analysis it is clear that the pisoliths in the study area were formed from the precipitation of haematite grains, carbonate, and zeolite. Many of the pisolitic sandstone outcrops are pale turquoise in colour, signifying a degree of bleaching. This suggests a hydrothermal influence which is most likely to have originated from the intrusive activity in the area at that time. Areas of sandstone which develop pisoliths are also expected to be slightly coarser-grained than sandstone not containing pisoliths, or to have more interstitial spaces through which fluids can pass and minerals can precipitate. These textural differences, however, have not been evident either in hand specimen or thin-section.

The pisoliths are believed to form from the circulation of hydrothermal fluids, mobilised through heating of the interstitial water in the sediments by magma and lava flows, prior to the eruption events which produced the lower volcaniclastic breccia. The precipitated minerals, carbonate and haematite, forming the pisoliths have been concentrated in their present location and must have been transported some distance through the sandstone by hydrothermal fluids. This would allow the concentration of the carbonate and haematite in the fluids to increase before precipitation around a nucleus. It is less likely that direct baking of the sandstone by overlying basalt would be sufficient to concentrate the minerals in the pisoliths.

The development of the pisoliths can be divided into four main stages from their inception in the sandstone unit to their eventual deposition in the stream-flow deposit. These are:

1 - Incipient Pisolith Stage

2 - Semi-detached Pisolith Stage

3 - Loose / Detached Pisolith Stage

4 - Deposition Stage

Permeating hydrothermal fluids, driven by the intruding magma prior to eruption, began precipitating transported minerals around nuclei of sandstone aggregates (*Incipient Pisolith Stage*) (Figure 21, a and b). With continued hydrothermal activity the minerals in solution were precipitated in concentric layers growing outwards. The pisoliths developed as the hydrothermal minerals kept precipitating, bonding the sandstone particles together and making the pisoliths more resistant than the host sandstone. The more resistant the pisoliths became, the more they developed as individual structures, still bonded to the sandstone (*Semi-detached Pisolith Stage*) (Figure 22). The pisoliths are now unique features in the sandstone and not just a precipitation colour staining. When fully developed the pisoliths are almost completely detached from the host sandstone (Figure 23).

With the increase in basaltic material below, the water or hydrothermal fluids in the wet sandstone might have boiled, causing phreatic eruptions. It seems unlikely that such large-scale fracturing could have occurred without an eruption during faulting and subsidence of the volcanic complex, although parts of the sandstone outcrop (eg. the large megablocks around the edge of the volcanic complex) may have fractured and moved during the slumping of the subsidence structure. During the phreatic eruptions, part of the Clarens Formation sandstone was fractured and broken into angular fragments, but the pisoliths, more resistant to the fracturing, remained intact. Many of them were released from the sandstone during the eruptions and deposited as airfall deposits *(Loose Pisolith Stage)*. These airfall deposits are not preserved in the study area. Perhaps accompanying the termination of the phreatic eruptions, slumps or debris flows moved the ejected material into streams which redeposited the ejected sandstone fragments and pisoliths as stream-flow deposits within the volcanic complex (Figures 25, a and b) (*Deposition Stage*). The absence of basaltic clasts in the stream-flow deposits suggests a phreatic as opposed to

phreatomagmatic explosion (Figure 26). It also suggests that the phreatic eruptions and stream-flow deposition must have occurred prior to the emplacement of the Moshesh's Ford basalts. Only occasional glass fragments are encountered in the stream-flow deposits.

ased on the cross-bedding of the stream-flow deposit in Figure 25(a), and the coarse-grained nature of the sand grains and size of the sandstone clasts in all outcrops, it can be inferred that the environment of deposition of the material at this outcrop was that of an unidirectional stream flowing into a shallow lake or pond of water (Figure 68). The ripples (Figure 27) observed along the upper surface of a sandstone lense are symmetrical, and this implies a bidirectional movement of water. These ripples imply that the sandstone lense was deposited along the edges of a shallow lake or open body of water where small waves washed up the shore and back (Figure 68).

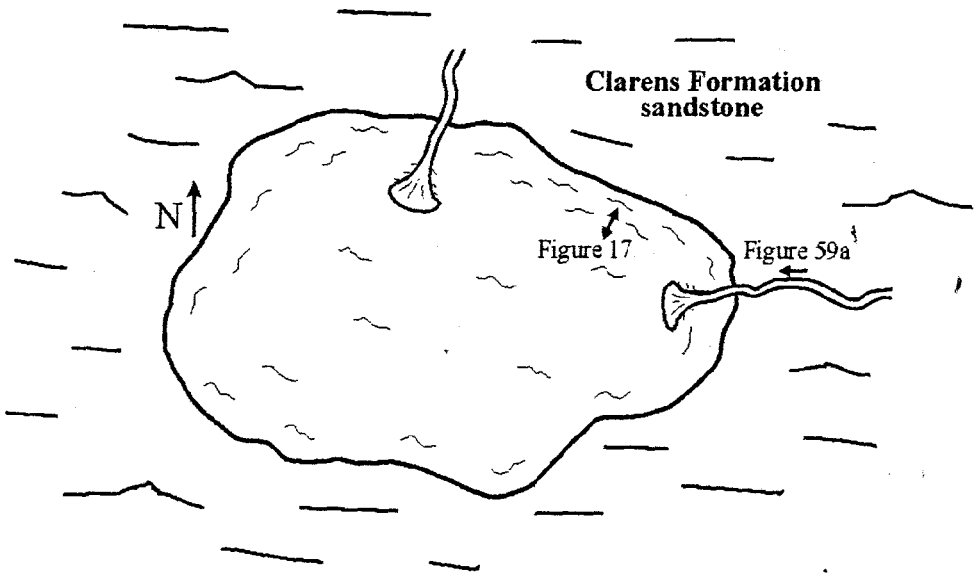

Figure 68: Inferred palaeoenvironment prior to the main explosive event forming the lower volcaniclastic breccia. Angular sandstone sediment washed down the streams, forming stream-flow deposits (Figure 25a), while symmetrical ripples formed around the edges of the basin like those preserved on the upper surface of the sandstone unit in Figure 27. Due to the lack of basalt clasts in the stream-flow deposits it is believed that no basalt lavas were yet present around the lake or pond.

A number of Clarens sandstone fragments containing pisoliths are observed, predominantly in the lower volcaniclastic breccia (Figure 69). These represent areas of sandstone which avoided the initial phreatic eruptions and were later fractured by phreatomagmatic eruptions which produced the breccia deposit as more magma was added to the system from below. Alternatively, the sandstone fragments could be derived from the stream-flow deposits prior to them becoming consolidated.

Figure 69: Fragment of sandstone containing pisoliths in lower volcaniclastic breccia. Note how pisoliths along the edge of the sandstone fragment have resisted fragmentation and retained their spherical shape, even protruding from the edge of the sandstone fragment. Sample from volcaniclastic breccia west of altitude reference in northwest corner of Figure 16.

The mineralogical differences of the pisoliths possibly reflect compositional variations in hydrothermal fluids at the different sample sites. Permeating fluids would assimilate elements from the minerals in the rocks or sediment through which they passed. Subsequently their own

chemical composition might have changed enough to permit different minerals to precipitate in different areas. Iron would have been assimilated from fluid movement through the Elliot Formation sediments which are rich in haematite and precipitated as concentric rings of haematite in the Clarens Formation sandstones.

The majority of the stream-flow deposits are layered with alternating fine-grained layers and coarser, more clastic layers. The clastic layers occasionally display a crude upward-coarsening trend, suggesting gravitational sieving of the sandstone fragments and pisoliths within the layer. This is a characteristic of debris flow deposits. Upward-fining and deformed and twisted or chaotic layers have also been encountered, but the upward-coarsening and deformed sequences appear to be the most common.

The distances between the pisoliths in the *Incipient Pisolith Stage* and the stream-flow deposits vary between a few metres, and a few tens of metres, which is not significantly great. This makes accurate calculation of palaeoflow directions difficult. Generally the stream-flow outcrops lie to the east of the pisolitic sandstone outcrops, or towards the centre of the volcanic complex. This, however, assumes that the sandstones responsible for the pisoliths in the stream-flow deposits were near to the sandstones containing *Incipient Stage* pisoliths. This is probably an inaccurate assumption as the pisoliths in the stream-flow deposits are mature, while the *Incipient Stage* pisoliths are very immature. It seems more likely that the stream-flow pisoliths were formed further away from the *Incipient Stage* pisoliths at a site where hydrothermal fluid movement had occurred for a greater period of time.

A 600 x 400m megablock in the southwestern edge of the study area (400m to the north of Log 8 (see Map, Appendix B)) consists of Clarens sandstone grading upwards into pisolitic sandstone, overlain by stream-flow deposits which are covered by a basalt flow. If the pisoliths are only formed in close proximity to basalt flows, as suggested by this occurrence, then the presence of the basalt flow *above* the stream-flow deposit, rather than between the sandstone and the stream-flow deposit, is confusing. However, any lava flow above the sandstone would have been fractured with the sandstone and basalt fragments would be observed in the stream-flow deposits. Only an accessory amount of basaltic glass is observed in the stream-flow deposits. Possibly the stream-flow deposit originated elsewhere, where basalt was close enough to the sandstone to initiate pisolith growth but far enough to avoid being erupted during the phreatic eruptions and redeposited with the stream-flow deposit. The stream-flow deposit was then emplaced directly above Clarens sandstone and overlain by a subsequent basalt flow.

10.4 Palaeoenvironment of Study Area

The present shape of the volcanic complex and the fault along the western margin, suggest that the complex represents a subsidence structure in which the lower volcaniclastic breccia ponded. Shallow lakes formed in the subsidence structure a number of times throughout the period, from the deposition of the Clarens Formation to sometime during the emplacement of the flood basalts. The lacustrine units described in section 7.5 are the deposits formed by these shallow lakes.

Thin gravel lags (erosional and depositional structures) towards the top of the Clarens Formation (Figure 70) suggest a wet environment with small, low energy streams flowing into the subsidence structure, removing the fines and leaving small gravel lags of shale clasts and

sandstone fragments. The gravel lag deposits, as well as the *in situ* blocky peperites along the sandstone-basalt contacts are only observed on large sandstone blocks on the edge of the volcanic complex. Sandstone outcrops immediately outside the structure show no small channel lags or peperite development where in contact with basalt flows. This implies that the sandstone within the structure was wetter than the sandstone outside the structure where the basalt conformably overlies sandstone with no evidence of any peperite generation.

Although no evidence exists that proves that a lake was present in the volcanic complex at the time of the explosive eruptions forming the lower volcaniclastic breccia, there is much evidence that *wet* sediment interacted with the intruding magma (peperite development, channel lag deposits towards the top of the Clarens Formation sandstone). As the subsidence structure did not form until the eruptions began, it seems that there was already a topographic depression of some size containing water, which the intruding magma vaporised. Based on the palaeolake deposits observed interbedded with the basalt lava flows (below) and the presence of pillow lavas on Tafelkop it can be inferred that a similar environment, fed by small perennial or sporadic streams existed in a topographic depression at the time of the formation of the lower volcaniclastic breccia.

Intruding magma formed peperite when interacting with wet sediment, and this lead to an explosive FCI-type interaction. The depression was faulted and deepened during the eruption and emplacement of the lower volcaniclastic breccia, in the manner of caldera collapse due to the evacuation of a large volume of sub-surface peperite. The hypotheses for the mechanisms of eruption and emplacement of the lower volcaniclastic breccia are discussed later (Section 10.6). The faulting only occurred along the western boundary of the complex while the eastern

boundary appears to have remained unaffected. This is referred to as a "trapdoor" system where only one side is downthrown. Some tilting of the surrounding Clarens Formation sandstone along the north and northwestern boundary of the subsidence structure is apparent, and the sandstone dips towards and under the lower volcaniclastic breccia (Figure 10).

Figure 70: A thin, channelised structure in the Clarens Formation sandstone near Modena in the north of the study area consists of large shale and sandstone clasts suggesting a wet environment where fines are removed from the sediment by low energy stream action, leaving thin gravel lags. These gravel lags are evident towards the top of the Clarens Formation sandstone unit, just outside the volcanic complex. Evidence of wet sediments in the study area suggests a collecting of groundwater, which suggests that there was groundwater movement, as well as streams feeding water into a depression in the centre of the study area.

At least three palaeolakes are inferred to have formed in the subsidence structure. This number is based on the identification of three, thin, laterally extensive lacustrine deposits within the subsidence structure. The size of the palaeolakes varied slightly, however, the extent of the

lacustrine deposits interbedded with the basalts is uncertain due to the lack of outcrop. Presumably with the infilling of the subsidence structure with volcaniclastic breccia and lava flows, the size and depth of the depression decreased. Consequently the areal extent of the subsequent palaeolakes also decreased.

10.5 PEPERITE AND ITS SIGNIFICANCE

Fluidisation of wet sediment by water vapour may occur by heating, or by pressure relief during the opening of fractures. Fluidisation by heating is unlikely to occur at pressures greater than 312bars. This is because the pressure of vapour within unconsolidated wet sediments must be greater than the hydrostatic and lithostatic pressure from the overlying sediment and water columns in order to vapourise the water. This pressure of 312bars is equivalent to approximately 1.6km of wet sediment, assuming a density of $2g/cm^3$ (Kokelaar, 1982).

The intimate intermixing of magma and host at a submillimetre scale is attributed to fluid instabilities developed along the magma-vapour-host interface (Busby-Spera and White, 1987). Such intimate intermixing of magma and water-bearing fragmental debris is commonly a precursory step towards explosive hydrovolcanism (Busby-Spera and White, 1987).

The contact zone between the basalt and the sandstone host of the fluidal peperite resembles a mixture of two immiscible fluids of similar viscosity with "globules" of basalt enclosed in sandstone and vice versa (Figures 35 and 71). Very few blocky fragments and jigsaw puzzle clasts are present in the fluidal peperite. Fluidal peperites have clasts shaped by effects of surface tension into drop-like bodies. They form only if a water-vapour film can be maintained more or

less continuously at the magma-sediment interface, insulating the magma. The vapour film prevents the magma from being hydroclastically fragmented by thermal shocking. This results from rapid contraction of the basalt on cooling (Busby-Spera and White, 1987).

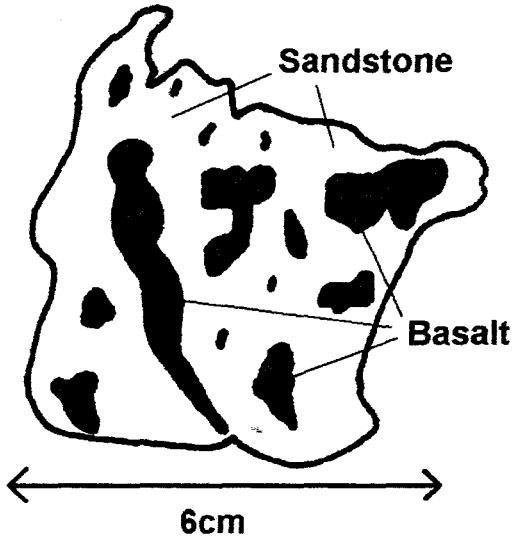

Figure 71: Sketch of typical fluidal peperite fragment within the lower volcaniclastic breccia, containing blebs of basalt mixed in with wet sediment.

Fragmentation, and the formation of blocky peperite, due to thermal contraction is termed "granulation" (Fischer and Schmincke, 1984). It occurs when the steam envelope or vapour film between the basalt and the host sediment is unable to maintain itself and breaks down. This is often as a result of many host clasts being too large to entrain in a vapour film at the magma-host interface (Busby-Spera and White, 1987). The result is rapid quenching and increased brittleness. Grain size of the host is thus an important determinant of peperite style because large clasts cannot be entrained along the magma-wet sediment interface. This process is necessary for the production of fluidal, sediment-displacive peperites (Busby-Spera and White, 1987). In some blocky peperites in the present study area, jigsaw puzzle clasts are evident, but in the majority of cases the basalt is too dispersed. A degree of fragment dispersion appears to have occurred.

This is probably the result of explosive expansion of water-laden host sediment engulfed in the magma by a process described by Busby-Spera and White (1987) as "clast blocking" (Figure 72).

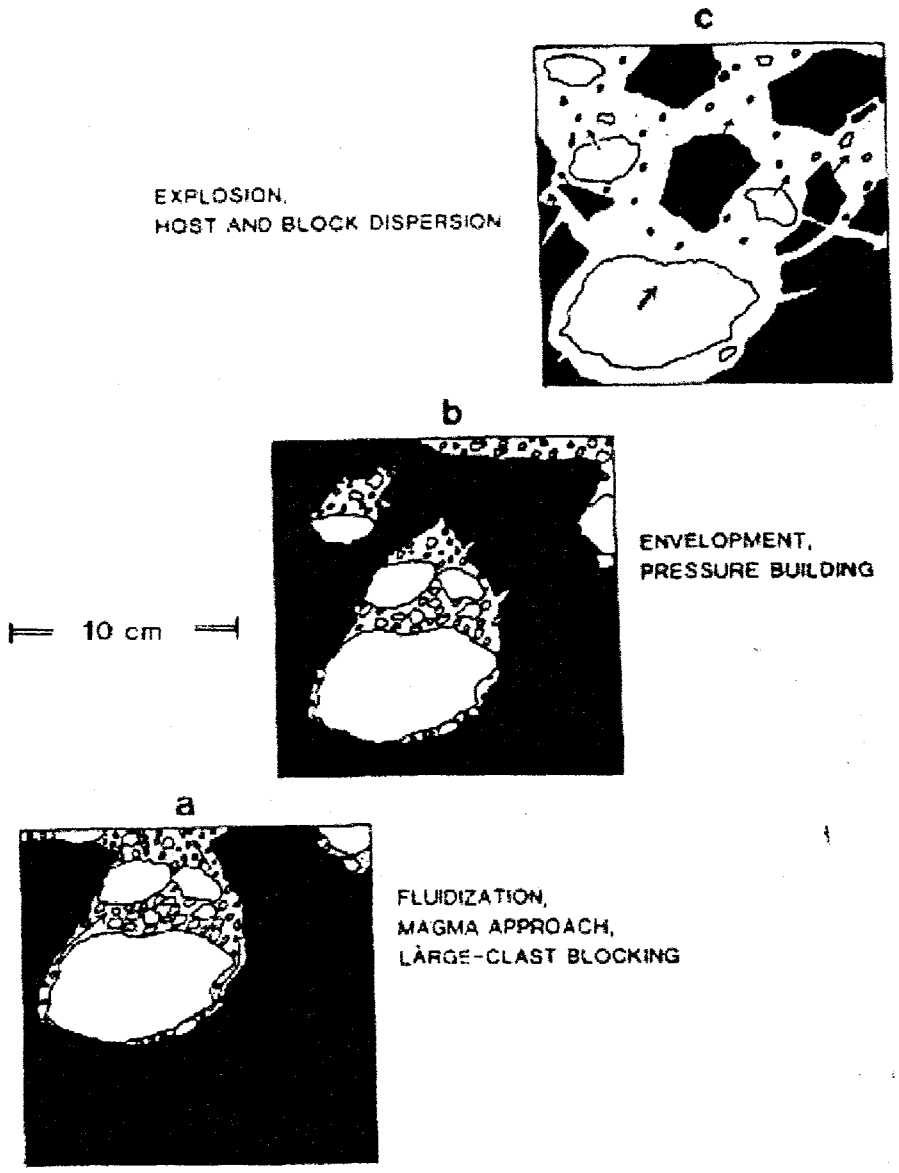

Figure 72: Schematic diagram illustrating "clast blocking". A large clast (light) within a permeable, poorly-sorted lithic lapilli tuff breccia is enveloped by magma (dark material), along with a small pocket of wet tephra in its "shadow". The surface of the magma cools rapidly during intrusion into coarse-grained, permeable host material and is broken into blocks and dispersed into the host when water enclosed within tephra pockets is vaporised. After Busby-Spera and White (1987).

The intruding magma frequently encounters large clasts or aggregates of grains which it engulfs, along with water-laden matrix in "shadows" behind the clast. The enclosed water is thus confined in zones behind such large "blocking clasts", and simple vaporisation of pockets of interstitial water violently breaks apart the rapidly chilling magma into blocks and mixes it with partially fluidised host sediment (Busby-Spera and White, 1987).

The volcaniclastic breccias can be considered to be similar to the "erupted peperites" in Scotland described by Sanders and Johnston (1989). They were formed through the mixing of basaltic magma with wet sediment. Fluidal peperite clasts are observed in the lower volcaniclastic breccia, and are inferred to have formed from the mixing of magma with wet sediment prior to the eruption of the breccia. The lower volcaniclastic breccia formed explosively, as more magma was introduced to the system from below, and lithified clasts of fluidal peperite were incorporated in the breccia.

Fluidal peperite development along the dolerite-sandstone contact on the northwestern boundary of the complex (Figure 76) is very similar in appearance to the clasts of peperite in the lower volcaniclastic breccia unit. It is possible that the dolerite intrusion was responsible for the production of at least some of the fluidal peperite clasts observed in the lower breccia. In that case this dolerite or similar body would have had to have intruded prior to the development of the breccia to produce fluidal peperite to be included as clasts in the breccia.

10.6 Mechanisms of Eruption and Mode of Emplacement of Volcaniclastic Breccias

The Brosterlea Complex subsidence structure contains two volcaniclastic breccias with slightly different physical characteristics. The process forming these deposits, and the mode of emplacement of each deposit is vital to understanding the subsidence structure as a whole. While it is clear that the upper volcaniclastic breccia originated outside the study area, the lower breccia may have been produced within the Brosterlea Complex as a proximal backflow or backfall. The various possible processes of formation and modes of emplacement are considered here.

Hypothesis 1: "Typical" maar-diatreme structure

The complex could represent an extremely large structure like a maar-diatreme where the lower volcaniclastic breccia has filled the vent of a diatreme, or group of coalesced vents in a roughly circular-shape. Diatremes are tephra-filled volcanic necks exposed below the erupted surface, and are believed to be the subsurface roots of maars and related volcanoes. Maar volcanoes consist of a low, broad, fallout- and surge-deposited pyroclastic apron surrounding a central crater cut below the pre-eruptive surface (White, 1991). Basaltic diatremes form when rising magma encounters groundwater in sediment or rock at shallow depths below the surface. The two can mix together and heat from the magma instantaneously vaporises the water, as an explosive thermal reaction. This reaction has been classified as a Fuel Coolant Interaction (FCI) by Wohletz (1986), and can produce a powerful blast below the surface that fragments and ejects the overlying country rock and sediment. In the volcanic complex the interaction between the rising magma and the wet sediment is estimated to have been near the base of the Clarens Formation (approximately 60m below the palaeosurface), as the sedimentary clasts observed in

the volcaniclastic breccias are predominantly Clarens Formation sandstone, rather than Elliot Formation sandstone and shale. The presence of some Elliot Formation sandstone and shale clasts suggests that the eruptions excavated further (at least to 100m, judging from the depth of the volcanic complex), into the rocks below the Clarens Formation.

According to Busby-Spera and White (1987) FCIs occur when a hot liquid (termed the fuel) comes into contact with a cooler liquid (the coolant) whose temperature of vaporisation is less than the temperature of the fuel. Although the interactions can cause nonexplosive vaporisation of the coolant, highly explosive interactions are also common. In these cases a rapid transfer of heat from the fuel to the coolant, upon mixing of the two, results in sudden vaporisation of the coolant and explosive disruption of the whole system (Wohletz, 1986; Busby-Spera and White, 1987). The presence of fluidal peperite in the Brosterlea complex may represent a precursory stage to the development of FCIs (Busby-Spera and White, 1987). This implies that FCIs may have been responsible for the formation of the volcaniclastic breccias.

In the Brosterlea Complex the rock fragments formed from a diatreme eruption would have been mixed and redeposited in the vent of the diatreme as massive, poorly sorted, well mixed deposits (Figure 73). Diatreme-maars are characterised by steep-sided fault contacts, like the fault contact in the southwest of the study area (Map, Appendix B, Figure 16). Subsidence, as described in the study area, also occurs in diatreme-maars (Lorenz, 1986). Large sections of Clarens Formation along the edge of the diatreme might have broken from their *in situ* positions and slumped into the vent as large sandstone blocks.

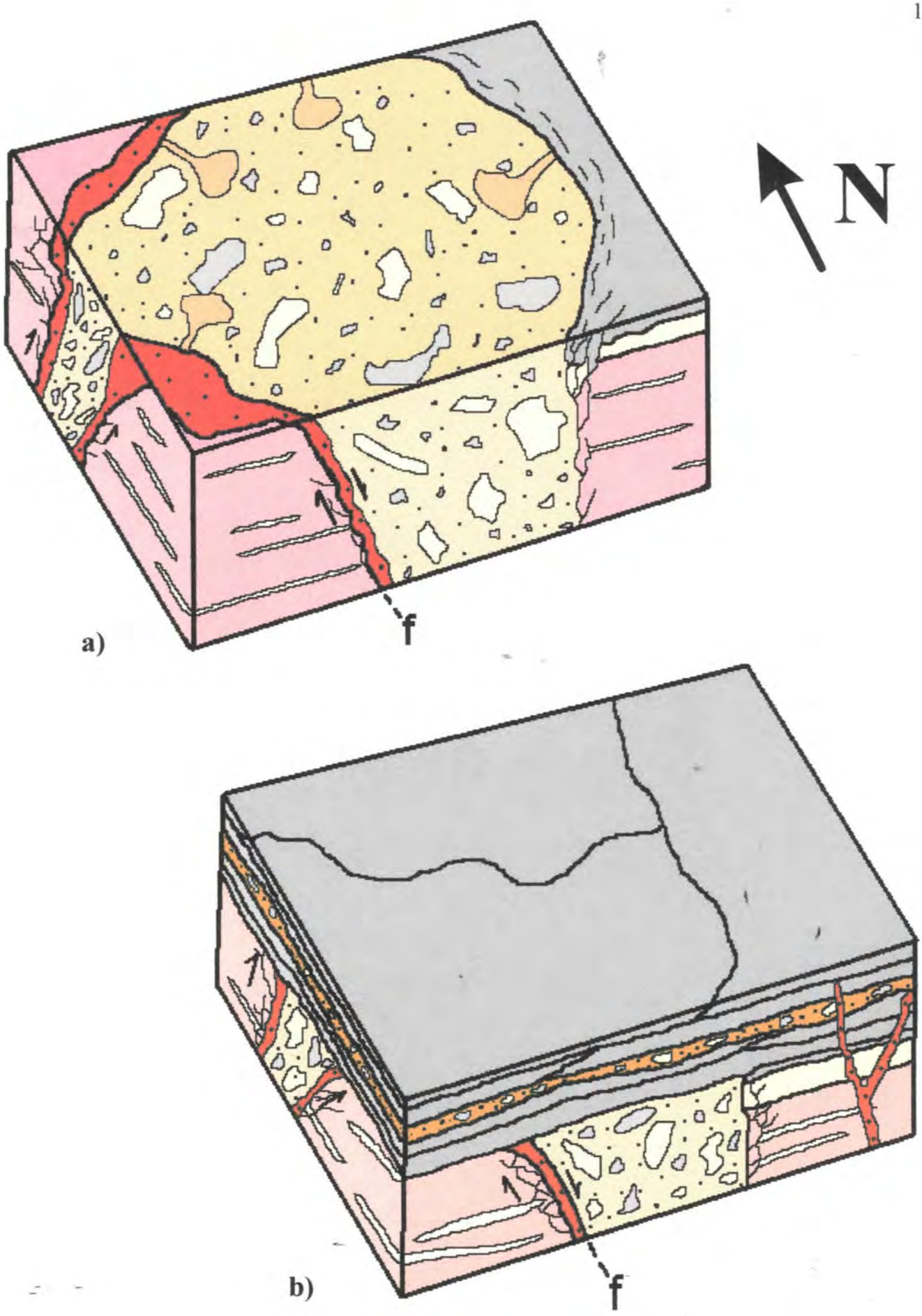

Figure 73: Hypothesis 1 ("Typical" maar-diatreme structure): a) - Formation of large diatreme vent and faulting along western boundary. The northern-most half of the fault plane along the western boundary of the vent was intruded by a dolerite body. The vent was refilled with the material erupted from the diatreme. b) - The subsequent extrusion of basalt flows covered the vent and the lower volcaniclastic breccia, and the thin, upper volcaniclastic breccia was emplaced between basalt flows. The upper volcaniclastic breccia originated outside the study area from an eruption similar to that which produced the lower volcaniclastic breccia. Dyke intrusions continued throughout the emplacement of the exposed basalt flows.

However, it is highly unlikely that typical diatreme-maar eruptions could produce the volumes of volcaniclastic breccia observed in the field area. Considering a "typical" cone-shaped diatreme-maar crater between 100m and 2km in diameter, with a depth of 1 to 2km (Lorenz, 1973), the volume of the crater would range from $0.003km^3$ to $2.1km^3$. Since the lower volcaniclastic breccia has an estimated volume of $27km^3$, it could not fill the neck of a typical diatreme-maar. No direct and conclusive evidence exists to support the theory that the complex is a composite of a number of smaller vents either. Evidence for the presence of a number of smaller vents would include a number of breccia units with differing physical and chemical characteristics, portions of unaffected Clarens and Elliot Formation outcropping at altitudes in accordance with the altitudes of the Elliot and Clarens formations outside the subsidence structure, and a number of individual breccia units interbedded with each other.

Hypothesis 2: Intrusion of dolerite along fault plane and eruption of breccias

The presence of the dolerite intrusion to the west, together with the evidence of a fault-like contact in the southwestern corner of the study area and dramatic differences in elevation of the Clarens Formation sandstone just north of the study area and the Clarens sandstone outcrops ~500m to the south, within the study area, suggests that a zone of faulting occurs along the entire western boundary. This subsidence of the original shallow depression is almost certainly due to the eruption of the lower breccia, in the manner of caldera collapse. The presence of an inferred palaeodepression suggests that if the lower volcaniclastic breccia was generated outside the boundaries of the study area, it may have flowed as a laharic debris flow and ponded in the depression (Figure 74). Internal structures which would indicate a palaeoflow direction for the breccia are not evident.

Grapes *et al.* (1973) described a volcaniclastic deposit which formed from the end of a shallow doleritic intrusion in the Allan Hills region of Antarctica. In a similar manner, the large doleritic intrusion along the western boundary of the Brosterlea Complex may have produced at least some of the lower volcaniclastic breccia. Figure 75 demonstrates Grapes *et al.*'s inferred mechanism of intrusion of a sill, and formation of volcaniclastic breccia. As the sill intrudes below the sedimentary units, an expansion space is formed at the head of the sill. Voids are also produced as the overlying sedimentary beds are forced to slip over one another. The resultant decrease in pressure in these areas, and tensional fractures that develop in the crests of the folds allow magma to move into and enlarge the voids.

Water present in the sedimentary units would cause an explosive magma-water interaction and further rotation of the overlying units at the head of the intrusion would result in blocks of Clarens Formation sandstone being broken off and incorporated into the dolerite magma (Grapes *et al.*, 1973). Grapes *et al.* observed that many of the sandstone blocks have been partially fused from interaction with magma and the sandstone is now composed of ragged quartz and feldspar grains within a clouded granophyric intergrowth of quartz and feldspar. They stress that the interaction between the sediment and the doleritic intrusion can only occur at shallow depths where folding and bedding plane slip is possible. Similar angular grains and intergrowths were observed in thin-sections from most of the sandstone blocks sampled in the Brosterlea Complex. Partial and completely fused sandstone blocks are observed within the very similar Sterkspruit complex near Rhodes, in the Barkly East area (Skilling, pers.com.).

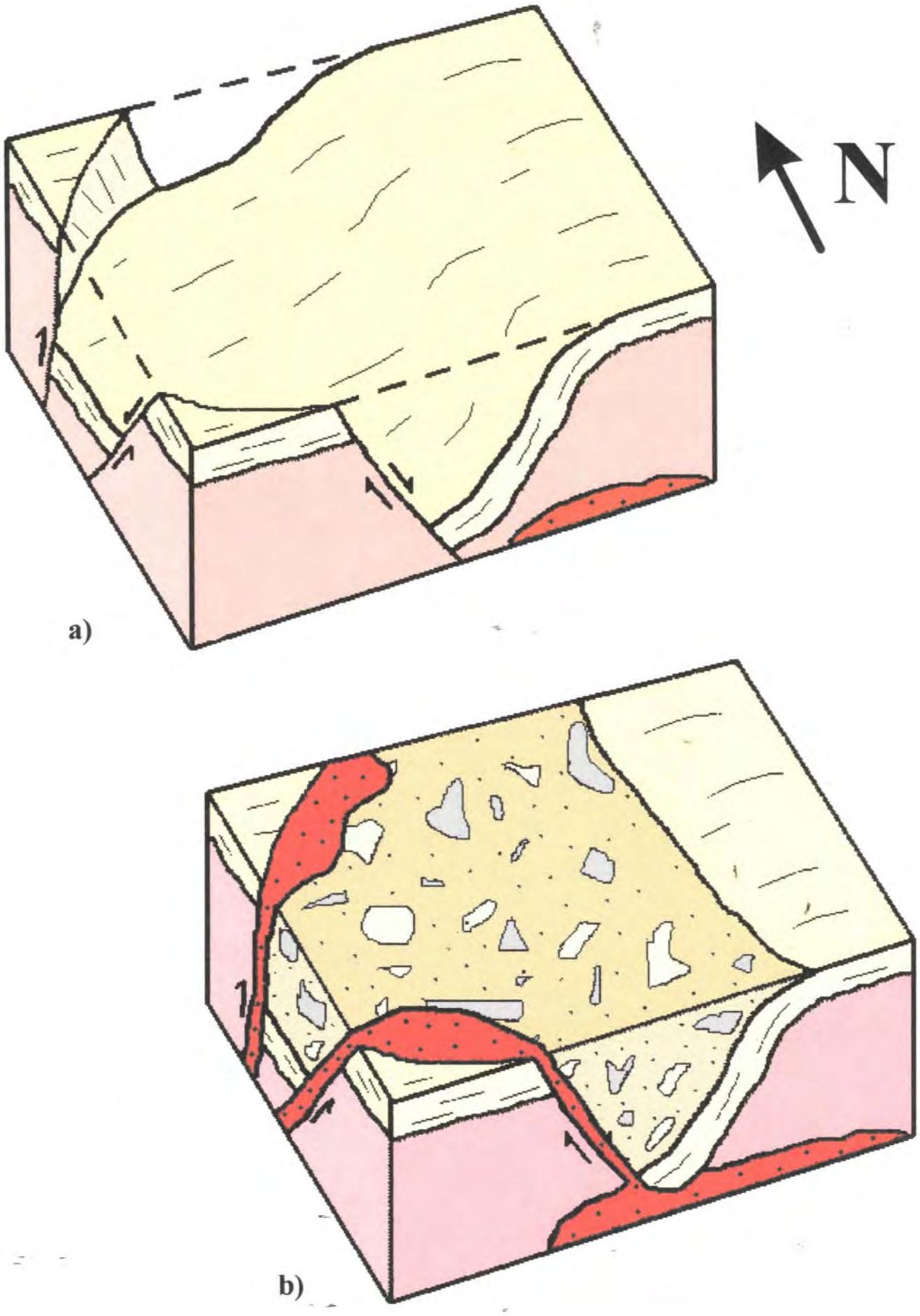

Figure 74: Hypothesis 2 (Intrusion of dolerite along fault plane and eruption of breccias): Block diagrams depicting the development of the subsidence structure and the in-filling of the depression with volcaniclastic breccia. a) - Faulting along the western margin and down-sagging occurred to form the subsidence structure. b) - Intrusion of dolerite along the fault plane and ponding of laharic volcaniclastic breccia in the depression. From the possible relationship between the dolerite and the volcaniclastic breccia observed in the north-western corner of the study area, it appears that the dolerite may be related to the formation of at least some of the breccia through a similar process to that described by Grapes et al. (1973).

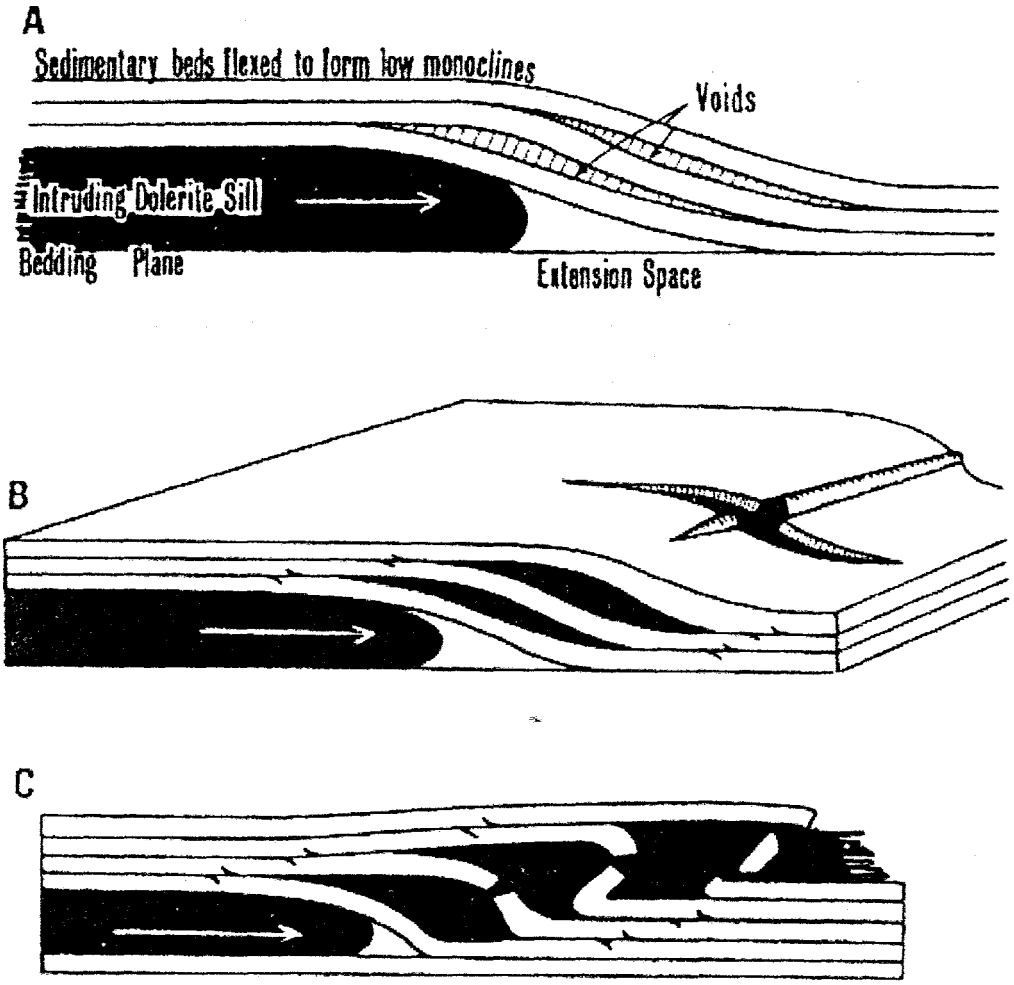

Figure 75: Diagrammatic reconstruction of the mechanism of intrusion of a sill. A- Development of voids caused by the overlying beds slipping over one another forward of the intruding sill to form low monoclines. B- Tensional fractures develop in the crests of the folds allowing magma to rise into and enlarge the voids. C- Extreme differential slip disrupts the overlying beds causing rotation and inclusion of sediment blocks in dolerite. After Grapes *et al.* (1973).

Pollard and Johnson (1973) and Kerr and Pollard (1998) disagree with this mechanism, and feel it is unlikely for the overlying beds to slip past each other, creating voids at the head of the intrusion. This is because the head of the intrusion is the zone of greatest compression, and the overlying beds should be compressed together, not forced apart.

In the case of the Brosterlea Complex there is no evidence of disruption of the edge of the dolerite intrusion, folding of the Elliot and Clarens formation units, or a decrease in clast size away from the dolerite. A small outcrop of volcaniclastic breccia is, however, observed between the dolerite and the partly-consolidated sandstone host rock (Figure 76). This outcrop suggests that a small fissure of dolerite may have formed volcaniclastic breccia upon interaction with the wet sedimentary rocks.

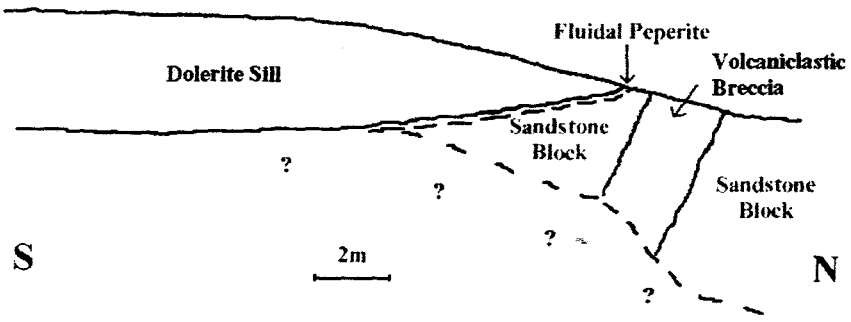

Figure 76: Sketch of outcrop of northern edge of dolerite intrusion along western edge of study area. Volcaniclastic breccia might be associated with the dolerite body, and may possibly have formed in similar fashion to breccia described by Grapes *et al.* (1973).

It seems unlikely that the observed doleritic intrusion could be responsible for such a large volume of volcaniclastic breccia without exhibiting a zone of disrupted material close to or along the length of its outcrop where the intrusion interacted with the sedimentary rocks and the lower volcaniclastic breccia was produced. One would expect a gradational contact between the dolerite and the breccia as the edges of the dolerite became more and more fragmented to produce the breccia, but the contact is sharp.

Hypothesis 3: Underplating of large area of wet sediments by dolerite sills and homogenous boiling of the sediment

The most likely hypothesis for the mechanism of eruption of the lower volcaniclastic breccia is that of dolerite sills underplating the entire volcanic complex. Sills which existed immediately prior to the eruptions forming the lower breccia may have been large enough to have heated and boiled the overlying sediment, producing the observed volume of the lower volcaniclastic breccia.

Considering the volume of breccia in the subsidence structure, a hydrovolcanic eruption would require wet sediment to be continuously added to prolong the eruption event and produce the required volume of volcaniclastic breccia. Such an eruption might closely resemble the unusual, smaller-scaled eruptions on White Island, New Zealand (Houghton and Nairn, 1991). Here the low discharge rate of the magma over an extended time period was delicately balanced with a continual input of unconsolidated sediment either through erosion of adjacent topographical highs, or through collapse of the weak conduit walls. In the present study area, the continued deposition of Clarens sandstone might have provided the sediment to prolong the phreatomagmatic eruptions. However, since the deposition in one locality would not have been rapid enough to sustain the eruptions, the eruptions may have had to occur simultaneously at several related point or linear sources within the volcanic complex. No evidence for multiple sources is observed in the complex. The volume of the breccias are too high to have formed from this mechanism, therefore, it is most likely that interaction of magma and wet sediment ($15km^3$) occurred over a large subsurface interface at any one time, as an essentially single catastrophic event.

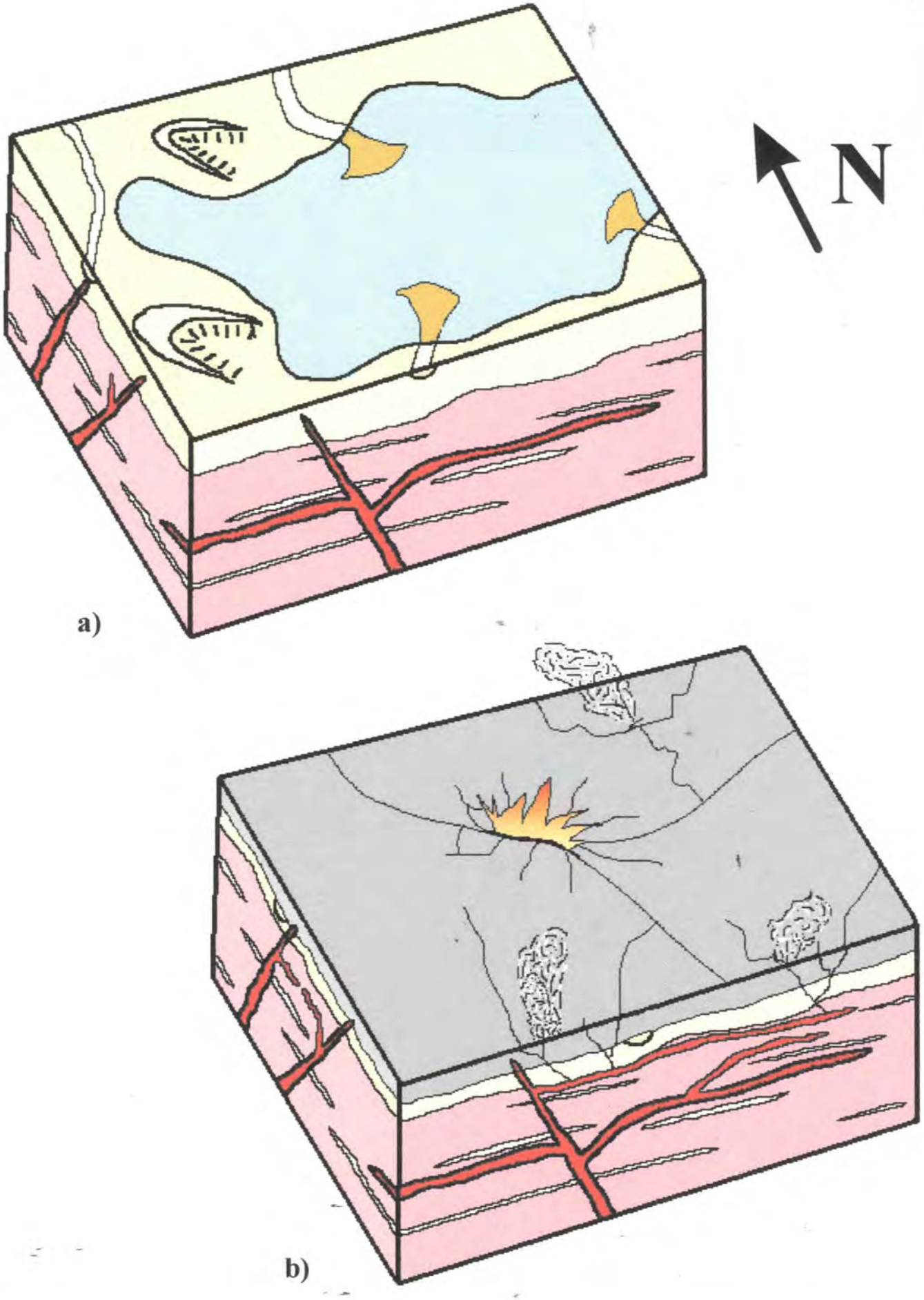

Figure 77: Hypothesis 3 (Underplating of large area of wet sediments by dolerite sills and homogenous boiling of the sediment): Block diagrams depicting palaeoenvironment and evolution of the lower volcaniclastic breccia in the subsidence structure. a) - Deposition of the Elliot Formation shales and sandstones followed by the deposition of Clarens Formation sandstone and the formation of a shallow lake in the palaeodepression. b) - The extrusion of Moshesh's Ford basalts over the lake capped the system. This allowed a buildup of pressure fromthe vaporising of water in the lake sediments below the lava flows. The explosive expansion of volatiles caused fracturing of the Clarens and Elliot Formation rocks, as well as the Moshesh's Ford basalt flows.

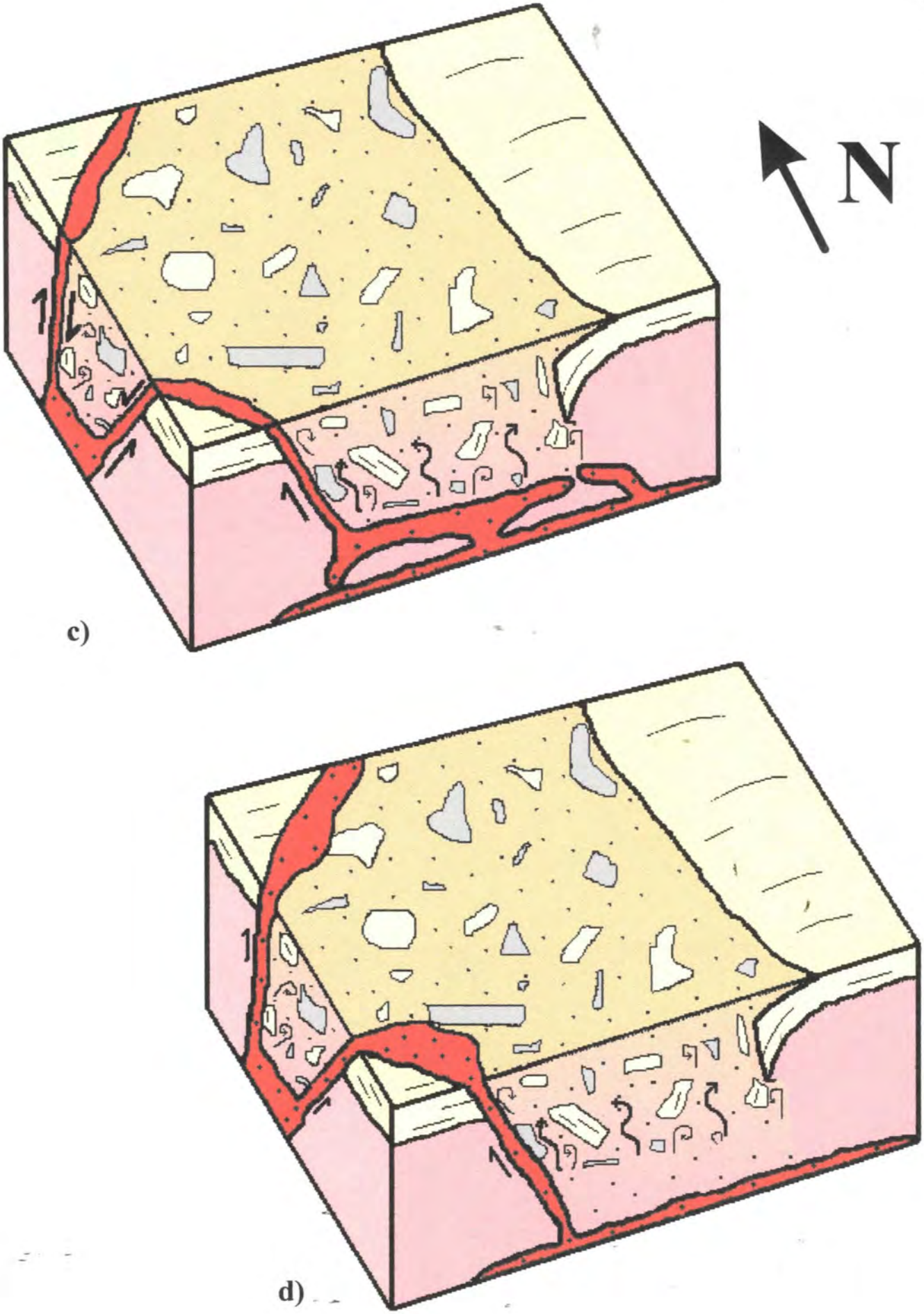

Figure 77: (cont.) Block diagrams depicting the formation of the volcaniclastic breccia through intrusion of the Elliot and Clarens Formations by dolerite sills, heating and boiling the ground and surface water, and possibly building more pressure under a few basalt flows. Subsequent eruptions fragmented the overlying sediment, forming the volcaniclastic breccia (c). d) - The underlying doleritic intrusions may have solidified *in situ*, may have erupted as dykes at a later stage, or most likely have been incorporated into the lower breccia.

A problem arises when considering how sufficient pressure built up in unconsolidated sediments to cause explosive eruptions of the sediments and basalt magma to form the lower volcaniclastic breccia. Simply capping the system with a few basalt flows would not be sufficient, as fractures forming in the cooling basalt would release any pressure. Basalt lava flows are in fact common aquifers in many parts of the world. A large sequence of basalt capping would be required, but an estimated maximum thickness of only 10-15m is inferred for the basalt capping prior to the generation of the lower volcaniclastic breccia. This thickness is calculated from the volume of basalt clasts in the lower breccia divided by the area of the volcanic complex. Only the Moshesh's Ford basalts are included in the lower breccia and are therefore the only lava flows emplaced prior to the phreatomagmatic eruptions. They would not have provided enough of a cap to contain the building pressure.

Alternatively, if the sediment in the volcanic complex was underplated by dolerite, the sediment may just have boiled over a large area, as in a cauldron, mixing with the dolerite. The dolerite sills may have vapourised the water in the sediments, causing an initial phreatic followed by phreatomagmatic explosion due probably to homogenous boiling. This was accompanied by fragmentation of the sedimentary and volcanic material. The coarse-grained basalt clasts in the lower breccia suggest that the sills did exist below the volcanic complex and were fragmented and incorporated into the breccia as the breccia formed. A volume of 6.8km^3 of juvenile glass is estimated to be in the lower volcaniclastic breccia. It is believed to have interacted with approximately 15km^3 of consolidated and unconsolidated sediment (Elliot and Clarens formations). This represents a ~60m package of sedimentary material over the area of the volcanic complex. This is the preferred hypothesis for the formation of the lower volcaniclastic

breccia. The underplating and formation of the subsidence structure and formation of the breccia is depicted in Figure 77.

Transport of volcaniclastic breccias

Depending on which mechanism of eruption hypothesis is considered, the mode of emplacement of the lower volcaniclastic breccia differs. No evidence exists to suggest that the lower breccia was transported into the volcanic complex from a source outside the study area. However, for completeness that possibility is considered later with the discussion on the mode of emplacement of the upper breccia. Based on the three hypotheses discussed previously, it seems more likely that the lower breccia was transported only a short distance (a few hundred metres at most) into the volcanic complex. The lower breccia is believed to have been formed within the volcanic complex and as a result would not have moved far from its source to its present position. The possible modes of emplacement for the lower breccia thus include generation *in situ*, eruption into the air, falling directly back into the complex, and eruption or "boiling over" of material and return to the complex as lahars.

Because no evidence of bedding or layering exists in the lower breccia (except a small section along the western slope of Perdekop) material ejected from the volcanic complex as a slurry would have to have flowed back into the complex before cooling. If the breccia was returned to the complex as secondary lahars one would expect to observe some sort of internal structure in the predominantly massive unit. Glass shards, as observed in the breccia would also not survive transport for any distance.

The majority of the massive, poorly-sorted breccia was most likely generated *in situ* by the boiling of the wet sediment, with occasional eruptions of dense, wet jets (probably of Surtseyan-type) which either fell directly back into the complex, or were ejected a short distance from the complex. Strombolian eruptions accompanied the eruption of the breccias. These eruptions generated cored and ribbon bombs, forming isolated bomb-rich layers within the lower breccia (eg. subunits on the western slope of Perdekop).

The sheet-like, interbedded nature of the upper volcaniclastic breccia with the lava flows, with lateral continuity even outside the study area and no obvious associated vent, suggests that it was transported into the complex from a source outside the study area. The reason why the upper volcaniclastic breccia is finer-grained than the lower breccia is possibly due to the upper breccia in the area being further from its source than the lower breccia. Clasts of volcaniclastic breccia within the upper breccia imply that a cohesive or cemented breccia was picked up during eruption or transport of the upper breccia.

The mechanisms by which the upper breccia (and perhaps locally, the lower breccia) may have been transported depend on the temperature of the material. The temperature is dependant on the time period from the start of the eruption of the fragmental material to the emplacement in the subsidence structure of the upper and lower volcaniclastic breccias, as well as the temperature of the eruption. The two most likely flow mechanisms to have moved the breccias into the complex are pyroclastic flows and lahars.

A pyroclastic flow is a hot (>100°C), gas-driven, gravity mass-flow deposit of juvenile pyroclastic debris in which the proportion of particles to gas by volume is high (Cas and Wright,

1991; Yamamoto *et al.*, 1993; Waitt, 1989). No gas-escape structures are observed in the volcaniclastic breccias, however; a feature sometimes present in pyroclastic flows. The expanding gas in pyroclastic flows inflates the flow. As very little welding is observed within the volcaniclastic breccias it is unlikely that they were emplaced above 100°C.

De Rita *et al.* (1991), state that almost all mafic pyroclastic flow deposits described to date are commonly unwelded and of a smaller volume relative to felsic flows. In the western Cascade Range a 15m-thick basaltic, welded ash flow tuff of andesite (53-54 wt% SiO^2) composition was traced for 12 km (Taylor, 1969, 1981; from De Rita *et al.*, 1991). In rare cases, the mafic flows can behave more like felsic magma flows, as is the case of a caldera erupting basaltic pyroclastic flows on Gran Canaria (Freundt and Schmincke, 1995). They describe the types of deposits, covering more than a 45km diameter, and emplacement mechanisms of basaltic magma that "erupted under conditions designed for felsic magmas". The eruptive behaviour was very similar to felsic magma, with the basalts having low viscosities, but high discharge rates. This produced a voluminous deposit from low pyroclastic fountains (<1000m high). The material was hot during transport and deposition, and welding and high temperature devitrification occurred. This is not, however, observed in the study area where the unwelded upper and lower breccias, containing unconsolidated sediment, each cover more than 270km^2 (15 x 18km). It is thus unlikely that a pyroclastic flow was responsible for the emplacement of the volcaniclastic breccias.

The upper breccia is most likely to have been emplaced as lahars, which are unsorted or poorly-sorted, water-mobilised, hyperconcentrated, mass-flows of debris from a volcanic eruption (Mullineaux and Crandell, 1962; Waitt, 1989; Hanson and Elliot, 1996). The term "lahar"

includes the whole textural range of water-lubricated debris flows and hyper-concentrated flood flows of a volcanic origin. The water in the flows may be derived from almost any source. These include eruptions through a crater lake or wet sediment, eruptions during heavy rain storms, eruptions causing the melting of snow and ice, flowing of pyroclastic flows or surges into streams and rivers, meteoric water, or magmatic water released during eruptions (Mullineaux and Crandell, 1962; Waitt, 1989).

The difference in temperature between hot (above ambient temperature to 100°C) and cold (ambient temperature) lahars is usually a result of the way in which they formed. Hot lahars are generated during or soon after an actual eruption, and are heated by accumulation of the material being erupted. Cold lahars on the other hand, may take place after the eruption (and thus not be associated at all with the eruption), from the collapsing of the rim of a crater lake, heavy rain, or melting of snow and ice. These provide large volumes of water to saturate and lubricate a pre-existing mantle of volcanic debris.

Mullineaux and Crandell (1962), and Hanson and Elliot (1996) state that lahars tend to be very variable in texture and composition. This is clearly observed in the present field area. Best (1992) emphasises that a wide range of facies may be generated from a single flow, and that deposits can display significant vertical, lateral, and proximal-distal variations. The breccias in the study area are poorly sorted, not because the flows were turbulent, but because the high density of clasts within the flow and the lack of gas expansion prohibited the shifting and sorting of the clasts. The breccias were possibly emplaced by plug flow or laminar flow.

Based on the discussion above, it is believed that the emplacement mechanism of the upper breccia (and possibly, locally the lower breccia) was laharic in nature, though it is possible that the upper breccia may have initially travelled as a pyroclastic flow before being deposited. Reworking of the pyroclastic deposit at a later stage may have generated a lahar that deposited the volcaniclastic breccia in the study area.

10.7 Strombolian Eruptions

According to MacDonald (1972) and Houghton and Nairn (1991) Strombolian eruptions contain small proportions of well-formed fusiform or spheroidal bombs and/or lapilli. The Strombolian eruptions can be associated with phreatomagmatic eruptions and are the inferred source of the cored and ribbon bombs encountered in the lower volcaniclastic breccia. Strombolian scoria cones are composed of loose, steeply piled pyroclasts and the easily erodible tephra cones can be rapidly destroyed (Francis, 1993). No crater remnant is observed in the study area, although a near-vent, bomb-rich deposit, associated with very similar volcaniclastic breccias has been observed in the Sterkspruit valley, approximately 100km to the north-east near Rhodes in the Barkly East area (Skilling, pers.com.).

The Strombolian clasts in the lower volcaniclastic breccia may have been picked up from an earlier Strombolian deposit, or they may have been erupted directly onto the surface of the breccia. The is no evidence of any Strombolian activity in the complex prior to the formation of the lower volcaniclastic breccia to have produced Strombolian clasts. Any such clasts would have been picked up and distributed throughout the lower volcaniclastic breccia, not restricted to a small subunit towards the top of the lower breccia. It is unlikely that the Strombolian clasts

were transported to the volcanic complex from a source like the Strombolian vent in the Sterkspruit valley as no volcaniclastic breccia outcrops links the two sites directly, and unless unconsolidated, such a transport of material would most likely include fragments of volcaniclastic breccia also present in the valley. No clasts of volcaniclastic breccia are present in the lower breccia in the volcanic complex.

No evidence of sediment in the Strombolian clasts suggests that little, if any, mixing of sediment and basalt occurred. This implies that the Strombolian eruptions were almost exclusively juvenile basalt. It is suggested that during the formation of the lower breccia isolated Strombolian eruptions of basalt with little sediment interaction may have occurred, possibly towards the eastern edge of the volcanic complex. The Strombolian clasts may have been erupted onto the surface of the breccia, or onto the edges of the complex, along with some volcaniclastic breccia that had previously boiled over, and then returned to the complex as lahars. This would result in the isolated subunit containing Strombolian clasts on the western slope of Perdekop. This also suggests that the lower volcaniclastic breccia may have been emplaced in a number of pulses, marking a slight change in the environment between eruptions, to allow for the containment of Strombolian clasts in a small area of the complex.

11.0 CONCLUSIONS

The fault contact along the western boundary of the volcanic complex, and the tilted Clarens Formation sandstone dipping under the structure indicates the presence of a subsidence structure. The eastern boundary remained unfaulted while the western boundary was downthrown into the structure, and as a result the structure is inferred to have formed as a "trapdoor" system. The tilted Clarens Formation sandstone observed dipping under the lower volcaniclastic breccia in the north of the study area suggests that the faulting dragged the Clarens sandstone downwards. It is believed that the contact, or fault plane in the southwest corner of the study area is a continuation of the fault along the northern and western margin.

The presence of a palaeolake or ponding of water at the time of the volcanic eruptions is suggested by the presence of blocky peperite development in the subsidence structure, the fluvial reworking of sandstone and volcaniclastic breccia above the fault outcrop in the southeast of the structure, and channel-lags in the upper part of the Clarens Formation sandstone, which are confined to the structure. Ponding of water suggests that abundant groundwater was also present providing an environment for the interaction of basalt with wet sediment and the formation of FCIs.

A large dolerite intrusion along the western boundary of the subsidence structure has intruded along the fault plane along the western contact. This intrusion implies that intrusive activity may have occurred in close proximity to the ponded water, and suggests that the eruption mechanisms forming the volcaniclastic breccia may have been related to interaction between the intrusions

and wet sediment. While it is difficult to be certain if the coarse-grained basaltic clasts in the lower volcaniclastic breccia are related to doleritic intrusions or thick basalt flows, clasts from doleritic intrusions would confirm that other intrusions existed close to the subsidence structure, possibly underplating the wet sediments. The hydrothermal circulation of groundwater, heated by these intrusions caused the precipitation of pisoliths in the Clarens Formation sandstone. The fluidal peperite clasts in the breccias also have basalt which is generally extensively hydrothermally altered.

Both phreatic and phreatomagmatic eruptions are inferred to have been generated within the subsidence structure through the intrusion and underplating of wet sediments by dolerite sills, and vaporisation of the water in the lake and the lake sediments. A period of phreatic eruptions is believed to have occurred prior to the main phreatomagmatic eruptive event. This is based on the nature of stream-flow deposits which outcrop stratigraphically between the Clarens Formation and the lower volcaniclastic breccia. Consolidated and unconsolidated sandstone was fractured by steam explosions and erupted with little or no juvenile basalt content. This sediment included pisolitic sandstone which was fragmented, freeing the pisoliths. The pisoliths and pisolitic sandstone were redeposited in stream-flow deposits along with angular sandstone fragments.

Fluidal peperite formed prior to the phreatomagmatic eruptions in areas where unconsolidated sand and mud were intruded by small amounts of basalt. Subsequently clasts of peperite were included in the lower volcaniclastic breccia. An increase in the volume of magma below the subsidence structure introduced more basalt to the system. This increase in the magma:water ratio led to the formation of FCIs that resulted in a transition from phreatic to phreatomagmatic eruptions which produced the lower volcaniclastic breccia ($27km^3$). The breccia is inferred to

have formed by eruption as superheated wet sediment mixed with intruding magma and redeposition by a combination of backfall and backflow in the subsidence structure through boiling of the fluid in the partly-consolidated sediments. Minimal transport is inferred for the lower breccia. An approximate 25 vol% juvenile glass in the lower breccia ($6.8km^3$) represents the volume of intrusive material which interacted with approximately 30 vol% unconsolidated sediment ($8.1km^3$), ~25 vol% lithic sedimentary clasts, and ~20 vol% lithic basalt ($5.4km^3$).

It is unclear how pressure was able to build up in the unconsolidated sediments to generate the erupted products. Geochemical analyses of basalt clasts taken from the lower volcaniclastic breccia revealed that they have a geochemical signature of the Moshesh's Ford basalts, which outcrop around the subsidence structure, but are absent within it. It is believed that the Moshesh's Ford basalts were emplaced prior to the generation of the lower volcaniclastic breccia, and the phreatomagmatic eruptions fragmented the basalt in the subsidence structure, incorporating it into the breccia. However, the Moshesh's Ford basalts are estimated to have been only 10-15m thick in the subsidence structure, based on the volume of Moshesh's Ford basalt fragments in the lower volcaniclastic breccia. Due to cooling fractures, thermal joints and the presence of vesicles in the basalts, this would not have provided enough of a capping to the system to build up the pressure required. It is more likely that dolerite sills underplated wet sediments over a wide area, causing homogeneous boiling of the water in the sediments, in an uncapped system.

With a localised drying-out of the system, Strombolian eruptions occurred and their clasts were incorporated into the lower breccia. The Strombolian eruptions may have occurred *during* the eruption of the lower volcaniclastic breccia. As the cored and composite lapilli and cored bombs

are geographically restricted to a small area on the western slope of Perdekop, it is believed that the Strombolian eruptions occurred nearby. However, as the Strombolian clasts are dispersed vertically throughout the subunit, and are not isolated in lenses or lateral zones within the breccia, it suggests that the subunit has been transported a short distance, mixing the constituents of the subunit during transportation.

A mechanism of eruption similar to that described for the lower volcaniclastic breccia is inferred for the upper volcaniclastic breccia. This breccia was not erupted from the subsidence structure and was transported from a source outside the study area as a laharic debris flow. A greater proportion of basalt clasts in the upper breccia indicates an increase in the volume of lava flow emplaced during the time between emplacement of the lower and the upper volcaniclastic breccias. Increased lava flows may possibly have given rise to higher explosivity and a greater degree of inflation of the upper breccia compared to the lower one.

Similarities between the breccias in the Brosterlea Volcanic Complex and the Prebble Formation in Antarctica are significant as they suggest a similar palaeoenvironment and eruptive style. This allows correlation between the deposits in Southern Africa and those in Antarctica, and field evidence observed on the one continent may help to understand and describe the palaeoenvironment and geological features on the other.

Widespread basaltic lahars such as those in the Brosterlea Volcanic Complex are very rare. It is possible that such deposits characterise pre-flood basalt volcanism in other areas, eg. pyroclastic rocks occur at the base of the Siberian Traps (Sharma, 1997), but they have not been

described. It is also possible that similar deposits may exist at the base of other flood basalt provinces and as yet have not been identified or described.

12.0 REFERENCES

Anderson, D.L., Zhang, Y.S-., Tanimoto, T. 1992. Plume heads, continental lithosphere, flood basalts and tomography, in *Magmatism and the Causes of Continental Break-up*, Spec. Publ., **68**. edited by B.C. Storey, T. Alabaster and R.J. Pankhurst. 99-124, The Geological Society, London.

Best, J.L. 1992. *Sedimentology and event timing of a catastrophic volcaniclastic mass flow, Volcan Hudson, Southern Chile*. Bulletin of Volcanology. **54**: 299-318.

Blatt, H. 1982. *Sedimentary Petrology*. W.H. Freeman and Company, San Francisco.

Blatt, H., Middleton, G., Murray, R. 1980. *Origin of Sedimentary Rocks*. Prentice-Hall, Inc., New Jersey.

Boggs, S (Jnr.). 1987. *Principles of Sedimentology and Stratigraphy*. Macmillan Publishing Company, New York.

Botha, B.J.V. 1968. *The Stratigraphy of the Red Beds stage, Karroo System, at Elliot, C.P.* Transactions of the geological Society of Southern Africa. **71**: 101-117.

Bristow, J.W., Saggerson, E.P. 1983. *A Review of Karoo Vulcanicity in Southern Africa*. Bulletin of Volcanology. **46-2**: 135-159.

Busby-Spera, C.J., White, J.D.L. 1987. *Variation in peperite textures associated with differing host-sediment properties.* Bulletin of Volcanology. **49**: 765-775.

Cas, R.A.F., Wright, J.V. 1991. *Subaqueous pyroclastic flows and ignimbrites: an assessment.* Bulletin of Volcanology. **53**: 357-380.

Cox, K.G. 1970. *Tectonics and Vulcanism of the Karroo Period and their Bearing on the Postulated Fragmentation of Gondwanaland.* **In**: Clifford, T.N. and Gass, I.G. (Eds). African Magmatism and Tectonics. Oliver and Boyd, Edinburgh. 211-235.

Deer, W.A., Howie, R.A., Zussman, J. 1996. *An Introduction to the Rock-Forming Minerals.* Addison Wesley Longman Ltd.

De Rita, D., Frazzetta, G., Romano, R. 1991. *The Biancavilla-Montalto ignimbrite (Etna, Sicily).* Bulletin of Volcanology. **53**: 121-131.

Dingle, R.V., Siesser, W.G. Newton, A.R. 1983. *Mesozoic and Tertiary Geology of Southern Africa.* A.A. Balkema, Rotterdam.

Duncan, R.A., Hooper, P.R., Rehacek, J., Hooper, P.R., Marsh, J.S., Duncan, A.R. 1996. *The Timing and Duration of the Karoo Igneous Event, Southern Gondwana.* Journal of Geophysical Research.

Du Toit, A.L. 1904. *Geological survey of Aliwal North, Herschel, Barkly East and part of Woodehouse.* 9th Annual Rep. Geol. Commission, Colony of the Cape of Good Hope. 69-110.

---------- 1954. *The Geology of South Africa.* Oliver and Boyd, London.

Eales, H.V., Marsh, J.S., Cox, K.G. 1984. The Karoo Igneous Province: an Introduction. in *Petrogenesis of the Volcanic Rocks of the Karoo Province*, edited by Erlank, A.J., Special Publication No. 13. The Geological Society of South Africa.

Eriksson, P.G. 1981. *A Palaeoenvironmental Analysis of the Clarens Formation in the Natal Drakensberg.* Transactions of the geological Society of Southern Africa. **84**: 7-17.

--------- 1984. *A palaeoenvironmental analysis of the Molteno Formation on the Natal Drakensberg and NE Orange Free State.* Transactions of the geological Society of Southern Africa. **87**: 237-244.

--------- 1985. *The depositional palaeoenvironment of the Elliot Formation in the Natal Drakensberg area.* Transactions of the geological Society of Southern Africa. **88**: 19-26.

--------- 1986. *Aeolian dune and alluvial fan deposits in the Clarens Formation of the Natal Drakensberg.* Transactions of the geological Society of Southern Africa. **89**: 389-393.

Eriksson, P.G., McCourt, S., Snyman, C.P. 1994. *A note on the petrography of upper Karoo sandstones in the Natal Drakensberg: implications for the Clarens Formation palaeoenvironment.* South African Journal of Geology. **97(1)**: 101-103.

Fischer, R.V., Schmincke, H.-U. 1984. *Pyroclastic Rocks.* Springer Berlin Heidelberg New York Tokyo. pp. 1-472.

Francis, P. 1993. *Volcanoes: A Planetary Perspective.* Oxford University Press Inc., New York.

Friedman, G.M.(ed.). 1969. *Depositional Environments in Carbonate Rocks.* Society of Economic Paleontologists and Mineralogists. Special Publication No. 14.

Friedman, G.M., Sanders, J.E. 1978. *Principles of Sedimentology.* John Wiley & Sons.

Freundt, A., Schmincke, H. -U. 1995. *Eruption and emplacement of a basaltic welded ignimbrite during caldera formation on Gran Canaria.* Bulletin of Volcanology. **56**: 640-659.

Füchtbauer, H., Peryt, T. 1980. *The Zechstein Basin with Emphasis on Carbonate Sequences.* E. Schweizerbart'sche Verlagsbuchhandlung, Stuttgart.

Gevers, T.W. 1928. *The Volcanic Vents of the Western Stormberg.* Transactions of the geological Society of Southern Africa. **31**: 43-62.

Grapes, R.H., Reid, D.L., McPherson, J.G. 1973. *Shallow dolerite intrusion and phreatic eruption in the Allan Hills region, Antarctica.* New Zealand Journal of Geology and Geophysics, 17 (3): 563-577.

Greensmith, J.T. 1989. *Petrology of the Sedimentary Rocks.* Unwin Hyman, London.

Hanson, R.E., Elliot, D.H. 1996. *Rift-related Jurassic basaltic phreatomagmatic volcanism in the central Transantarctic Mountains: precursory stage to flood-basalt effusion.* Bulletin of Volcanology. **58**: 327-347. Springer-Verlag.

Hooper, P.R. 1997. The Columbia River Flood Basalt Province: Current Status. in *Large Igneous Provinces: Continental, Oceanic, and Planetary Flood Volcanism.* edited by Mahoney, J.J., Coffin, M.F. Geophysical Monograph 100. American Geophysical Union, Washington.

Houghton, B.F., Nairn, I.A. 1991. *The 1976-1982 Strombolian and phreatomagmatic eruptions of White Island, New Zealand: eruptive and depositional mechanisms at a 'wet' volcano.* Bulletin of Volcanology. **54**: 25-49.

Houghton, B.F., Wilson, C.J.N. 1989. *A vesicularity index for pyroclastic deposits.* Bulletin of Volcanology. **51**: 451-462.

Kerr, A.C., Pollard, D.D. 1998. *Towards more realistic formulas for the analysis of laccoliths.* Journal of Structural Geology. 20: 1783-.

Kerr, A. C., Tarney, J., Marriner, G.F., Nivia, A., Saunders, A.D. 1997. The Caribbean-Colombian Cretaceous Igneous Province: The Internal Anatomy of an Oceanic Plateau. in *Large Igneous Provinces: Continental, Oceanic, and Planetary Flood Volcanism.* edited by Mahoney, J.J., Coffin, M.F. Geophysical Monograph 100. American Geophysical Union, Washington.

Kokelaar, B.P., 1982. *Fluidisation of wet sediments during the emplacement and cooling of various igneous bodies.* Journal of the geological Society of London. **139**: 21-33.

Leat, P.T., Thompson, R.N. 1988. *Miocene hydrovolcanism in NW Colorado, USA, fuelled by explosive mixing of basic magma and wet, unconsolidated sediment.* Bulletin of Volcanology. **50**: 229-243.

Lock, B.E. 1978. *Ultrahigh-Temperature Volcanic Mudflows Amongst the Drakensberg Volcanic Rocks: New Criteria for their Recognition.* Transactions of the geological Society of Southern Africa. **81:** 55-59.

Lock, B.E., Paverd, A.L., Broderick, T.J. 1974. *Stratigraphy of the Karroo Volcanic Rocks of the Barkly East District.* Transactions of the geological Society of Southern Africa. 77: 117-129.

Lorenz, V. 1973. *On the Formation of Maars.* Bulletin of Volcanology. **37**: 183-204.

--------- 1986. *On the growth of maars and diatremes and its relevance to the formation of tuff rings.* Bulletin of Volcanology. **48**: 265-274.

Macdonald, G.A. 1972. *Volcanoes.* Prentice-Hall Inc. Englewood Cliffs, New Jersey.

Mahoney, J.J., Coffin, M.F. 1997. Preface in *Large Igneous Provinces: Continental, Oceanic, and Planetary Flood Volcanism.* edited by Mahoney, J.J., Coffin, M.F. Geophysical Monograph 100. American Geophysical Union, Washington.

Makadzange, T. 1998. *Geochemical Stratigraphy of Karoo basalts of the Brosterlea area, around Bakenkop, Driehoek, and Perdekop Hills, Eastern Cape Province, South Africa.* Unpublished Honours Project, Rhodes University, South Africa.

Marsh, J.S., Eales, H.V. 1984. The Chemistry and Petrogenesis of Igneous Rocks of the Karoo Central Area, Southern Africa. in *Petrogenesis of the Volcanic Rocks of the Karoo Province*, edited by Erlank, A.J., Special Publication No. 13. The Geological Society of South Africa.

Marsh, J.S., Hooper, P.R., Rehacek, J., Duncan, R.A., Duncan, A.R. 1997. Stratigraphy and Age of Karoo Basalts of Lesotho and Implications for Correlations Within the Karoo Igneous Province. in *Large Igneous Provinces: Continental, Oceanic, and Planetary Flood Volcanism.* edited by Mahoney, J.J., Coffin, M.F. Geophysical Monograph 100. American Geophysical Union, Washington.

Marsh, J.S., Skilling, I.P. 1998. Field Excursion Guide Book A3: *Karoo Volcanic and Intrusive Rocks, Eastern Cape.* IAVCEI International Volcanological Congress. Cape Town.

Masokwane, A. 1997. *Geochemical Stratigraphy of Karoo basalts of the Brosterlea area, around the farms Klipfontein and Noodhoek, Eastern Cape, South Africa.* Unpublished Honours Project, Rhodes University, South Africa.

McPhie, J., Doyle, M., Allen, R. 1993. *Volcanic Textures: A Guide to the Interpretation of Textures in Volcanic Rocks.* Centre for Ore Deposition and Exploration Studies, University of Tasmania.

Mountain, E.D. 1960. *Felsic Material in Karroo Dolerite.* Transactions of the geological Society of Southern Africa. **63:** 137-152.

Mullineaux, D.R., Crandell, D.R. 1962. *Recent Lahars from Mount St. Helens, Washington.* Bulletin of the geological society of America. **73**: 855-870.

Mumpton, F.A. 1981. (Ed). *Reviews in Mineralogy: Natural Zeolites.* Vol.4. Mineralogical Society of America.

North, F.J. 1930. *Limestones: Their Origins, Distribution, and Uses.* Thomas Murby and Co., London.

Peate, D.W. 1997. The Paraná-Etendeka Province. in *Large Igneous Provinces: Continental, Oceanic, and Planetary Flood Volcanism.* edited by Mahoney, J.J., Coffin, M.F. Geophysical Monograph 100. American Geophysical Union, Washington.

Pollard, D.D., Johnson, A.M. 1973. *Mechanics of Growth of some Laccolithic Intrusions in the Henry Mountains, Utah, II: Bending and Failure of Overburden Layers and Sill Formation.* Tectonophysics. **18**: 311-354.

Randell, L.M. 1996. *The Geology of the Area around the farms Lindisfarne, Hentland, and Caerlaverock, Barkly East, Rhodes, North-Eastern Cape, South Africa.* Unpublished Honours Project, Rhodes University, South Africa.

Reading, H.G. (ed.) 1996. *Sedimentary Environments: Processes, Facies and Stratigraphy.* 3rd Ed. Blackwell Science Limited.

Robey, J. 1973. *A Study of the Telemachus Kop and Modderfontein Volcanic Vents, west of Jamestown. Cape Province.* Unpublished Rhodes University Honours Project.

Rogers, A.W., Du Toit, A.L. 1909. *An Introduction to the Geology of Cape Colony*. Longmans, Green and Co.

Rollinson, H. R. 1993. *Using Geochemical Data: Evaluation, Presentation, Interpretation.* Longman Group UK Limited.

Rumble, K.C. 1979. *The Geochemistry and Petrology of the Karoo Andesites and Associated Basalts of the North-Eastern Cape Province.* Unpublished MSc thesis, Rhodes University, South Africa.

Saggerson, E.P. 1986. *A Handbook of Minerals Under the Microscope.* University of Natal Press, Pietermaritzburg.

Sanders, I.S., Johnston, J.D. 1989. *The Torridonian Stac Fada Member: an extrusion of fluidised peperite?* Transactions of the Royal Society of Edinburgh: Earth Sciences, **80**: 1-4.

Saunders, A.D., Fitton, J.G., Kerr, A.C., Norry, M.J., Kent, R.W. 1997. The North Atlantic Igneous Province. in *Large Igneous Provinces: Continental, Oceanic, and Planetary Flood Volcanism.* edited by Mahoney, J.J., Coffin, M.F. Geophysical Monograph 100. American Geophysical Union, Washington.

Scarth, A. 1994. *Volcanoes.* UCL Press Limited, University College London, London.

Sharma, M. 1997. Siberian Traps. in *Large Igneous Provinces: Continental, Oceanic, and Planetary Flood Volcanism.* edited by Mahoney, J.J., Coffin, M.F. Geophysical Monograph 100. American Geophysical Union, Washington.

Shelley, David. *Optical Mineralogy.*

Smith, R.M.H. 1986. *Sedimentation and palaeoenvironments of Late Cretaceous crater-lake deposits in Bushmanland, South Africa.* Sedimentology. **33**: 369-386.

Smith, R.M.H., Eriksson, P.G., Botha, W.J. 1993. *A Review of the Stratigraphy and Sedimentary Environments of the Karoo-aged basins of Southern Africa.* Journal of African Earth Science. **16**: 143-169.

South African Committee of Stratigraphy (SACS). 1980. Handbook 8. *Lithostratigraphy of the Republic of South Africa, Namibia, and the Republics of Bophutatswana, Transkei and Venda.* 1-690.

Tankard, A.J., Jackson, M.P.A., Eriksson, K.A., Hobday, D.K., Hunter, D.R., Minter, W.E.L. 1982. *Crustal Evolution of Southern Africa; 3.8 Billion years of Earth History.* Springer-Verlag. 396-399.

Tucker, M.E. 1981. *Sedimentary Petrology: An Introduction.* Blackwell Scientific Publications.

Turner, B.R. 1986. *Tectonic and climatic controls on continental depositional facies in the Karoo Basin of northern Natal, South Africa.* Sedimentary Geology. **46**: 231-257.

Visser, J.N.J. 1984. *A Review of the Stormberg Group and Drakensberg Volcanics in Southern Africa.* Palaeontology Africa (Palaeont. afr.). **25**: 5-27.

Visser, J.N.J., Botha, B.J.V. 1980. *Meander channel, point bar, crevasse splay and aeolian deposits from the Elliot Formation in Barkly Pass, North-eastern Cape.* Transactions of the geological Society of Southern Africa. **83**: 55-62.

Waitt, R.B. 1989. *Swift snowmelt and floods (lahars) caused by great pyroclastic surge at Mount St Helens volcano, Washington, 18 May 1980.* Bulletin of Volcanology. **52**: 138-157.

Walker, G.P.L. 1984. *Downsag Calderas, Ring Faults, Caldera Sizes, and Incremental Caldera Growth.* Journal of Geophysical Research. **89**: 8407-8416.

White, J.D.L. 1989. *Basic elements of maar-crater deposits in the Hopi Buttes volcanic field, North-eastern Arizona, USA.* Journal of Geology. **97**: 117-125.

-------- 1990. *Depositional architecture of a maar-pitted playa: sedimentation in the Hopi Buttes volcanic field, North-eastern Arizona, USA.* Sedimentary Geology. **67**: 55-84.

-------- 1991. *Maar-diatreme phreatomagmatism at Hopi Buttes, Navajo Nation (Arizona), USA*. Bulletin of Volcanology. **53**: 239-258.

White, R.S., McKenzie, D. 1989. *Magmatism at rift zones: the generation of volcanic continental margins and flood basalts*. Journal of Geophysical Research, **94**: 7685-7729.

White, R.S., McKenzie, D. 1995. *Mantle plumes and flood basalts*. Journal of Geophysical Research. **100, B9**: 17 543 - 17 585.

Wohletz, K.H. 1986. *Explosive magma-water interactions: thermodynamics, explosion mechanisms, and field studies*. Bulletin of Volcanology. **48**: 245-264.

Yamamoto, T., Takarada, S., Suto, S. 1993. *Pyroclastic flows from the 1991 eruption of Unzen volcano, Japan*. Bulletin of Volcanology. **55**: 166-175.

APPENDIX A

TRACE MIN	Sample #	GBS-124	GBS-125	GBS-126	GBS-127	GBS-128	GBS-129	GBS-130	GBS-131	GBS-133	GBS-134	GBS-135	GBS-136	GBS-137
Barium	Conc.	141.2	127.3	239.8	134.5	285.4		131.1	156.8	242.2	242.5	132.3	362.8	301.5
Scandium	Conc.	33	32.3	34.8	32.5	34.7		32.4	35.7	33.4	33.3	33.2	36.3	35.9
Thorium	Conc.	ND	LLD	3.0	LLD	2.0	LLD	1.6	LLD	LLD	3.5	LLD	2.6	2.9
Lead	Conc.	LLD	2.1	4.2	1.9	3.7	LLD	2.6	LLD	3.1	5.0	LLD	4.4	4.7
Cerium	Conc.	18.2	13.9	29.8	16.8	34.5	18.3	15.2	17.5	30.8	31.6	17.7	34.6	30.5
Neodymium	Conc.	11.4	8.1	17.6	10.6	17.5	10.2	9.9	11.1	17.9	16.3	10.6	20	18.1
Lanthanum	Conc.	6.4	5.8	12.8	5.6	12	6.4	6.7	5.6	14.7	13.5	6.8	13	13
Niobium	Conc.	5.7	4.2	8.1	4.5	8.8	5.7	4.1	5.7	9.9	8.7	5.1	9.4	9.5
Zirconium	Conc.	71	69.1	105.6	68.6	109.1	78.6	72.4	77.4	104.3	105.7	77.1	109.9	109.9
Yttrium	Conc.	25.4	24.4	29.8	23.6	31.8	24.1	25.6	27	29	30.1	27.1	28.8	30.6
Strontium	Conc.	190	192.5	260.4	184.1	283.5	189.1	183.4	219.3	384.9	172.8	185.3	333.6	236.4
Rubidium	Conc.	7.5	6.7	15.7	7.4	19.3	9.7	7	5.3	17.4	25.8	5.7	19.7	29.8
Cobalt	Conc.	45.9	45.1	35.8	46.6	39.4	42	47.8		34.8	38.5	42.6	37.7	37.6
Chromium	Conc.	333.1	346.1	305.7	343.7	317.1	352	330.2		306.8	329.6	294.2	319.1	332.9
Vanadium	Conc.	251.3	246.3	245	246.7	253.5	252.7	253.3		238.6	241.4	250.4	258	248.2
Zinc	Conc.	85.6	82	86.5	84.2	97.4	76.4	81.4	92.5	87.3	89.3	86.9	92	91.2
Copper	Conc.	98.1	96.2	34.6	96.7	40	70.8	101.6	115.8	32.6	35.6	90.1	35.6	39.5
Nickel	Conc.	106.2	106.1	21.5	117.2	26.2	112.4	105.3	71.7	22.1	24.6	98.6	23.1	24

	Sample #	GBS-124	GBS-125	GBS-126	GBS-127	GBS-128	GBS-129	GBS-130	GBS-131	GBS-133	GBS-134	GBS-135	GBS-136	GBS-137
Major Oxide														
SiO2		51.782	51.49	53.927	51.441	53.19	51.95	51.418	50.298	51.333	50.93	50.756	51.699	52.8
TiO2		0.887	0.847	1.041	0.856	1.096	0.926	0.916	0.96	1.042	1.077	0.958	1.068	1.094
Al2O3		15.745	15.659	14.726	15.527	15.124	15.084	15.317	14.849	14.696	15.411	15.267	15.409	15.203
Fe2O3		11.12	10.529	9.792	11.027	10.273	10.606	11.264	10.92	9.776	10.345	11.832	10.117	10.232
MnO		0.176	0.17	0.169	0.183	0.173	0.172	0.179	0.169	0.156	0.163	0.165	0.143	0.156
MgO		7.444	7.198	6.034	7.54	6.07	6.888	7.257	5.983	5.989	6	6.132	6.369	6.318
CaO		10.767	11.033	9.463	10.696	9.487	11.25	10.891	9.235	9.399	9.945	11.423	8.482	8.601
Na2O		2.498	2.423	1.93	2.479	2.455	2.522	2.476	4.095	2.032	2.236	2.398	2.223	2.95
K2O		0.432	0.425	0.796	0.454	1.037	0.481	0.437	0.425	0.903	0.985	0.42	0.98	1.279
P2O5		0.139	0.138	0.222	0.14	0.227	0.145	0.141	0.143	0.22	0.219	0.155	0.225	0.226
Ti		5322	5082	6246	5136	6576	5556	5496	5760	6252	6462	5748	6408	6564
TiO2 / Zr		0.012493	0.012258	0.009858	0.012478	0.010046	0.011781	0.012652	0.012403	0.00999	0.010189	0.012425	0.009718	0.009955
P2O5 / Zr		0.001958	0.001997	0.002102	0.002041	0.002081	0.001845	0.001948	0.001848	0.002109	0.002072	0.00201	0.002047	0.002056
P		607.43	603.06	970.14	611.8	991.99	633.65	616.17	624.91	961.4	957.03	677.35	983.25	987.62
Zr / Y		2.795276	2.831967	3.543624	2.90678	3.430818	3.261411	2.828125	2.866667	3.596552	3.511628	2.845018	3.815972	3.591503
P / Zr		8.555352	8.727352	9.186932	8.918367	9.092484	8.061705	8.510635	8.073773	9.217641	9.05421	8.785344	8.94677	8.986533
Zr / Y		2.795276	2.831967	3.543624	2.90678	3.430818	3.261411	2.828125	2.866667	3.596552	3.511628	2.845018	3.815972	3.591503
Ti / Zr		74.95775	73.54559	59.14773	74.8688	60.27498	70.68702	75.9116	74.4186	59.94247	61.13529	74.55253	58.30755	59.72702
Zr / Nb		12.45614	16.45238	13.03704	15.24444	12.39773	13.78947	17.65854	13.57895	10.53535	12.14943	15.11765	11.69149	11.56842
TOTAL	Major	100.99	99.912	98.1	100.343	99.132	100.024	100.296	97.077	95.546	97.311	99.506	96.715	98.859

TRACE MIN	Sample #	BCP1	BCP2	BCP1960	BCP1969	BCP1989	BP 1938	BP 1943	BP 2025	BP 2029	BP 2039	BP 2128	BP 2131
Barium	Conc.	450.9	501.0	383.3	396.2	283.5	254.9	256.8	138.5	135.8	195.0	270.2	228.2
Scandium	Conc.	34	22.9	29.1	30.2	27.8	27.1	26.5	31.7	30.9	33.4	30.5	31.4
Thorium	Conc.	2.2	4.7	2.4	2.7	1.5	2.5	LLD	LLD	LLD	LLD	1.8	LLD
Lead	Conc.	2.3	8.3	3.1	3.2	2.9	2.3	LLD	1.8	LLD	2.2	LLD	LLD
Cerium	Conc.	43.87	40.84	42.83	41.22	45.15	41.45	39.61	16.81	20.4	24.94	35.66	29.4
Neodymium	Conc.	23.22	22.29	20.38	22.27	21.32	20.35	20.25	10.94	11.83	14.16	20.32	16.82
Lanthanum	Conc.	17.65	15.39	20.29	18.05	17.76	16.64	15.35	6.13	9.16	9.58	16.11	11.77
Niobium	Conc.	22.84	17.89	19.81	22.75	22.47	21.88	21.05	6.52	5.93	10.77	15.31	11.77
Zirconium	Conc.	154.99	213.89	130.13	138.78	143.2	139.53	139.15	71.66	72.3	88.08	122.9	100.32
Yttrium	Conc.	29.89	26.62	26.34	27.82	26.65	27.96	27.85	24.43	25.33	25.49	31.53	27.08
Strontium	Conc.	353.33	252.13	308.75	355.84	316.31	311.13	315.01	191	195.38	235.58	235.14	243.26
Rubidium	Conc.	22.89	39.88	31.01	18.41	9.34	18.7	18.08	4.58	5.51	14.63	16.62	12.84
Cobalt	Conc.	39.4	27	34.6	37.4	35.3	37.2	37.7	46	47.3	45.8	41.6	44.7
Chromium	Conc.	297	174.1	302.3	267	271.4	274.8	266.1	331.9	338	265.5	216.8	211.8
Vanadium	Conc.	268.3	156.3	246.2	249.3	224.4	226.5	219.8	248.8	242.9	255.5	246	213.6
Zinc	Conc.	96.7	77.7	83.7	91.7	87.3	78.6	76.7	85.3	81.9	91.7	90.3	95.8
Copper	Conc.	87.5	55.8	68.5	79.5	43.3	75.8	75.3	102.6	99.8	94.9	91.2	100.6
Nickel	Conc.	68.1	41.8	60.3	63	64.9	68.6	70	109.9	108.7	81.7	65.9	72.3

TRACE MIN	Sample #	BB 1779	BB 1978	BB 1999	BB 2037	BB 2096	BB 2105	BB 2109	BCD 1	BCD 2	BCD3	BCD4	BCD5	BCB 1750
Barium	Conc.	182.6	139.8	132.9	127.9	277	276.3	276.3	296.1	352.4	436.5	246.6	396.6	205.8
Scandium	Conc.	30.4	31.2	27.9	30.3	33.4	33.4	33.7	28.9	30.1	28.1	33.8	28.1	30.4
Thorium	Conc.	LLD	LLD	1.0	LLD 2.41		1.95	2.7	LLD 2.2		3.59	2.23	2.49	LLD
Lead	Conc.	LLD	LLD	1.99	1.87	3.88	3.95	5.08	2.13	3.55	4.6	4.68	3.08	2.49
Cerium	Conc.	28.63	18.15	17.54	15.86	36.46	32.23	32.63	42.27	42.46	42.63	29.39	34.42	28.24
Neodymium	Conc.	17.04	11.82	12.18	10.49	20.06	19.49	19.02	22.13	21.41	23.06	15.69	19.61	17.05
Lanthanum	Conc.	10.89	5.12	5.2	4.2	15.32	11.67	13.87	17.98	18.41	18.2	12.74	18.36	11.91
Niobium	Conc.	10.8	4.78	4.59	3.75	10.44	9.32	8.4	23.79	22.07	21.03	5.92	22.95	13.52
Zirconium	Conc.	90.25	66.98	64.78	62.01	109.72	109.91	111.46	145.84	143.65	171.78	101.49	162.38	97.26
Yttrium	Conc.	26	24.53	22.02	21.59	29.23	28.69	29.83	29.85	29.04	28.6	28.62	27.69	27.58
Strontium	Conc.	240.26	197.58	195.12	181.69	241.26	238.49	239.97	342.02	313.37	270.68	238.8	252.57	235.29
Rubidium	Conc.	13.73	7.76	6.67	5.35	21.29	20.57	22.15	7.98	23.93	44.13	16.19	40.34	12.19
Cobalt	Conc.	46.1	44.8	45.3	51.1	36.3	36.6	36.6	41	39.6	33.6	40.6	35	45.7
Chromium	Conc.	238.2	259.3	341.3	401.9	312.6	316.1	314.4	272.6	251.8	241.7	313.6	256.4	227.1
Vanadium	Conc.	239	243.1	212.6	233.3	242.5	243.5	242	242.4	245	215	253.1	221.7	250.4
Zinc	Conc.	87.6	79.9	76.8	79.3	93.2	91.8	94.2	96.6	93.9	82.8	91.3	86	93
Copper	Conc.	93.1	98.8	97.8	88.4	37.6	38	39.8	89.8	87.6	70.5	36.3	71.8	100.3
Nickel	Conc.	81.3	94.7	113.7	132.3	23.8	24.6	24.6	69.7	59.6	56.5	21.9	63.6	73.3

TRACE MIN	Sample #	BD 1802	BD 1863	BD 1878	BD 1896	BD 1911	BD 1916	BD 1944	BD 1969	BD 1987	BD 2038	BD 2044	BD 2059	BD 2063
Barium	Conc.	126.2	73.1	336.9	121.2	123	125.7	87.5	107.1	146.1	310	287.3	259.5	267
Scandium	Conc.	28.2	32.7	33.4	30.4	27.6	28	24	29.2	31.2	34.4	35.4	35.1	35.1
Thorium	Conc.	LLD	LLD	LLD	LLD	LLD	LLD	LLD	LLD	LLD	1.67	LLD	2.32	2.01
Lead	Conc.	LLD	LLD	LLD	LLD	LLD	LLD	1.93	2.41	2.04	3.28	2.55	4.31	3.49
Cerium	Conc.	12.57	18.79	14.99	14.17	14.65	14.54	15.01	14	19.21	34.22	37.62	31.53	32.56
Neodymium	Conc.	9.09	13.17	9.85	10.4	10.81	10.2	8.07	9.97	11.57	19.75	21.7	19.07	19.64
Lanthanum	Conc.	6.84	7.87	4.52	4.14	4.47	4.98	5.84	5.41	6.33	14.12	14.33	13.95	15.03
Niobium	Conc.	4.35	4.9	3.64	3.94	4.32	4.72	5.04	4.45	5.5	9.5	9.8	9.44	8.92
Zirconium	Conc.	57.36	71.17	62.91	58.17	58.68	64.1	53.41	61.15	73.01	108.88	107.45	109.29	110.05
Yttrium	Conc.	21.27	24.57	22.9	21.77	20.47	21.11	18.55	20.66	26.1	30.71	29.42	29.87	31.02
Strontium	Conc.	188.82	197.23	776.9	174.97	186.83	189.97	182.43	164.43	190.39	216	215.16	226.36	221.81
Rubidium	Conc.	7.15	LLD	4.78	7.83	7.92	8.34	6.03	3.78	5.56	27.36	17.23	27.04	29.36
Cobalt	Conc.	53.5	46.7	44.7	57	52.7	51.2	61.7	66.4	46.6	37.4	37.5	38.3	37.4
Chromium	Conc.	344.9	320.5	324.5	424.2	354.1	366.8	428.5	462.7	311.4	322.9	321.7	334.6	329.8
Vanadium	Conc.	211.2	250.9	240.3	225.7	208.1	216.6	186.6	222.5	244.1	248.9	250.3	251.3	252.2
Zinc	Conc.	81.1	86.8	81.3	83.9	80.9	77.4	76.7	87.4	82.2	93.6	93.9	91.6	93.9
Copper	Conc.	91.4	99.9	85.4	93.5	90	87.1	69.7	96.9	99.2	37.6	38.5	41.6	40.5
Nickel	Conc.	170.7	109.9	104.7	174.1	166.7	156.5	241.7	243.8	102.4	24.2	26.3	27.4	27.9

Major Oxide	Sample #	BCP1	BCP2	BCP1960	BCP1969	BCP1989	BP 1938	BP 1943	BP 2025	BP 2029	BP 2039	BP 2128	BP 2131
SiO2		50.4	60.651	50.600	51.405	52.265	51.599	51.601	51.384	51.160	51.093	52.400	52.064
TiO2		1.124	0.807	0.987	1.051	1.069	1.068	1.051	0.893	0.865	1.066	1.215	1.079
Al2O3		15.7	13.417	16.363	15.436	15.729	15.750	15.872	15.423	15.487	15.265	15.233	15.422
Fe2O3		10.4	7.279	8.704	10.188	10.472	10.407	10.244	11.126	10.959	11.417	11.523	11.902
MnO		0.188	0.133	0.156	0.184	0.175	0.159	0.162	0.180	0.180	0.168	0.172	0.186
MgO		6.103	3.554	5.655	5.940	5.840	5.502	5.389	7.598	7.665	7.275	6.306	6.554
CaO		8.917	5.460	9.873	8.204	10.271	10.125	9.992	10.791	10.901	10.475	10.194	10.441
Na2O		2.969	3.428	2.718	3.127	2.819	2.419	2.336	2.485	2.413	2.261	2.707	2.720
K2O		1.04	1.963	1.690	1.080	0.713	1.006	0.948	0.385	0.258	0.690	0.911	0.762
P2O5		0.228	0.155	0.207	0.207	0.225	0.219	0.218	0.137	0.138	0.210	0.286	0.226
LOI		2.347	2.730	2.503	2.349	0.962	1.338	1.218	0.414	0.704	0.585	0.280	0.123
Ti		6744	4842	5922	6306	6414	6408	6306	5358	5190	6396	7290	6474
P		996.36	677.35	904.59	904.59	983.25	957.03	952.66	598.69	603.06	917.7	1249.82	987.62
Ti/Zr		43.51248	22.6378	45.50834	45.43882	44.7905	45.92561	45.318	74.76975	71.78423	72.6158	59.31652	64.53349
P/Zr		6.428544	3.166815	6.951433	6.518158	6.866271	6.858955	6.846281	8.354591	8.341079	10.41894	10.16941	9.844697
Zr/Y		5.185346	8.034936	4.940395	4.988497	5.373358	4.990343	4.996409	2.933279	2.854323	3.455473	3.897875	3.704579
Zr/Nb		6.785902	11.95584	6.568905	6.10022	6.372942	6.377057	6.610451	10.9908	12.19224	8.178273	8.027433	8.523364
TOTAL	Major	99.377	99.577	99.456	99.171	100.54	99.592	99.031	100.816	100.73	100.505	101.227	101.479

Major Oxide	Sample #	BB 1779	BB 1978	BB 1999	BB 2037	BB 2096	BB 2105	BB 2109	BCD 1	BCD 2	BCD3	BCD4	BCD5
SiO2		51.917	50.853	50.702	50.411	54.277	54.983	54.837	50.941	50.185	52.514	52.804	51.867
TiO2		1.064	0.833	0.790	0.805	1.103	1.096	1.099	1.100	1.092	0.968	1.312	1.009
Al2O3		15.455	15.997	16.213	15.348	15.198	15.364	15.145	16.522	16.290	15.160	15.270	15.470
Fe2O3		11.376	10.872	10.541	10.795	9.749	9.488	9.418	10.469	10.545	9.239	10.562	9.607
MnO		0.185	0.179	0.173	0.170	0.160	0.153	0.154	0.168	0.134	0.164	0.228	0.148
MgO		7.225	7.040	7.697	8.409	6.056	5.946	5.805	5.335	5.693	5.345	4.770	5.754
CaO		10.803	10.860	11.040	10.836	9.518	9.497	9.586	9.098	9.443	7.663	9.248	7.331
Na2O		2.583	2.329	2.344	2.345	2.427	2.439	2.437	3.387	2.913	3.428	2.233	3.171
K2O		0.673	0.420	0.428	0.383	0.992	0.994	1.015	0.764	1.218	1.722	0.771	1.670
P2O5		0.210	0.131	0.128	0.127	0.228	0.231	0.230	0.219	0.220	0.189	0.206	0.199
LOI		0.276	0.561	0.739	1.420	0.638	0.599	0.771	1.809	2.061	2.568	1.799	2.696
Ti		6384	4998	4740	4830	6618	6576	6594	6600	6552	5808	7872	6054
P		917.7	572.47	559.36	554.99	996.36	1009.47	1005.1	957.03	961.4	825.93	900.22	869.63
Ti/Zr		70.73684	74.61929	73.17073	77.89066	60.31717	59.83077	59.16024	45.25507	45.61086	33.81069	77.56429	37.28292
P/Zr		10.16842	8.54688	8.634764	8.950008	9.080933	9.184515	9.017585	6.562191	6.692656	4.808068	8.870036	5.355524
Zr/Y		3.471154	2.730534	2.941871	2.872163	3.753678	3.830952	3.736507	4.885762	4.946625	6.006294	3.546122	5.864211
Zr/Nb		8.356481	14.01255	14.11329	16.536	10.50958	11.79292	13.26905	6.130307	6.508836	8.168331	17.14358	7.075381
TOTAL	Major	101.767	100.075	100.795	101.049	100.346	100.79	100.497	99.812	99.794	98.96	99.203	98.922

Major Oxide	Sample #	BD 1802	BD 1863	BD 1878	BD 1896	BD 1911	BD 1916	BD 1944	BD 1969	BD 1987	BD 2038	BD 2044	BD 2059	BD 2063
SiO2		50.329	49.723	46.972	50.524	50.378	50.824	48.809	49.334	51.230	52.321	52.617	52.816	53.059
TiO2		0.738	0.877	0.807	0.763	0.741	0.772	0.656	0.755	0.908	1.103	1.083	1.097	1.102
Al2O3		16.024	15.738	16.042	15.139	15.953	16.371	15.481	13.630	15.439	15.102	15.219	15.375	15.296
Fe2O3		10.911	10.771	9.913	11.440	10.911	10.515	10.695	12.099	11.005	10.167	10.253	10.351	10.287
MnO		0.173	0.184	0.148	0.175	0.171	0.171	0.166	0.189	0.178	0.154	0.148	0.167	0.168
MgO		9.184	7.080	7.250	9.605	9.216	8.864	11.700	11.880	7.429	6.227	6.440	6.441	6.480
CaO		10.385	11.246	9.515	10.339	10.468	10.607	9.851	9.650	10.904	9.354	9.470	9.657	9.458
Na2O		2.362	2.026	3.061	2.326	2.391	2.285	1.859	1.929	2.411	2.306	2.265	2.403	2.483
K2O		0.360	0.248	0.381	0.382	0.369	0.392	0.199	0.202	0.277	1.219	1.006	1.178	1.209
P2O5		0.117	0.139	0.127	0.122	0.119	0.129	0.109	0.123	0.144	0.224	0.225	0.224	0.227
LOI		0.461	1.039	5.160	0.645	0.507	0.335	0.912	0.924	0.668	0.800	0.882	0.419	0.362
Ti		4428	5262	4842	4578	4446	4632	3936	4530	5448	6618	6498	6582	6612
P		511.29	607.43	554.99	533.14	520.03	563.73	476.33	537.51	629.28	978.88	983.25	978.88	991.99
Ti/Zr		77.19665	73.93565	76.9671	78.70036	75.76687	72.26209	73.69406	74.08013	74.61992	60.78251	60.47464	60.22509	60.08178
P/Zr		8.913703	8.534916	8.821968	9.165205	8.862134	8.79454	8.918367	8.790025	8.619093	8.990448	9.150768	8.956721	9.013994
Zr/Y		2.696756	2.896622	2.747162	2.672026	2.866634	3.036476	2.879245	2.959826	2.797318	3.545425	3.652277	3.658855	3.547711
Zr/Nb		13.18621	14.52449	17.28297	14.76396	13.58333	13.58051	10.59722	13.74157	13.27455	11.46105	10.96429	11.57733	12.33744
TOTAL	Major	101.044	99.071	99.376	101.46	101.224	101.265	100.437	100.715	100.593	98.977	99.608	100.128	100.131